Photochemistry on Nonreactive and Reactive (Semiconductor) Surfaces

Prashant V. Kamat

Radiation Laboratory, University of Notre Dame, Notre Dame, Indiana 46556-0579

Contents

I. Introduction

Photochemical processes in heterogeneous systems have gained wide popularity in recent years because of their wide applications in xerography, photography, chemical synthesis, and conversion and storage of solar light energy. Of particular interest are the photochemical processes on inorganic oxide surfaces. Several excellent review articles and books have appeared in recent years which highlight the various possible ways with which the support materials control the photochemical behavior of an adsorbed substrate.[1-11] Such support materials can be broadly classified into two categories: (i) *nonreactive surfaces*, such as silica or alumina which provide an ordered two-dimensional environment for effecting and controlling photochemical processes more efficiently than can be attained in homogeneous solutions (see for example, refs 7–11); (ii) *reactive surfaces*, such as titania or metal chalcogenides, which directly participate in photochemical reactions by absorbing the incident photon and transferring charge to an adsorbed molecule or by quenching the excited state of the adsorbed molecule (see for example refs 12–35). The scheme described in Figure 1 highlights the principle of these two categories.

The role of a nonreactive support material illustrated in Figure 1a is to assist the electron transfer between two adsorbed molecules. However, a reactive support such as TiO_2 can directly quench the excited molecule on its surface and then reduce another adsorbed molecule (Figure 1b). The surface as well as intrinsic properties of the support material plays an important role in influencing the course of a photochemical reaction. A detailed account of the mechanistic and kinetic aspects of these surface photochemical processes will be covered in this review. In particular, emphasis is laid on the discussion related to issues which have not been dealt with in past reviews. The surface photochemical reactions involving adsorption of simple gas-phase molecules on single-crystal surfaces are

Prashant V. Kamat is a native of Binaga, India. He received his *Ph.D. degree in Physical Chemistry from Bombay University in 1979.* He carried out his postdoctoral research in the area of solar photochemistry with Prof. Norman N. Lichtin at Boston University (1979–1981) and with Prof. Marye Anne Fox at the University of Texas at Austin (1981–1983). He joined the research staff at Notre Dame Radiation Laboratory in 1983 as an Assistant Professional Specialist. He was promoted to the ranks of Associate Professional Specialist in 1988 and Professional Specialist in 1992. His primary research interests include photochemistry in heterogeneous media, charge-transfer processes in semiconductor colloids, dye sensitization, and chemical and electrochemical deposition of thin semiconductor films.
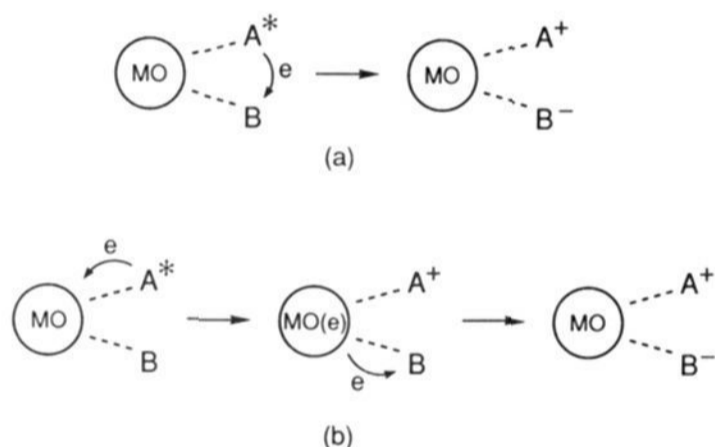

Figure 1. Role of support material in promoting the photochemical process.

beyond the scope of the present review. Review articles which discuss the spectroscopic study of these solid/gas-phase reactions can be found elsewhere (see for example refs 36 and 37).

II. Adsorption of Molecules

A. Interaction of Surface with the Adsorbed Substrate

In the particulate form, support materials (e.g., metal oxides) are usually covered with hydroxyl groups on their surfaces as well as physisorbed water. The physisorbed water can be removed from the surface by heat treatment (373–1273 K). The fraction of hydroxyl groups left on the surface can easily be monitored by fluorescent molecules like acridine or 9-anthroic acid which are excellent probes for Bronsted acidity and basicity of the surfaces.[37] In colloidal suspensions, the surface-active groups are useful in promoting adsorption via electrostatic, hydrophobic, or hydrogen bonding.

a. Aggregation Effects

The strong interactions between the surface and the adsorbed molecules often lead to aggregation effects.
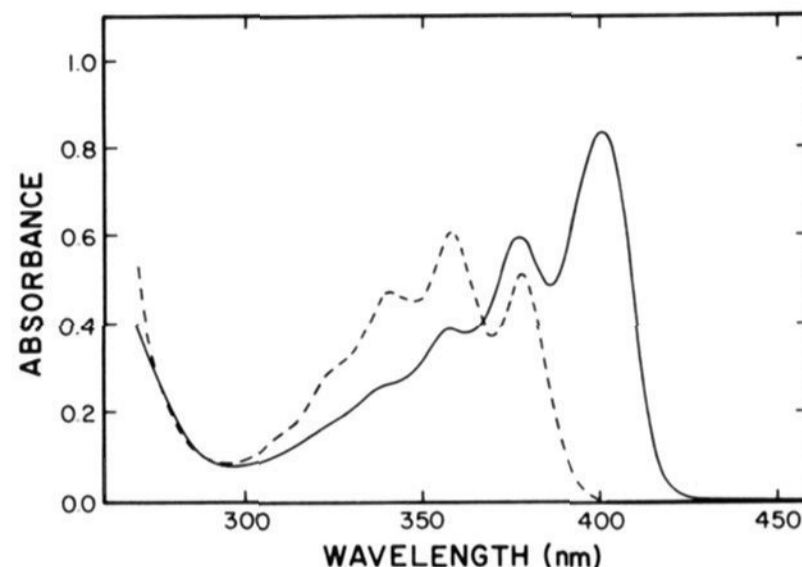
Figure 2. Absorption spectra of 2AS (133 μM) in aqueous 1×10^{-4} M HCl with (—) and without (- - -) alumina-coated silica (3.15 g/L) particles. Reprinted from ref 45. Copyright 1989 American Chemical Society.
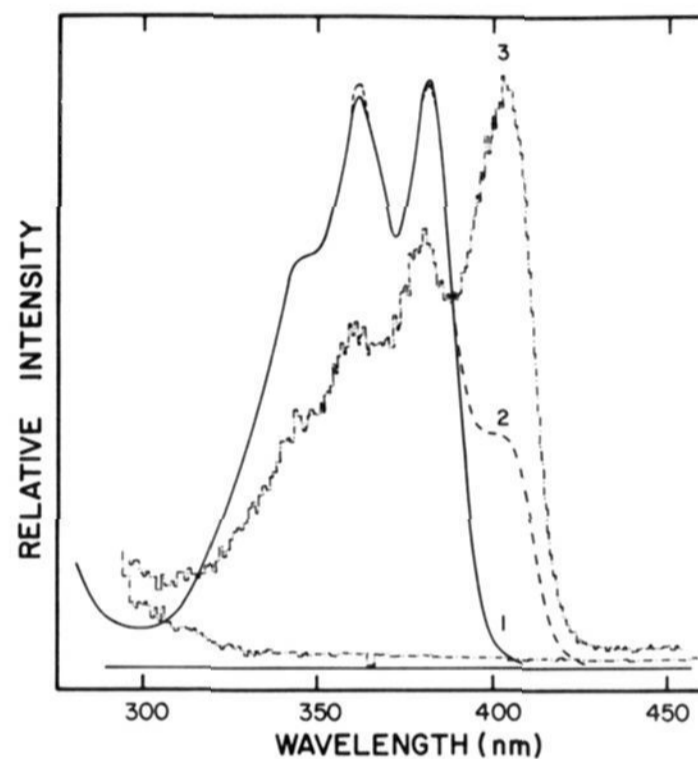
Figure 3. Fluorescence excitation spectra of 50 μM 2AS in aqueous 1×10^{-4} M HCl with and without 1.2 g/L alumina-coated silica particles. Curve 1 (solid) without SiO_2/Al_2O_3; emission monitored at 435 nm (rel instrumental sensitivity 1); curve 2 (dashed) with SiO_2/Al_2O_3, emission monitored at 435 nm (rel sensitivity 7); and curve 3 (dashed-dotted) with SiO_2/Al_2O_3, emission monitored at 560 nm (rel sensitivity 900). Reprinted from ref 45. Copyright 1989 American Chemical Society.

Absorption and emission studies of photoactive molecules on solid surfaces provide an insight to the aggregation process. For example, broadening of the absorption as well as increase in the dimer absorption has been observed when dyes such as phenosafranine,[38] rose bengal,[39] thionine,[40] diphenylisobenzofuran,[41] pyrene,[42] rhodamine B,[43] and derivatized Ru(bpy)$_3^{2+}$[44] were adsorbed on silica or alumina surfaces.

Anthracene-2-sulfonate molecules (2AS) dimerized upon adsorption from aqueous solution onto positively charged alumina-coated silica particles.[45] The ground-state dimerization which occurs even when fewer than 1% of available adsorption sites are occupied is accompanied by an intensification and red-shift (from 370 to 401 nm) of the 0–0 absorption band and a large decrease in the fluorescence yield (Figures 2 and 3). The spectral properties of the dimer of 2AS investigated in this study resemble those of the stable dimer of

anthracene, in which the long molecular axes in the dimer are parallel and the angle between the short axes is close to 60°. Anthracene-1,5-disulfonate and anthracene-1-sulfonate molecules adsorbed on these particles under similar experimental conditions did not dimerize. This suggested that subtle orientational effects can be important in controlling dimer formation. Similarly, coordination compounds of ruthenium(II) adsorbates with a single eight or twelve carbon atom alkyl side chain attached to one bipyridine ligand formed close-packed two-dimensional aggregates on negative oxide surfaces.[44] Thus adsorption onto particles is a convenient means of preparing samples of suitable aggregate geometry for the purpose of spectroscopic characterization. For example, the picosecond pump–probe technique has been employed to measure the electronic energy relaxation in J aggregates of pseudoisocyanines on 40-Å colloidal silica particles.[46,47]

Aggregation effects are also seen when photoactive molecules are incorporated in swollen clays.[48–50] Clay materials such as montmorillonite and kaolinite have unique structural features which facilitate intercalation of molecules between their layers. Such a strong interaction between the neighboring molecules often leads to the deactivation of the excited state via self-quenching processes.[50] On the other hand, molecules adsorbed on porous Vycor glass[51–53] or embedded in silica gel glass[54] do not exhibit any aggregation even at high substrate concentrations.

b. Charge-Transfer Interactions

The hydroxylated surfaces of oxides (e.g., colloidal TiO_2) are capable of undergoing charge-transfer interaction with specific functional groups of the adsorbed molecule. The charge-transfer interaction between the oxide surface and the adsorbed molecule can be probed with electronic absorption and emission as the energetics of the ground and excited states are altered. These spectral changes include displacement or broadening of the absorption bands, appearance of new charge-transfer bands, and changes in the extinction coefficient of absorption. For example, the absorption changes observed during the interaction of a squaraine dye with colloidal TiO_2 are shown in Figure 4.[55] The red-shifted absorption, which corresponds mainly to the dye associated with TiO_2, has been used to determine the association constant by the Benesi–Hildebrand method. The values of the associated constants and the spectral changes associated with surface interaction are summarized in Table I.

Similar charge-transfer surface interactions have important implications in improving the photosensitization properties of the semiconductor material, details of which will be discussed in a later section of this paper.

B. Determination of Binding Capacity

In order to elucidate the kinetics of surface photochemical process it is essential that one determine the concentration of adsorbed material first. There are various techniques employed in such studies, a few of which will be described here.

a. Adsorption Isotherms

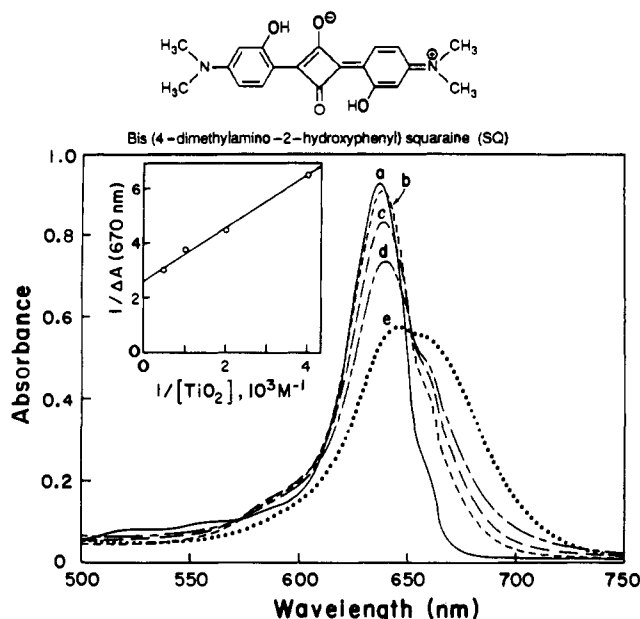Langmuir and Langmuir–Hinshelwood analysis is commonly employed to determine the adsorption

Figure 4. Absorption spectra of SQ (3 mM) in 40% methylene chloride and 60% acetonitrile containing: (a) 0, (b) 0.25, (c) 0.5, (d) 1.0, and (e) 2 mM colloidal TiO_2. The insert shows the fitting of the 670-nm absorption to the Benesi–Hildebrand plot. Reprinted from ref 55. Copyright 1991 Elsevier Science Publishers, B. V.

equilibrium between adsorbed and unadsorbed species in suspensions containing a support material. The principle and technique of this method are described elsewhere.[1,62,63] Adsorption of $Ru(bpy)_3^{2+}$ and methyl viologen derivatives at silica-, alumina-, RuO_2-, and TiO_2/aqueous electrolyte interfaces have been studied in detail by Furlong and Sasse.[44]

b. Benesi–Hildebrand Method

This method[64] is appropriate when the interaction between the surface modifier (S) and the support (M) results in a spectroscopically distinguishable absorption band of the complex. The absorption changes occurring

$$[S] + [M] \leftrightarrow [S\cdots M] \tag{1}$$

as a result of surface complexation can be utilized to obtain the association constant (K_a) of equilibrium 1. The insert in Figure 4 shows an example of such an analysis. The association constants determined by this method for several dye/TiO_2 systems are summarized in Table I.

c. Use of Nonbinding Probes

This method is similar to the one employed for obtaining binding data in micelle and colloidal inorganic systems.[65,66] The method involves determination of the decay rate constant of a nonbinding probe (e.g., $Ru(bpy)_3^{2+*}$ in a positively charged colloidal suspension) before and after the addition of a colloidal suspension containing the nonbinding probe and the quencher which binds to the colloids. For example, positively charged SiO_2/Al_2O_3 particles selectively adsorb the negatively charged quencher, 2,2'-azinobis(3-ethylbenzothiazoline-6-sulfonate) ($ABTS^{2-}$), molecules so that the rate of quenching of a nonbinding probe $Ru(bpy)_3^{2+*}$ by $ABTS^{2-}$ decreased (see Figure 5).[67] The concen-

Table I. Surface Modification of TiO₂ Colloids

support	surface modifier	apparent association constant (M^{-1})	spectral changes	ref
TiO_2	SCN^-	3.5×10^2	charge transfer band at 285 nm	60
TiO_2	chlorophyllin	2.0×10^3	increase in molar absorbancy	59
TiO_2	anthracene-9-carboxylic acid	6.0×10^3	increase in molar absorbancy and red-shift in the absorption maxima	56
TiO_2	thionine	2.75×10^5	red-shift ($\sim$20 nm) in the absorption maximum	58
TiO_2	bis[4-(dimethylamino)-2-hydroxy-phenyl]squaraine	2.7×10^3	red-shift ($\sim$20 nm) in the absorption maximum	55
CdS	diethyldithiocarbamate	9×10^2	new absorption band at 610 nm	303
SiO_2/Al_2O_3	RuL_3^{4-} (L = bathophenanthroline sulfonate)	1.2×10^4	red-shift ($\sim$10 nm) in the absorption maximum	143
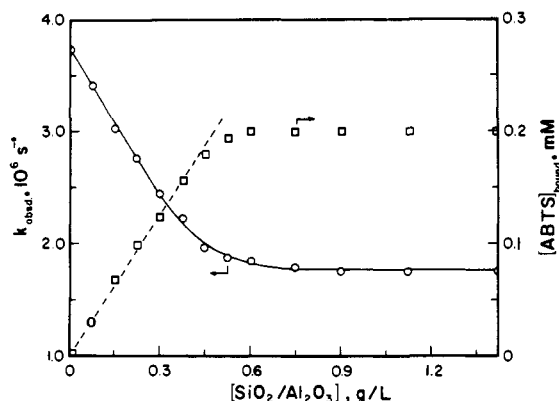
Figure 5. Effect of SiO_2/Al_2O_3 on the luminescence decay rate constant of $Ru(bpy)_3^{2+}$ in aqueous solution containing $ABTS^{2-}$ (O). The corresponding values of $[ABTS^{2-}]$ bound calculated according to eq 2 are also shown (□). The concentrations of $Ru(bpy)_3^{2+}$ and $[ABTS^{2-}]$ were 40 and 200 μM respectively. Reprinted from ref 67. Copyright 1989 American Chemical Society.

tration of $ABTS^{2-}$ in the solution phase was determined from

$$[ABTS^{2-}]_{soln.} = (k_{obsd} - k_0)/k_q \qquad (2a)$$

where k_0 is the rate constant for the intrinsic decay of $Ru(bpy)_3^{2+*}$ and k_q is the bimolecular rate constant for quenching by $ABTS^{2-}$ in the solution phase. The concentration of $ABTS^{2-}$ removed from solution due to adsorption, $[ABTS^{2-}]_{bound}$, was thus determined by eq 2b. The dependence of $[ABTS^{2-}]_{bound}$ on the concen-

$$[ABTS^{2-}]_{bound} = [ABTS^{2-}]_{total} - [(k_{obsd} - k_0)/k_q] \qquad (2b)$$

tration of SiO_2/Al_2O_3 particles is also shown in Figure 5, the initial slope of which gave the binding capacity of these particles for $ABTS^{2-}$. This capacity was found to be 0.42 mmol of $ABTS^{2-}$ per gram of SiO_2/Al_2O_3 particles, which corresponds to 40 $Å^2$ of surface area per adsorbed molecule.

III. Photochemistry on Nonreactive Surfaces

Although research in the area of surface photochemistry was initiated several decades ago,[68-70] it is still an intriguing topic in many respects. Early work on the photophysical studies of organic molecules adsorbed on oxide supports has been reviewed by Nicholls and Leermakers.[70] Although inorganic oxide supports such as silica, alumina, or zeolites are photochemically inert, they often alter the course of a photochemical reaction. Some representative examples which highlight the role
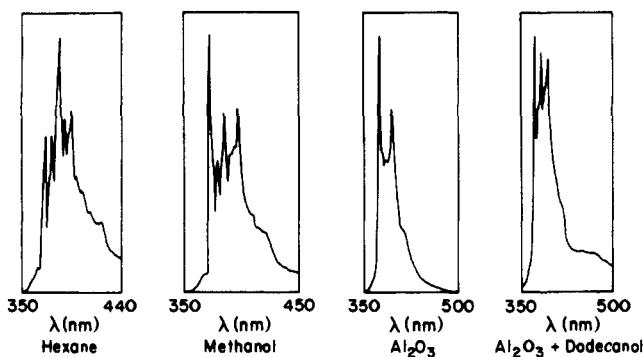

Figure 6. Fluorescence spectra of pyrene in hexane, methanol, adsorbed on alumina (1 mg/g Al_2O_3), and adsorbed on alumina together with dodecanol (100 mg/Al_2O_3). Reprinted from ref 91. Copyright 1985 Elsevier Science Publishers, B. V.

of nonreactive surfaces in influencing the excited-state behavior of photoactive molecules will be presented.

A. Excited-State Properties

a. Singlet Excited State

In all the surface photochemical work carried out so far, pyrene seems to have been the most attractive probe molecule because of its long fluorescence lifetime, its ability to form excimers, and its spectral sensitivity to the polarity of its environment. A wide variety of surfaces has been probed with pyrene and its derivatives. These include silica,[69-88] alumina,[89-92] zeolites,[93-95] clays,[96-98] and calcium fluoride.[73] The vibrational structure of pyrene is known to be strongly dependent on the polarity of the environment.[99] The changes in the fluorescence peaks I (370 nm) and III (391 nm) are commonly used to monitor the polarity or hydrophobic microenvironment on the surface of SiO_2 and Al_2O_3.[91] With increasing polarity of the solvent, an increase in the fluorescence intensity of peak I is seen as the symmetry-forbidden 0-0 band of the $S_0 \rightarrow S_1$ transition is favored.[91] For example, the decrease in the fluorescence intensity ratio III/I of pyrene on alumina is similar to that observed in polar solvents (e.g., methanol), suggesting thereby the microenvironment on alumina surface is polar (see Figure 6). Coadsorption of dodecanol increases the hydrophobicity of the alumina surface as indicated by the increase in the fluorescence intensity ratio of peaks III/I. Similar changes in the surface hydrophobicity of silica which were derivatized with tetramethylsilane and poly(dimethylsiloxane) have been probed by monitoring the intensity changes in the pyrene fluorescence peaks.[83]

Tsubomura and his co-workers[100-102] and De Mayo and his co-workers[72-75,81] have utilized emission prop-
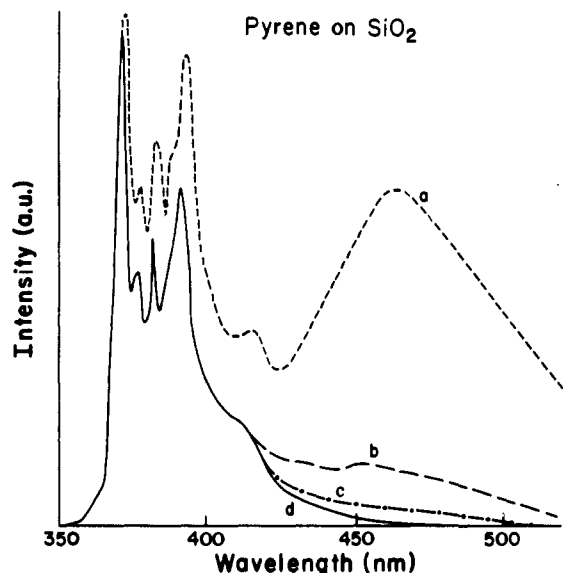
Figure 7. Emission spectra of adsorbed pyrene as a function of surface coverage: (a) at 3% (λ_{ex} 341 nm), (b) at 1% (λ_{ex} 341 nm), (c) at 0.2% (λ_{ex} 341 nm), and (d) at 0.2% (λ_{ex} 331 nm). Reprinted from ref 72. Copyright 1982 American Chemical Society.

erties of naphthalene, pyrene, and anthracene to probe the aggregation effects as well as the surface mobility of adsorbed molecules. For example, surface coverage plays an important role in influencing the emission characteristics of these probe molecules. The dependence of pyrene emission on the surface coverage is shown in Figure 7. At lower surface coverages, the emission spectrum at shorter wavelengths closely resembles that of monomer emission observed in solutions. A broad excimer-like emission band at longer wavelength can also be seen even at submonolayer coverages. This longer wavelength emission is clearly enhanced at higher coverages. Time-resolved emission studies[42,72-77,81] indicate that preferred sites available on the silica surface lead to the inhomogeneous distribution of pyrene consisting of weakly bound ground-state bimolecular association product. Hydrogen-bonding interaction with the π-system of the hydrocarbon is considered to play an important role in stabilizing this bimolecular association of pyrene and makes it behave in a manner different from that in hydroxylated solvents. Coadsorption of long-chain alcohol and polyalcohol which block the accessibility of silanol groups on the silica surface, greatly diminishes the tendency to bimolecular ground-state association. However, a substantial contribution to the dynamic excimer emission is observed when a mobile phase (e.g., water/methanol) is introduced.[78,103] Ground-state association of pyrene has also been observed in zeolites.[78] Excimers in the supercages were found to exist if the zeolite has been dehydrated first.

The mobility of pyrene on chemically modified silica surfaces and its dependence on temperature has been studied by measuring the time dependence of pyrene excimer formation.[84] The rate constant for the excimer formation determined in this study was 1.2×10^8 M^{-1} s^{-1} at room temperature. The apparent activation energy for diffusion on silica was determined to be 20 kJ/mol. The occurrence of inter- and intragranular motion of several aromatic hydrocarbons on dry silica gel has been demonstrated by Bauer et al.[72] Inter-

granular motion of adsorbate occurred both under static and shaking conditions. Although molecules prefer certain sites on the silica gel at room temperature, kT provides enough energy for the translational motion. Pyrene and its analogues have also been used to probe the nature of adsorption sites in solid zeolites and clays.[95,98] In addition to substantial spectral shifts, excimer formation has been observed for pyrenealdehyde adsorbed on Na^+–zeolite Y's.

Both monomer- and excimer-like emissions of pyrene on silica surfaces exhibit multiexponential decay. Such a multiexponential decay of the excited state arises from the inhomogeneous interaction between pyrene and the adsorbing surface.[73] An example of an emission–time profile of pyrene adsorbed on silica is shown in Figure 8. The multiexponential decay curves are usually analyzed by a nonlinear least-squares procedure fitted to the two- or three-component decay law given by expression 3. James et al. have developed a method-

$$F(t) = a_1 \exp(-t/\tau_1) + a_2 \exp(-t/\tau_2) + a_3 \exp(-t/\tau_3)$$
(3)

ology to determine the average emission lifetime of a probe molecule adsorbed on a heterogeneous surface (expression 4). Although the values of a_1, a_2, τ_1, τ_2, etc. varied from one measurement to another, the average

$$\langle \tau \rangle = \sum a_i \tau_i^2 / \sum a_i \tau_i$$
(4)

lifetime $\langle \tau \rangle$ was reproducible. The average lifetime for the monomer emission of pyrene on silica, alumina, or CaF_2 is in the range of 195–290 ns. The average lifetime for the excimer-like emission was in the range of 85–125 ns.[73]

1,6-Diphenylhexatriene (DPH) exhibits S_2–S_1 dependent fluorescence lifetime since its S_1–S_0 transition is symmetry-forbidden.[105] As the S_2–S_1 energy difference decreases with increasing polarizability of the environment, the fluorescence lifetime also decreases. The long-lived component of DPH fluorescence on alumina is shifted to higher energies by 250 cm^{-1} and indicates a reduced polarizing environment. 1-(N,N-Dimethylamino)-4-benzonitrile adsorbed on silica exhibits a long wavelength emission, originating from the twisted charge-transfer excited state (CT^*).[106] The apparent surface polarity of the silica surface, estimated from the CT^* emission frequency, is comparable to that of ethanol.

Probe molecules are also being used to identify the acid sites on adsorbents such as silica, alumina, or zeolites. For example, the emission characteristics of 9,10-diazaphenanthrene embedded in calcinated Vycor glass have been used to establish proton transfer from the Bronsted acid surface site to a heterocyclic N-atom of the adsorbate.[107,108] Oelkrug and his co-workers[109-111] have shown that the photoluminescence and the decay of the aromatic bases and acids adsorbed on metal oxides are strongly dependent on the pretreatment of the adsorbent surface. Similarly, acridone and N-methylacridone have been used as probes to establish the role of hydrogen bonding in the surface interactions with silica.[112] Rhodamine B and other xanthene dyes have also been used as probes to investigate the surface structure and its adsorption-site distribution on organic single crystals, CaF_2, and quartz plates.[113,114] Absorp-
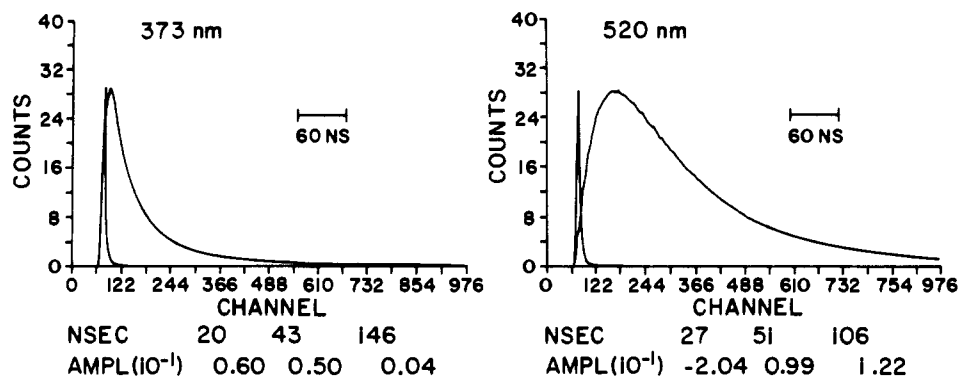
Figure 8. Rise and decay curves of the monomer (373 nm) and intramolecular excimer (520 nm) fluorescence of 1,3-di(1-pyrenyl)propane on silica coadsorbed with 1-octanol, fitted to three exponentials. The excitation pulse is also depicted in each case. Reprinted from ref 78. Copyright 1985 American Chemical Society.

tion characteristics of submonolayers of rhodamine 6G on a fused silica surface have been investigated by photochemical bleaching and polarization-dependent fluorescence measurements for the purpose of probing the geometry of the support.[115]

b. Excited Triplet State

One of the interesting aspects of probing the triplet excited state properties of molecules adsorbed on solid surfaces is their long survivability with lifetimes often approaching the values in rigid solvents. Aromatics adsorbed on alumina under high vacuum show phosphorescence with decay times on the order of seconds.[116-118] Such a long-lived excited state is beneficial in enhancing the efficiency of a photochemical or photocatalytic process. Attempts have been made to correlate the lifetime of the charge transfer triplet state of supported oxides (e.g., V_2O_5, MoO_3, or CrO_3 supported on porous Vycor glass) with their efficiency for photoreduction of CO.[119]

Triplet excited states of various aromatic molecules adsorbed on oxide surfaces have also been characterized by fast kinetic spectroscopy (e.g., diffuse reflectance laser flash photolysis) or ESR techniques. These systems include naphthalene, biphenyl, triphenylene,[120] acridine,[121] phenosafranin,[38] rose bengal,[39] thionine,[40] diphenylpolyenes,[122] benzophenone,[123-126] xanthone,[127] distyrylbenzenes,[128] pyrene,[91,120,129] and fullerenes (C_{60}[130] and C_{70}[131]). The T–T absorption spectra of some of these aromatic hydrocarbons are strikingly different from those observed in homogeneous solutions.[120] These differences have been attributed to the presence of charge-transfer states of the adsorbent–adsorbate systems and the occurrence of transitions to these triplet charge transfer states. Figure 9 shows the triplet–triplet absorption of benzophenone microcrystals deposited on a fused silica window. The triplet excited benzophenone which exhibits a maximum at 540 nm decays with mixed first- and second-order kinetics. Phosphorescence emission exhibits similarly a complex kinetics. In the case of xanthone adsorbed on silica gel, spectral evidence has been presented to show the formation of triplet excited state within 800 ps.[127] By restricting the mobility of β-phenylpropiophenone in the channels of sodalite, Casal and Scaiano[132,133] have achieved 5 orders of magnitude enhancement in the triplet lifetime. Schoonheydt et al.[134] have observed emission of proflavine dimers in bentonite clay.
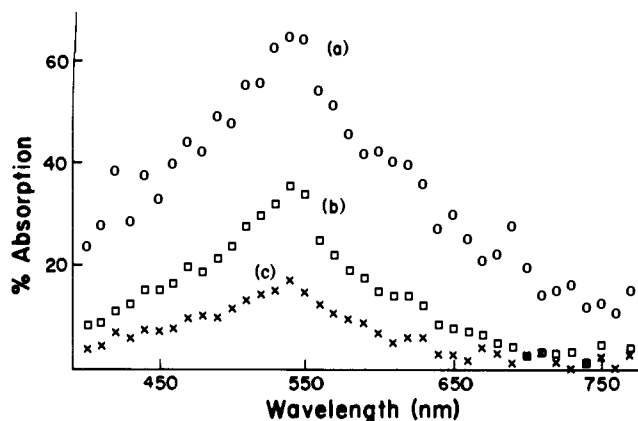

Figure 9. Time-resolved difference absorption spectrum of benzophenone triplet recorded following the 355-nm laser pulse excitation: (a) at maximum absorption, and (b) 1-μs and (c) 4-μs delay. Reprinted from ref 123. Copyright 1984 Elsevier Science Publishers, B. V.

$Ru(bpy)_3^{2+}$ is one of the most widely studied organometallic complexes in surface photochemical processes. Gafney and his co-workers have carried out an extensive investigation of photophysical and photochemical properties of $Ru(bpy)_3^{2+}$ adsorbed on porous Vycor glass.[11,51-53,135-137] Irrespective of the site of adsorption (interior cavities or into the crevices of outermost volume of PVG) the spectroscopic properties were unchanged. Slight changes in the absorption characteristics were observed between adsorbed $Ru(bpy)_3^{2+}$ and that in homogeneous solutions. Resonance Raman spectra of adsorbed $Ru(bpy)_3^{2+}$ indicate that its ground-state structure is equivalent to that in aqueous solution, whereas the excited-state structure differs from that in water.[137] Although the shapes of the emission band are similar in both media, the quantum yield and lifetime of $Ru(bpy)_3^{2+*}$ emission are significantly higher when adsorbed on PVG.[11,137] Adsorption onto PVG leads to an increase in the radiative rate constant, thus causing fundamental changes in the relaxation processes. The temperature dependence of emission quantum yield and lifetime for the ruthenium complex adsorbed on PVG has also been studied.[53]

The excited-state properties of ruthenium complexes have also been studied on a variety of other support materials such as silica, clay, and zeolite materials.[138-147] Absorption and emission properties of $Ru(bpy)_3^{2+}$ and $Cr(bpy)_3^{2+}$ in clay membranes were found to be de-
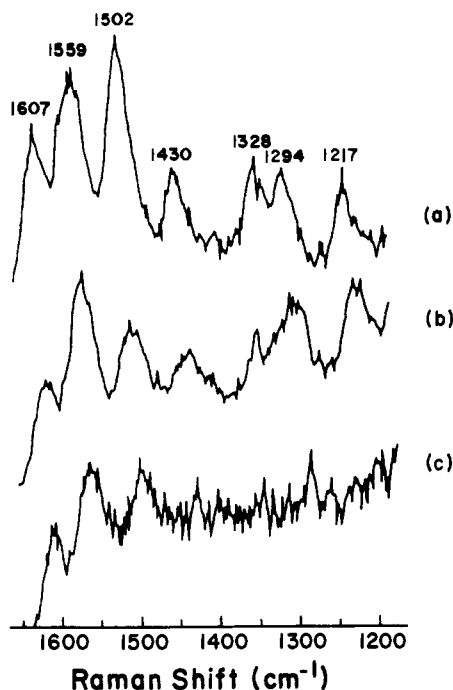
Figure 10. Pulsed UV resonance Raman spectra of zeolite Y: (a) 33, (b) 161, and (c) 200 μmol/g (excitation at 355 nm). Reprinted from ref 147. Copyright 1992 American Chemical Society.
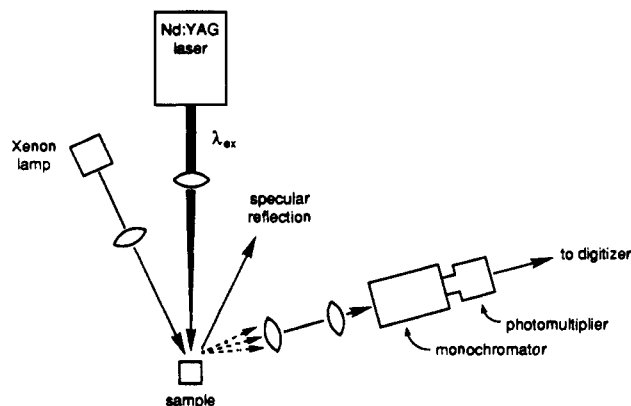

Figure 11. Schematic diagram of the diffuse reflectance laser flash photolysis setup. Reprinted from ref 39. Copyright 1989 American Chemical Society.

pendent on the water content.[141] It was concluded that covalently hydrated or slightly distorted bipyridyl ligands are formed when $Ru(bpy)_3^{2+}$ is adsorbed on the clay surface. Similar structural and excited-state dynamics have also been observed in zeolites.[146-147] Ordered arrangement of supercages within the zeolite crystal facilitates investigation of intermolecular interaction between $Ru(bpy)_3^{2+}$ molecules with a controlled degree of contact. Spectral properties of $Ru(bpy)_3^{2+}$ synthesized within zeolite Y cages indicate major spectral perturbations including a red-shift of the metal-to-ligand charge-transfer band by $\sim$40 nm, shifts in bipyridine ring breathing modes, and quenching of emission.[147] Figure 10 shows UV resonance Raman spectra of the ^{3}MLCT state of $Ru(bpy)_3^{2+}$ at various loadings. Although no frequency changes were observed as a function of loading, the intensities were weaker at higher loadings. Vibrations corresponding to the bpy$^{\cdot-}$ radical anion confirmed the formation of a charge localized ^{3}MLCT in these samples.[147]

Considerable interest has been shown recently in resolving organic and inorganic racemates on chirally modified clay supports.[148,149] Ghosh and his co-workers have shown the existence of remarkable absorption and emission spectral differences between enantiomeric and racemic poly(pyridyl)ruthenium complexes by ion exchanging the cationic forms of these complexes into montmorillonite and hectorite clays.[150-152] At least two different types of exchange sites for these clay systems have been proposed.[152] The distribution of poly(pyridyl)ruthenium (II) ions over these sites is controlled by the nature of the clay in question and by an interplay of chirality and ligand type of the probe. These differentiated sites have varying effects on spectral properties and quench the excited Ru(II) with different degrees of efficiency. Δ,Λ-$Ru(bpy)_3^{2+}$ resides in non-quenching exchange sites, the ions existing as small clusters within these zones. As a result of this cluster

formation, the preferential self-annihilation of lightly loaded Δ,Λ-$Ru(bpy)_3^{2+}$ has been observed at high-excitation flux. Also, coadsorbed $Zn(phen)_3^{2+}$ was found to suppress self-annihilation through pseudoracemic interaction with Ru(II). Chiral molecular recognition in intercalated zirconium phosphate has recently been demonstrated by Cao et al.[153]

B. Mechanism and Kinetics of Surface Photochemical Processes

a. Techniques

Spectroscopic techniques such as UV–visible absorption/diffuse reflectance, emission, FTIR, IR, XPS, and resonance Raman have been extensively employed to investigate the absorbate–adsorbent interactions as well as excited-state dynamics. These techniques are also useful in characterizing the products formed during the surface photochemical process. For photoactive molecules adsorbed on transparent colloids, conventional laser flash photolysis is convenient to probe the surface photochemistry of the adsorbate. However, for opaque samples, diffuse reflectance laser flash photolysis is regarded as a valuable technique that gives useful information regarding the photochemical transients as well as the kinetic details of the surface photochemical processes. The principle of diffuse reflectance laser flash photolysis is illustrated in Figure 11.

Theories which correlation the diffuse reflectance measurements to optical properties have been reviewed by Wendlandt and Hecht.[154,155] Diffuse reflectance measurements are usually analyzed on the basis of the Kubelka–Munk equation:

$$F(R) = k/s = (1 - R)^2/2R \qquad (5)$$

where k and s are absorption and scattering coefficients respectively and R is the reflectance at the front face. $F(R)$ is termed the Kubelka–Munk function[156] and is proportional to the concentration of the adsorbate molecules. However, for the analysis of the transient measurements a modified expression is employed.[121,157,158] If the intensity of analyzing light at the analyzing wavelength is I_0 and the diffusely reflected light is J_0, then the diffuse reflectance can be expressed as $R = J_0/I_0$. Thus the photoinduced changes in the surface concentration can be measured by monitoring

the reflectance R as a function of time. If R_B is the background reflectance and R_x is the total reflectance of the sample at the analyzing wavelength, then one can equate

$$[R_B - R_x]/R_B = 1 - R_t \qquad (6)$$

where $1 - R_t$ corresponds to the transient absorption as in the case of transmission flash photolysis.

Alternatively, if the exciting light is totally absorbed by the sample, the intensity of the diffused monitoring light from the sample (before and after photolysis) can be used to estimate the fractional absorption, A_d, of the transient formed at the surface (expression 7).[159] For

$$A_d = \ln (R_0/R_t) \qquad (7)$$

small fractional absorption ($A_0 \ll 1$), A_d is proportional to the concentration of the transient. Thus in a laser flash photolysis experiment the transient decay is followed by recording the changes in $1 - R_t$ or A_d with time. For a transient decaying by a unimolecular pathway, the rate constant can be obtained from the slope of a plot of $\ln [1 - F(R_t)]$ vs time (in the case of samples where transient concentration falls off exponentially), or $\ln [F(R_t)]$ vs time (in the case of samples where a homogeneous transient concentration exists beneath the sample surface) where $F(R_t)$ is the Kubelka–Munk function. Using this procedure the photochemistry of several molecules on various solid supports has been investigated. An example of the triplet excited spectra of benzophenone deposited on a fused silica window is shown in Figure 9.

The EPR technique has also been widely used to investigate the surface photochemical processes. Among these studies are photooxidation of quinoline on rutile,[160] methyl radicals on ZnO,[161] peroxy radicals on silica gel,[162] dibenzyl ketone on porous silica,[163] and carotenoid radicals on silica.[164] The forced Rayleigh scattering technique has also been employed to measure the self-diffusion coefficient of azobenzene in porous Vycor glass.[165]

b. Intermolecular Energy-Transfer Process

The mobility of the adsorbed molecules is greatly reduced when they are adsorbed on a solid surface. The lateral mobility of at least one of the adsorbed molecules is essential for carrying out bimolecular photochemical process on solid surfaces. Strong localized surface interactions restrict the mobility of the adsorbed molecule. Determination of the rate constants of exothermic bimolecular processes such as triplet–triplet energy transfer can yield valuable information regarding the surface diffusion. Turro et al.[124] have demonstrated the intermolecular triplet–triplet energy transfer between excited benzophenone and naphthalene on silica surfaces. By using diffuse reflectance laser flash photolysis they have demonstrated that triplet energy transfer occurs via both static and dynamic pathways on silica. The time-resolved absorption spectra recorded in these experiments are shown in Figure 12. Static energy transfer was instantaneous while the rate constants for the dynamic energy transfer were 7.3×10^{15} and 8.5×10^{15} dm^2 mol^{-1} s^{-1} on 95- and 225-Å-diameter silica, respectively. The silica surface was treated as a two-dimensional surface for the purpose of calculations. The dynamic quenching was attributed
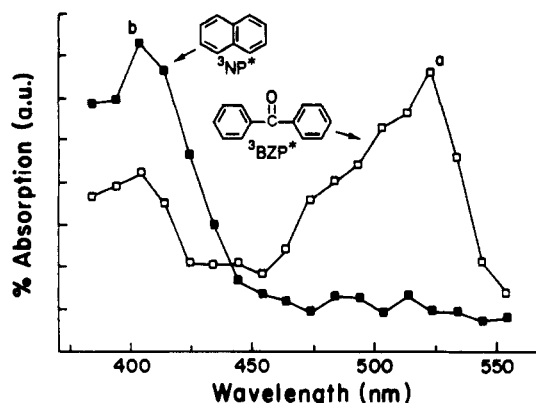

Figure 12. (a) Transient absorption spectrum obtained from irradiation of benzophenone on 95-Å silica 400 ns after the pulse and (b) transient absorption spectrum obtained from irradiation of benzophenone and naphthalene on 95-Å silica 5 μs after the pulse. Reprinted from ref 124. Copyright 1985 American Chemical Society.
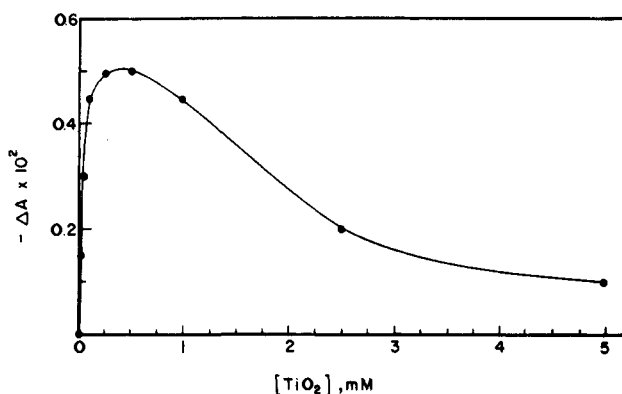

Figure 13. Dependence of the yield of the triplet excited state of Ox 725 on the concentration of TiO$_2$. The triplet yield was monitored by the bleaching of Ox 725 at 660 nm. The suspension contained 20 μM 9AC and 5 μM Ox 725. Excitation was at 355 nm where both the adsorbed and unadsorbed of 9AC had similar molar extinction coefficients. Reprinted from ref 56. Copyright 1987 Elsevier Science Publishers, B. V.

to collision-induced energy transfer resulting from the naphthalene surface diffusion.

By using anthracene-9-carboxylic acid (9AC) as the triplet sensitizer, efficient energy transfer to an oxazine dye, N,N'-tetraethyloxonine (Ox725), on the surface of colloidal TiO$_2$ has been carried out.[56] Static quenching was considered to be the dominant process since both 9AC and Ox725 were polar and strongly adsorbed onto the TiO$_2$ surface. The dependence of the Ox725 triplet yield on the concentration of TiO$_2$ (Figure 13) highlighted the role of the substrate in influencing the source of energy dissipation in heterogeneous systems. The energy-transfer efficiency increased steeply at low concentrations of TiO$_2$ as an increasing proportion of 9AC and Ox725 molecules in the system became adsorbed to the particles. The decrease in T–T energy transfer efficiency observed at higher TiO$_2$ concentrations is attributed to an increasing average distance separating the donor (9AC) and acceptor (Ox725) molecules on TiO$_2$ particles having submonolayer coverages. The maximum yield of Ox725 triplet corresponded to an energy-transfer efficiency of $90 \pm 5\%$.

Triplet–triplet energy transfer and heteroannihilation of triplet eosin and anthracene on a silica surface has

been carried out by Bryukhanov et al.[166] A concentrating effect of dye molecules in laponite clay suspensions has resulted in the electronic energy transfer from rhodamine 6G to a number of oxazine and thiazine dyes.[49] Both radiative and nonradiative energy-transfer mechanisms were found to be operative in the clay environment.

Klafter and Blumen[167] have proposed a generalized Förster-type equation for the survival probability of the donor. This model is commonly used to analyze direct energy and electronic energy-transfer processes on solid surfaces.[168,169] Fluorescence quenching of rhodamine B adsorbed on a single crystal of naphthalene and on glass, which occurred as a result of energy transfer from fluorescing monomer and dimer to nonfluorescing aggregate species, has been explained on the basis of a Förster-type energy transfer process.[113] Levitz et al.[168] have investigated possible geometrical cross-over and experimental constraints generally associated with the direct energy-transfer process. The singlet–singlet intermolecular electronic energy transfer between adsorbed rhodamine B (donor) and malachite green (acceptor) on silica surfaces has been analyzed to reveal the pore size effects on the fractal distribution of adsorbed acceptor molecules and to characterize the geometric size distribution of fractal structure of the support.[169-171] Fractallike exciton annihilation kinetic behavior has been observed for naphthalene embedded in Vycor glass samples.[172]

Avnir[173] has shown how various photophysical and photochemical properties of adsorbates are influenced by surface geometrical parameters such as intermolecular distances, surface concentrations, available surface for reaction and for excited intermediates, and surface heterogeneity. Both classical surface science tools and the use of surface science scaling laws which have been interpreted as reflecting fractal properties of the heterogeneous environment have been suggested in this study to correct the analysis of previously obtained experimental data from irregular surfaces.

c. Triplet Quenching by Oxygen

Interaction between the surface-bound triplet excited sensitizer and a gas-phase ground-state triplet oxygen molecule can yield important information regarding the morphology of the surface and kinetic details of the heterogeneous reactions at the gas/solid interface. Characterization and reactivity of molecular oxygen species on oxide surfaces have wide applications in generating singlet oxygen (reaction 8) as well as in elucidating heterogeneous catalytic reactions.[174] As

$$^3Sens^* + {}^3O_2 \rightarrow Sens + {}^1O_2^* \qquad (8)$$
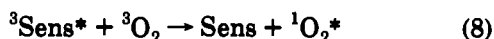
shown by Midden and Wang,[175] the use of a sensitizer anchored on a silica surface provides a "clean" method to generate gas-phase singlet oxygen, by keeping the sensitizer away from the solution phase.

It has already been shown[91,126,132,133,176] that profound differences exist between solution and surface quenching behavior of excited singlet and triplet states by gaseous quenchers. The overall kinetics of the reaction at the gas/solid interface involves some combination of processes such as (a) diffusion of the reactants to the surface, (b) adsorption of the reactants, (c) reaction at the surface site, (d) desorption of the products, and (e) diffusion of the products away from the surface.[126] The problem of the surface diffusion process has been discussed in detail by Freeman and Doll[177] and by Cuckier.[178] Apart from the surface diffusion of reactants and products, Langmuir-type adsorption/desorption processes play an important role in controlling the reaction kinetics. Wellner et al.[85] have shown that the pore size has a marked effect on the oxygen quenching efficiency of excited aromatic molecules adsorbed on porous silica. These researchers demonstrated a new surface catalytic effect associated with an increase in activity per unit area. Using the theoretical model of "target annihilation reactions" proposed by Bluemen et al.[179] Turro and his co-workers[126] have investigated the pore size dependence of quenching of triplet benzophenone by oxygen on a homologous series of silica gels. The benzophenone triplet annihilation rate constants were measured for each silica by measuring the survival probability $\Phi(t)$, of benzophenone triplet, as a function of oxygen pressure and fitting to a single exponential decay law

$$\Phi(t) \propto \exp(-k_{O_2}t) \qquad (9)$$

where

$$k_{O_2} = 1/\tau + k_q P_{O_2} \qquad (10)$$

The dependence of k_{O_2} on the oxygen pressure is shown in Figure 14a. The slope of this linear plot was used to determine the value of the target annihilation rate constant, k_q. The value of k_q was strongly dependent on the pore size of the lichrospher series of silica gels, the dependence of which is shown in Figure 14b. This linear scaling relationship was observed for oxygen pressures where the mean free path is greater than the mean pore size (Knudsen regime). In the Knudsen regime the annihilation reaction was modeled by a random walk picture in three dimensions.

The interaction between singlet oxygen and 1,3-diphenylisobenzofuran (DPBF) on an air-equilibrated oxide surface has recently been investigated by diffuse reflectance laser flash photolysis. The singlet oxygen which is produced via energy transfer from singlet and triplet excited DPBF reacts rapidly with the ground-state DPBF. The transient absorption spectra (Figure 15) recorded following the 532-nm excitation of DPBF adsorbed on TiO_2 show an increase in bleaching with time as ground-state DPBF reacts with singlet oxygen.[41] The half-life of self-sensitized degradation decreases as the surface coverage on alumina increases.[41,180] This is attributed to the participation of surface-bound oxygen which reacts more efficiently with DPBF than does atmospheric oxygen. $Ru(bpy)_3^{2+}$-exchanged zeolite Y has been shown to act as an effective sensitizer.[181] The photogenerated singlet oxygen freely diffuses to solution where it reacts with normal selectivity. The performance of zeolite-based sensitizer has been compared with other sensitizers in the oxygenation of 1-methyl-1-cyclohexene.

Oxygen quenching studies of a variety of ketones have indicated two different types of sites in the hydrophobic sodalite.[133] In the first case, the sites are more protected and are not readily accessible to oxygen. In the second case, quenching by oxygen occurs rapidly and efficiently, implying fast diffusion in these regions. This model
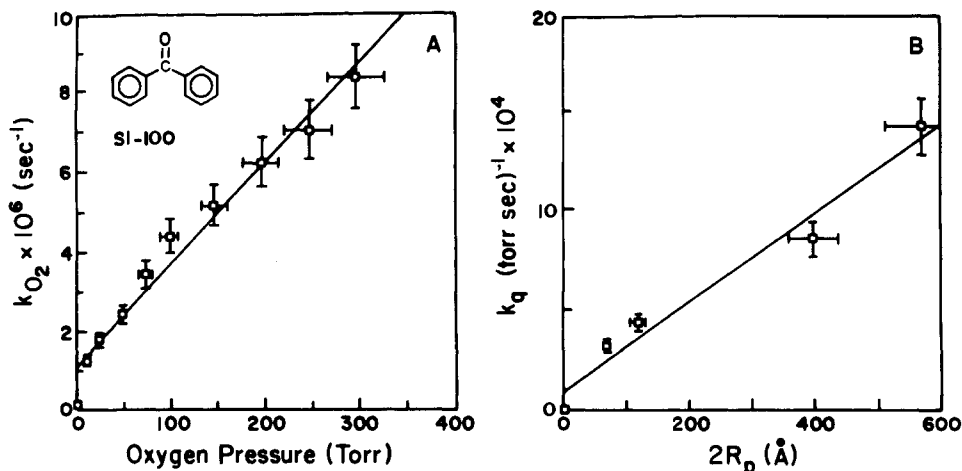
Figure 14. (A) Decay rate of benzophenone triplet adsorbed on Si-100 lichrospher silica at various pressures of oxygen and (B) bimolecular quenching rate of benzophenone triplet k_q vs the mean pore diameters for a series of lichrospher silicas at low surface coverage. θ_{BZP}: Si-100 = 3.15 × 10^4 mol/m^2; Si-300 = 4.37 × 10^4 mol/m^2, Si-500 = 6.63 × 10^4 mol/m^2, and Si-1000 = 7.00 × 10^4 mol/m^2. Reprinted from ref 126. Copyright 1988 American Chemical Society.
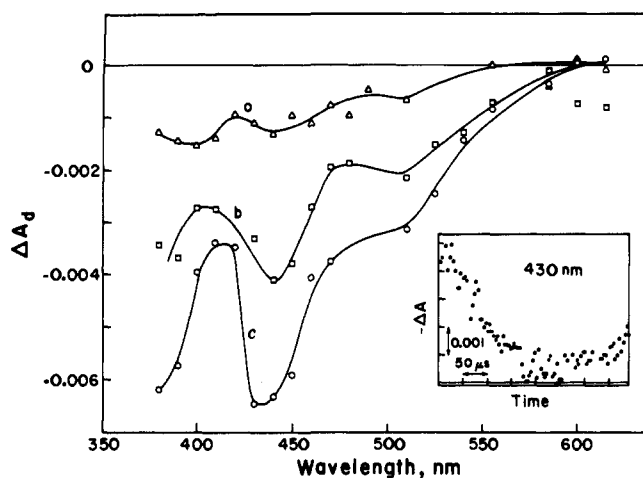

Figure 15. Time-resolved transient absorption spectra of air-equilibrated DPBF on TiO$_2$ recorded following 532-nm laser pulse excitation at (a) 1, (b) 27, and (c) 100 μs. Coverage corresponded to monolayer amounts (0.08 mmol of DPBF/g of TiO$_2$). Inset shows the bleaching growth corresponding to the reaction between singlet oxygen and ground-state DPBF. Reprinted from ref 41. Copyright 1992 American Chemical Society.

has been used to analyze the fast and slow component of triplet decay, and the results are summarized in Table II.

d. Photoionization

Photoionization of adsorbed molecules (e.g., conjugated hydrocarbons) has been carried out on insulators such as alumina.[91,122] Although the ionization potential of these adsorbed molecules is greater than 7.5 eV, laser pulses with energies of 3–4 eV are able to achieve photoionization. The photoionization on these surfaces is usually a biphotonic process and the role of surface is mainly to stabilize the cation radical. For example, active centers (e.g., Lewis acid sites) of the Al$_2$O$_3$ surface which have the ability to act as strong electron acceptors[182] facilitate the stabilization of the photoionization product. Diffuse reflectance laser flash photolysis has been extensively employed to characterize the cation radicals of pyrene and naphthalene,[91] diphenylpolyenes,[122] distyrylbenzenes,[122] and rose ben-

Table II. Quenching of Acetophenone Phosphorescence by Oxygen[a]

substrate	λ_{em} (nm)	k_q (s^{-1}) slow	k_q (s^{-1}) fast	% fast[b] quenching
acetophenone (20%)	254	1.6 × 10^4	~10^6	8
acetophenone (80%)	254	2.2 × 10^4	2.6 × 10^6	13
benzophenone	254/313	2.9 × 10^4	2.6 × 10^6	c
acetophenone/ valerophenone	254	<3 × 10^4	8 × 10^5	c
acetophenone/ 1-phenylhexane	254	6 × 10^3	8 × 10^5	30
	313	6 × 10^3	8.3 × 10^5	70
acetophenone/ 1-phenyl-3-pentanone	254	2 × 10^4	(1–3 × 10^5)	19
	313	2 × 10^4	3 × 10^5	45

[a] Compiled from ref 133. [b] Contribution of fast quenching to the total of quenching events. [c] Continuous variation does not allow a proper separation of the two components. Quenching is essentially complete for 1 atm of oxygen.

gal[39] on oxide surfaces. The photoionization promoted by Lewis acid sites on the alumina-coated silica particles is found to influence the decay kinetics and the emission yield of an anionic ruthenium(II) complex.[61]

Time-resolved diffuse reflectance transient absorption spectra recorded following the laser pulse (355 nm) excitation of o-, m-, and p-distyrylbenzenes (DSB) on surfaces of silica and alumina indicate short-lived triplet excited states and long-lived radical cations. The transient absorption spectra of cation radicals of o-, m-, and p-DSB are shown in Figure 16. Model calculations for one- and two-photon excitation processes give predictions that are in good agreement with the measurements of triplet excited state and radical cation production, respectively. The decay of the radical cation is nonexponential, with complete recovery taking place in minutes. This decay, which is independent of the coverages of adsorbate and the laser intensity, involves recombination of the originally produced radical cation–electron pair.

However in the case of rose bengal the photoionization was seen only on alumina and not on silica.[39] The transient spectra (Figure 17) recorded after 532-nm laser pulse excitation of rose bengal dye (RB) adsorbed on alumina surface show the formation of ^{3}RB* and radical cation RB$^{•+}$ in the degassed samples. Only the spectral features corresponding to RB$^{•+}$ are retained in air-
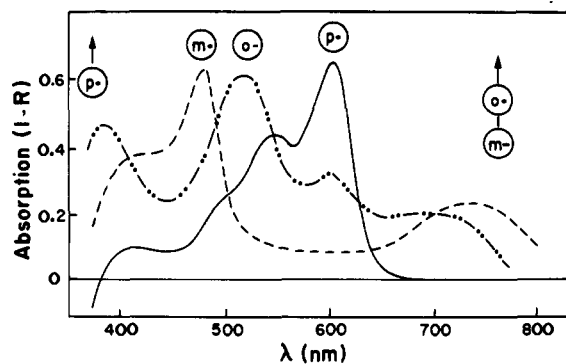
Figure 16. Diffuse reflectance transient absorption spectra of o-, m-, and p-DSB adsorbed on silica ($c = 7 \times 10^{-7}$ mol g^{-1}, T = 293 K), recorded with a 50-μs delay after laser pulse excitation at 354 nm. Reprinted from ref 122. Copyright 1988 American Chemical Society.
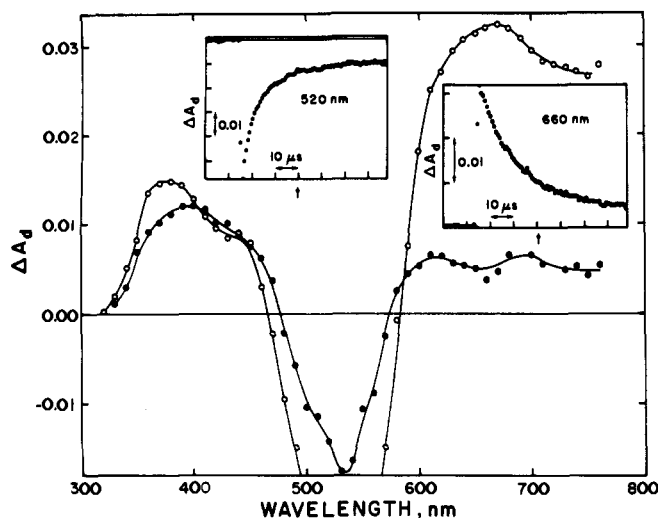

Figure 17. Transient absorption spectra of rose bengal dye on alumina (0.4 mg/g of Al$_2$O$_3$) recorded immediately after the 532-nm laser pulse excitation: (O) degassed and (●) air-equilibrated samples. (Inset show decay traces at 520 and 660 nm.) Reprinted from ref 39. Copyright 1989 American Chemical Society.

equilibrated samples. The dependence of RB$^{\bullet+}$ yield on the square of excitation intensity confirms that a biphotonic process is operative on the Al$_2$O$_3$ surface (reactions 11 and 12). The interaction between RB

$$RB + h\nu \rightarrow {}^1RB^* \rightarrow {}^3RB^* \qquad (11)$$

$${}^1RB^* \text{ (or } {}^3RB^*) + h\nu \rightarrow RB^{\bullet+} + e \qquad (12)$$
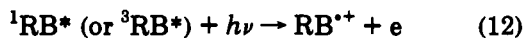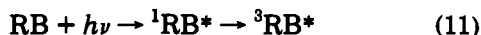
and the alumina surface plays an important role in promoting the photoionization process. This was evident from the dependence of RB$^{\bullet+}$ on the surface coverage of the dye. An increase in the RB$^{\bullet+}$ yield was seen with increasing RB surface coverage at submonolayer coverages. However, no increase in the RB$^{\bullet+}$ yield was seen at coverages greater than monolayer. Similar adsorbate-adsorbent interactions have also been highlighted in the study of diphenylpolyenes adsorbed on alumina.[122] Surface defects such as Al ions with tetrahedral coordination that have one or two coordinatively unsaturated sites (CUS) can act as electron acceptors and the energies of these unoccupied orbitals depend strongly on the distortion of the regular surface structure. Because of the high degree of hydroxylation
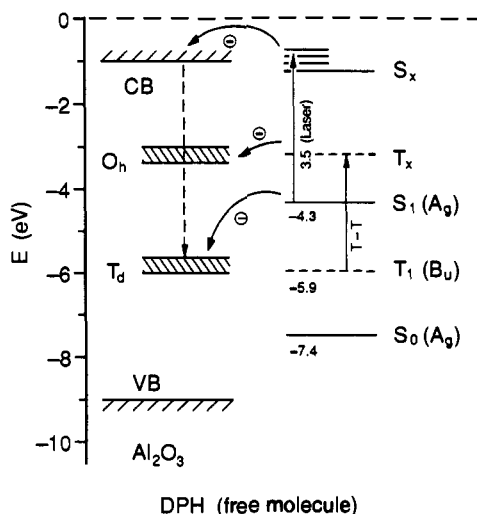

DPH (free molecule)

Figure 18. Energy level diagram of alumina showing the positions of the valence band (VB) and conduction band (CB) and including the approximate energies of the Al surface centers with T$_d$ and O$_h$ coordination. The energy levels of DPH relative to its ionization potential are also shown. Reprinted from ref 122. Copyright 1988 American Chemical Society.

of alumina surface very few adsorbate molecules are in direct contact with such CUS centers. However, the acceptor sites can be populated by electron tunneling, electron diffusion, or two photon excitation. It is also possible that the electron is taken up into the bulk of the alumina itself (Figure 18).

The quantum yield measurements of photoelectrons emitted from rhodamine B layers, which were adsorbed on cleaved faces of ionic crystals and on polished faces of amorphous quartz, have been used to estimate the effective densities of occupied dye states in a small energy range below the vacuum level.[114c]

e. Cis/Trans Isomerizations

Since the mobility of the adsorbed molecules is greatly restricted in the adsorbed state, the energy of adsorption acts as an additional barrier to rotation, vibration, or translation.[8] However, in many cases the absence of viscosity makes the reacting groups behave as if they were in vacuum. Many research groups have investigated the restrictions imposed by the surface adsorption on the excited state dynamics of the cis/trans isomerization process. Cis/trans photoisomerization of stilbene has been extensively studied in this regard.[69,183-185] It was demonstrated by Weis et al.[69] that the rate of cis → trans and trans → cis isomerization of stilbene on the silica surface is much slower than in cyclohexane.

Other cis/trans isomerization reactions studied include thioindigo on alumina,[186] thioindigo derivatives on silica,[187] and azo compounds on various oxides.[188-190] The adsorption on alumina from a solution containing trans- and cis-thioindigo was found to be stereospecific for the cis isomer.[186] While trans → cis isomerization was feasible under photoirradiation, cis-thioindigo was stable on the alumina surface and the isomerization could not be reversed. An inversion mechanism[191] has been proposed for the photoisomerization of trans-azobenzene which occurs on the surface at the same rate as in the solution phase. Along with the photoisomerization of trans-azobenzene, a fluorescent prod-
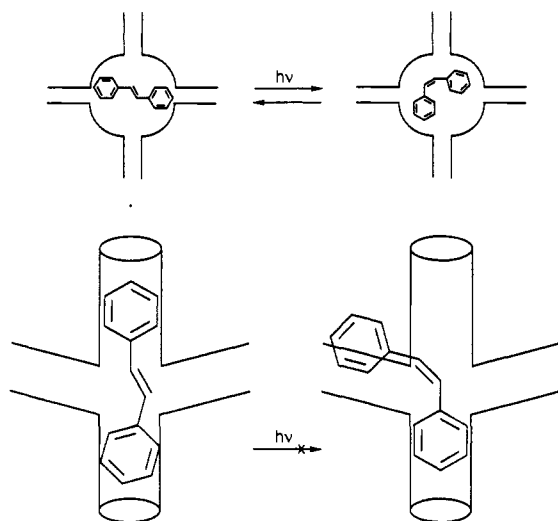
Figure 19. Inclusion of trans-stilbene in X type and in ZSM-5 zeolites. Required free volume for geometric isomerization is present in supercages of zeolite X and is absent in ZSM-5 channels. (V. Ramamurthy, private communication.)

uct 9,10-diazaphenanthrene is also formed due to ring closure. Similar ring-closure reactions have also been observed for trans-stilbene[183] and conjugated hydrocarbons[192] on alumina. Grutsch and Kutal[193] have shown the ability of an ionic transition-metal photosensitizer such as [Ir(bpy)₃OH]²⁺ adsorbed on silica to efficiently sensitize the valence isomerization of norbornadiene to quadricyclane. Takagi et al.[66] have observed high quantum yields of Ru(bpy)₃²⁺ sensitized cis → trans isomerization of N-methyl-4-β-styrylpyridinium in colloidal silica suspensions. Similarly Scaiano and his co-workers have demonstrated the use of silicalite (or dealuminized zeolite) in controlling the photostationary ratios in the sensitized cis/trans isomerization of stilbene.[194]

Ramamurthy et al.[184] have shown that a "tight fit" between the host (zeolite) and the guest (trans-stilbene) can result in marked selectivity of the included rotational conformers of trans-stilbene. Long-lived excited states from the flexible olefins have been observed in the faujasite and pentasil zeolites.[184,185] These two zeolites have different void space topologies with large spherical cages (diameter ~13 Å) for faujasite and only interconnecting channels (diameter ~5.5 Å) for pentasil. While both cis- and trans-stilbenes can be included into faujasites, only the latter was accommodated by pentasils (Figure 19). A similar difference in inclusion was noticed between trans,trans- and trans,-cis-diphenylbutadienes. The absence of photoisomerization indicated fully arrested rotation of trans isomers in pentasil while both trans and cis isomers underwent geometric isomerization inside the supercages of faujasites. These studies highlight the control of olefin photoisomerization with the void space topology of zeolites.

f. Intermolecular Electron-Transfer Processes

Achieving an efficient charge separation in a photochemical system is of great practical interest, especially in the area of conversion and storage of solar energy. Highly charged interfaces of oxides can be utilized to control the photoinduced electron-transfer reactions by regulating the relative reaction rates of
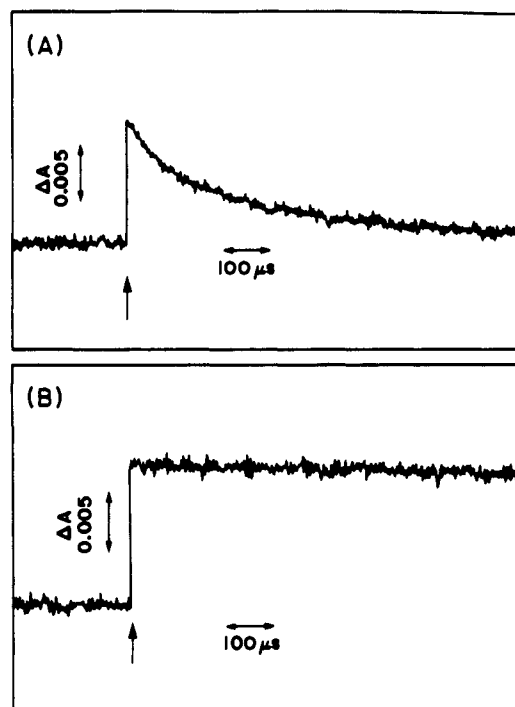

Figure 20. Transient absorption changes corresponding to the decay of PVS⁻ followed at 602 nm: (A) in homogeneous aqueous phase, pH 9.8; and (B) in a 0.2% SiO₂ colloidal suspension at pH 9.8. Concentrations of Ru(bpy)₃²⁺ and PVS⁰ were 36 μM and 4 mM, respectively. Reprinted from ref 138. Copyright 1981 American Chemical Society.

reactants and products. Either one or both of the reactants are strongly bound to the surface via electrostatic interaction. In the case of a photochemical system, Ru(bpy)₃²⁺, and a zwitterionic electron acceptor, propylviologensulfonate (PVS⁰), only positively charged Ru(bpy)₃²⁺ is bound to the negatively charged silica.[138] The photoinduced electron-transfer reaction is "uphill" by about 1.67 V. Therefore the back electron transfer

$$Ru(bpy)_3^{2+} + PVS^0 \rightarrow Ru(bpy)_3^{3+} + PVS^- \quad (13)$$

between the photoproducts is an exothermic process. In the homogeneous system the back electron transfer proceeds with a rate constant close to that of a diffusion-controlled process ($k = 7.9 \times 10^9$ M⁻¹ s⁻¹). However in SiO₂ suspension the back electron transfer is decreased by 2 orders of magnitude ($k = 5.7 \times 10^7$ M⁻¹ s⁻¹) as the reduced viologen (PVS⁻) is driven away from the negatively charged surface. The effect of SiO₂ in suppressing the back electron transfer is evident from the transient absorption decay of PVS⁻ shown in Figure 20. Thus, by controlling the surface charge, it is feasible to suppress back electron transfer process.

Efforts have also been made to study the photoinduced electron transfer between RuL₃⁴⁻ (L = bathophenanthroline disulfonate) and 2,2'-azinobis(3-ethylbenzothiazoline-6-sulfonate) (ABTS²⁻), which are electrostatically bound to positively charged alumina-coated silica particles suspended in water. Transient absorption spectra recorded after laser pulse excitation (532 nm) of solution containing RuL₃⁴⁻ and ABTS²⁻ in the presence and absence of SiO₂/Al₂O₃ particles are shown in Figure 21. The absorption bands at 415 and between 600 and 750 nm correspond to ABTS²⁻ and absorption band at 510 nm to RuL₃⁵⁻. The photo-
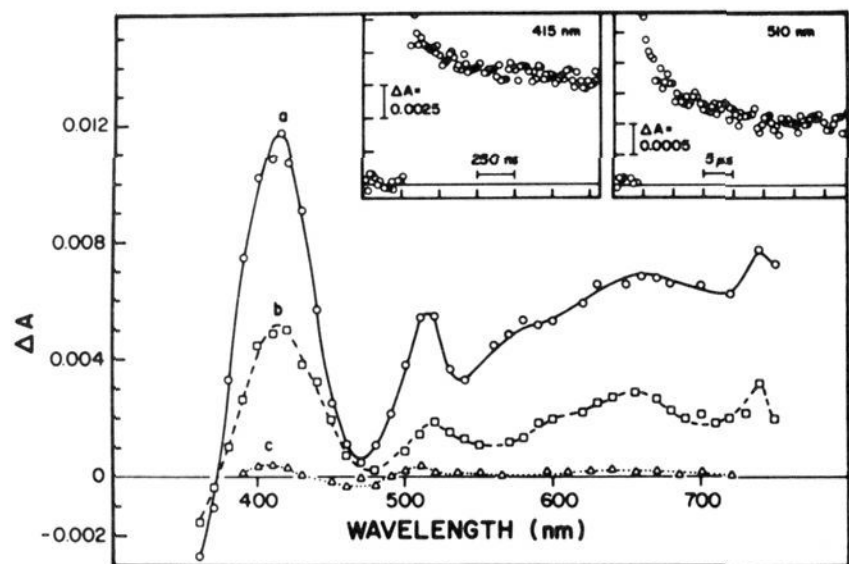
Figure 21. Transient difference absorption spectra obtained upon 532-nm laser pulse excitation of aqueous solutions of RuL_3^{4-} (40 μM) and $ABTS^{2-}$ (100 μM) with (spectra a and b) and without (spectrum c) SiO_2/Al_2O_3 particles (3.7 g/L). Spectrum a was obtained immediately and spectra b and c were recorded with a 25-μs delay. The insets show the kinetic traces recorded at 415 and 510 nm of the sample containing SiO_2/Al_2O_3 particles. Reprinted from ref 67. Copyright 1989 American Chemical Society.

chemical electron-transfer process is illustrated in reaction 14. The electron-transfer yield and quenching

$$(14)$$
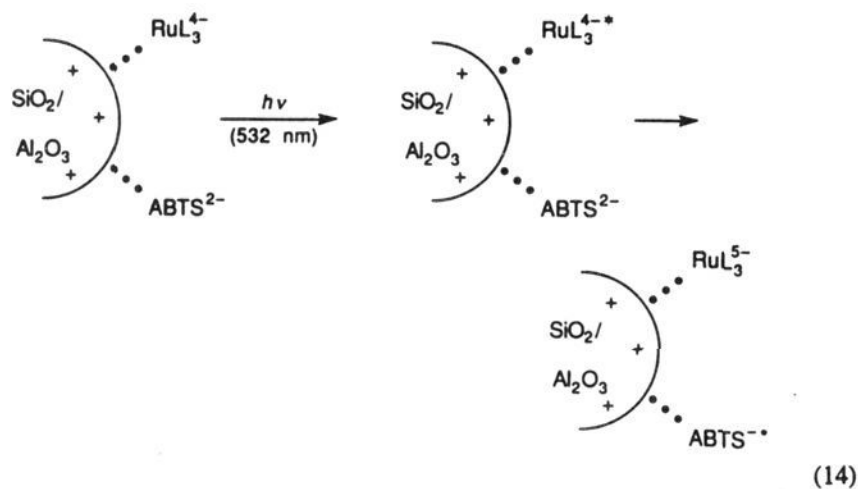
of RuL_3^{4-*} are strongly dependent on the concentration of SiO_2/Al_2O_3 colloids and are maximal when there is a monolayer coverage of reactants on the particles. The prompt formation of the electron transfer products (see inserts in Figure 21) shows the dominance of static over dynamic quenching on the SiO_2/Al_2O_3 particles presumably as a result of strong, localized interactions with the charged surface of SiO_2/Al_2O_3. Thus coadsorption onto colloidal SiO_2/Al_2O_3 particles greatly enhances the rate of electron transfer from $ABTS^{2-}$ to photoexcited RuL_3^{4-}. This enhancement is mainly due to high local concentration of the two species on the particle surface.

Size-exclusion and ion-exchange properties of zeolites have been used to promote light-driven vectorial transport in artificial photosynthetic systems.[195-200] Mallouk and his co-workers[197-200] have assembled sensitizer-electron acceptor/donor assemblies in zeolites (see, for example, Figure 22). Molecular electron transport chains composed of EDTA, zinc tetrakis(N-methyl-4-pyridyl)porphyrin (ZnTMPyP[4+]) and methyl viologen (MV[2+]), spatially organized by 1-mm-diameter zeolite L particles have been designed in this concentration.[197] Under visible light irradiation this compartmentalized, integrated system produces hydrogen from water via electron-transfer quenching of the excited porphyrin molecule. Spatial separation of the
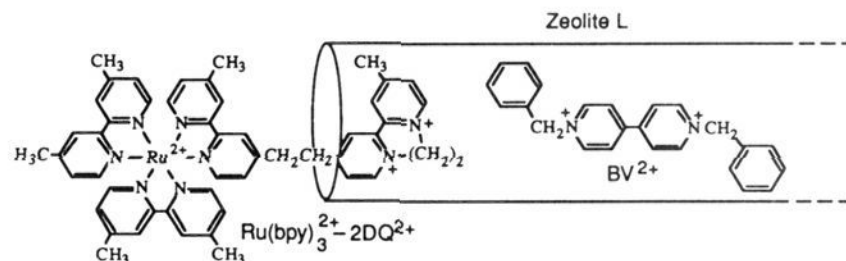

Figure 22. A zeolite-based compartmentalized photochemical system. (T. Mallouk, private communication.)
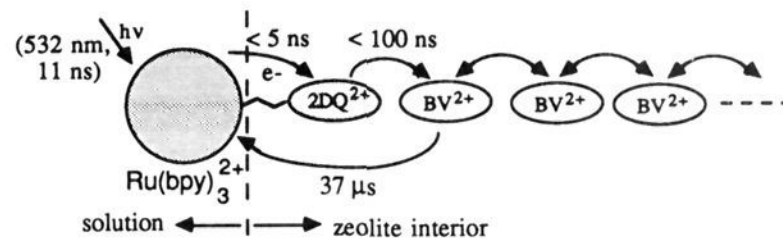

Figure 23. Possible molecular arrangement of donor–sensitizer–acceptor triad at the zeolite L/aqueous interface. Reprinted from ref 198. Copyright 1988 American Chemical Society.

hydrogen evolution catalyst and oxidized donor molecules facilitates the use of nonsacrificial donors in similar zeolite-based systems. In another study these researchers[200] have studied photoinduced electron-transfer reactions of $Ru(bpy)_3^{2+}$ and MV^{2+} ion-exchanged onto/into three different zeolites (L, Y, and mordenite). For large-pore L and Y zeolites, in which the photoredox pair $MV^{2+}/Ru(bpy)_3^{2+}$ is compartmentalized at the interface between the zeolite's interior volume and external surface, excited-state electron transfer is controlled by the diffusion of MV^{2+} within the zeolite channels. In both zeolites, unexpectedly high intrazeolite diffusion coefficients $\approx 10^{-7}$ cm^2 s^{-1} have been observed. The charge recombination kinetics was rather complex with a cage escape yield of 7–9%. In an earlier study, Dutta and Incavo[196] have succeeded in retarding the back electron transfer and stabilizing the electron-transfer products $Ru(bpy)_3^{3+}$ and MV^+ in zeolite supercages. It is likely that the size considerations play an important role in making the reactants reside in different cages and thus inhibit the back electron transfer. Long-lived charge separation has also been achieved in a self-assembling molecular triad at the zeolite/aqueous interface (Figure 23).[198] The diquat end of this molecule is small enough to fit through the 12-ring window of zeolite L or Y and is thought to protrude into the channel network leaving the size excluded Ru complex on the outside. Light-induced intramolecular electron transfer within the diad was rapid but the back electron transfer was slow. Ion-exchanged benzyl viologen (BV[2+]) further increased the lifetime of the charge-separated Ru^{3+}/BV^{*+} state to 37 μs.

Fluorescence quenching of pyrene by Cu^{2+} in zeolite X has been found to proceed via the Perrin electron-tunneling mechanism.[203] Photophysics and photochemistry of $Ru(bpy)_3^{2+}$ adsorbed into the layered solid zirconium phosphate sulfophenylphosphonate (ZrPS) has recently been investigated.[201,202] The quenching of $Ru(bpy)_3^{2+}$ by MV^{2+} occurs in ZrPS environment by dynamic and quasistatic quenching mechanisms. Similarly, electron-transfer reactions of reactants intercalated in clays have been studied by various research groups.[50,141,144,204]
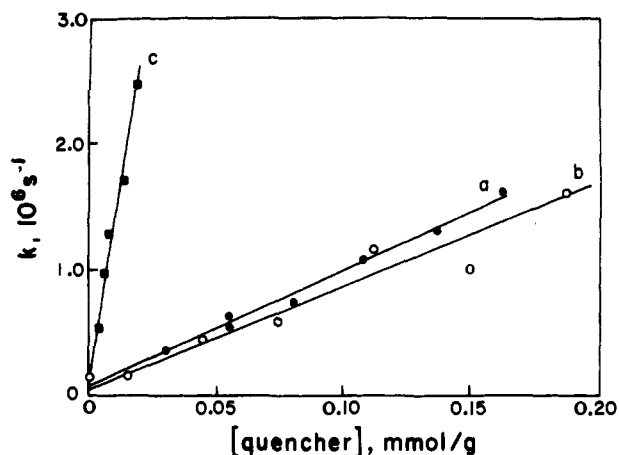
Figure 24. Plots of the rate constant for decay of triplet benzophenone on silica as a function of the concentration of the added quencher for (a) benzhydrol, (b) diphenylmethane, and (c) naphthalene. Reprinted from ref 206. Copyright 1991 American Chemical Society.

### g. Photochemistry of Other Organic Compounds

There have been several efforts to explore the novel effects imposed by the solid surfaces on the photochemical pathways by which many organic compounds undergo chemical changes. Since these aspects have been reviewed in many recent reviews,[4-7,205] only a brief account will be given here. On the basis of the dependence of photochemical behavior of ketones on the nature of silica surface, Turro and his co-workers have concluded that the silica surface consists of two major sites, one consisting of stronger binding sites (active silanol groups) and the other consisting of weaker binding sites (free silanol groups). The initial location of a ketone in one of the two binding sites is an important factor in controlling the product distribution on the silica surface. A similar effect of OH groups upon the excited states of alkyl ketones adsorbed on Vycor glass and their secondary radical processes on the surfaces has been investigated by IR spectroscopy.[5,10] The deactivation pathway involving surface OH-assisted photoenolization plays a significant role in determining the lifetime of the excited triplet state of ketone molecules adsorbed on Vycor glass by hydrogen bonding.

Johnston and her co-workers[206] have studied hydrogen abstraction by triplet benzophenone on the silica surface (reaction 15). The triplet decays with expo-

$$^3Ph_2CO^* + RH \rightarrow Ph_2{}^{\bullet}COH + R^{\bullet} \qquad (15)$$
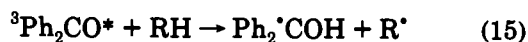
nential kinetics with rate constants that increase linearly with the hydrogen donor concentration (Figure 24). The rate constants for hydrogen abstraction (3.9×10^{14} and 4.4×10^{14} dm^2 mol^{-1} s^{-1} for diphenylmethane and benzhydrol, respectively) are 1 order of magnitude lower than that for energy transfer from triplet benzophenone to naphthalene. The ketyl radical formed on the silica surface decays slowly with a complex kinetics.

The photochemical behavior of a variety of ketones included in the hydrophobic zeolite, silicalite has been examined by Scaiano and his co-workers.[133,207,208] Diphenylmethyl radicals have been generated by 266-nm laser pulse excitation of 1,1,3,3-tetraphenylacetone adsorbed on silica gel as well as included in NaX, and silicalite zeolites (reaction 16).[208] Diphenylmethyl

$$Ph_2CHC(O)CHPh_2 \xrightarrow{h\nu}$$
$$Ph_2CH^{\bullet}CO + Ph_2{}^{\bullet}CH \rightarrow 2Ph_2{}^{\bullet}CH \qquad (16)$$
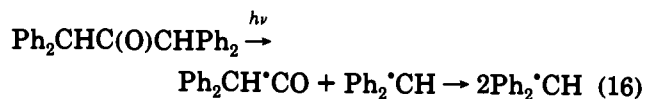
radicals exhibit a very wide range of lifetimes on these surfaces. This complex kinetic behavior has been explained on the basis of a wide range of possible sites or environments on the surface.

Although the "cage effect" introduced by the support material restricts the mobility and rotational and translational diffusion of the reactants (as well as primary and secondary photoproducts), the probability of certain encounters is greatly enhanced. The effect of surface adsorption on the dynamics of photolytically generated radical pairs has been investigated by several research groups (see for example refs 209–214). Baretz and Turro[95] have investigated the temperature and magnetic field effects on the photochemistry of the meso and d,l isomers of 2,4-diphenylpentan-3-one (DPP) in a variety of "super-cage" environments. Disproportionation of Ph$^{\bullet}$CHCH$_3$ radicals produced following the photolysis of DPP significantly increased in porous glass and silica environments.

Stable luminescent cations have been formed by adsorbing 9-phenylxanthen-9-ol on silica and alumina surfaces.[215] The observed luminescence has been attributed to the direct excitation of the cation as well as dehydroxylation of excited singlet of the starting material. The fluorescence of the cation ($\tau = 37 \pm 2$ ns) is readily quenched by oxygen with a rate constant of 1.5×10^4 Torr^{-1} s^{-1}.

IV. Photochemistry on Reactive Surfaces

During the past decade, the utilization of semiconductor particulate systems as a reactive heterogeneous medium has seen a tremendous growth in carrying out photochemical transformations of organic and inorganic compounds. By making use of the principles of photoelectrochemistry, semiconductor colloids, particles, and films have been employed in the conversion of light energy into electrical and chemical energy.[12-20] The application of semiconductor systems in initiating and controlling various photocatalytic processes has been reviewed recently by several researchers.[21-35,217-224]

Most of the studies reported to date focus on the development and characterization of novel photoelectrochemical systems composed of single crystal, polycrystalline and particulate semiconductors, as well as elucidation of the photophysical properties of the semiconductor colloids and the dynamics of the interfacial processes at the semiconductor–electrolyte interface.[29-34] One interesting development in this area is the development of 1–10-nm-size semiconductor clusters with hybrid molecular solid-state properties.[34] Various semiconductor colloids in this size regime have been synthesized to understand their behavior under optical excitation.

Under bandgap excitation semiconductor particles act as short-circuited microelectrodes and initiate the oxidation and reduction processes of the adsorbed substrate (Figure 25a). Alternatively an adsorbed molecule can inject charge from its excited state into the semiconductor particle and the oxidized form can then undergo transformation to give stable products. This process, which is commonly referred to as pho-
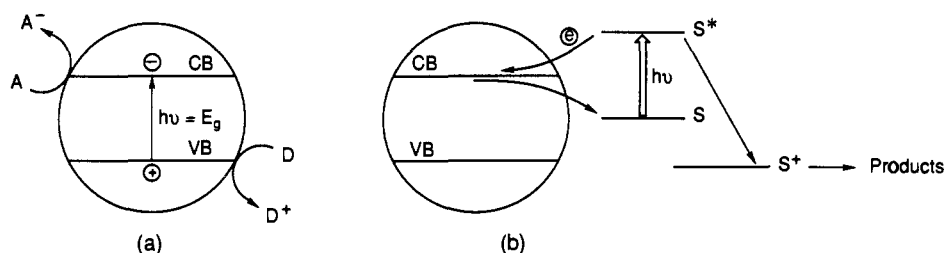
Figure 25. Charge transfer processes at a reactive semiconductor surface: (a) by direct bandgap excitation of the semiconductor and (b) by charge injection from excited state of the adsorbed molecule into the conduction band of the semiconductor.
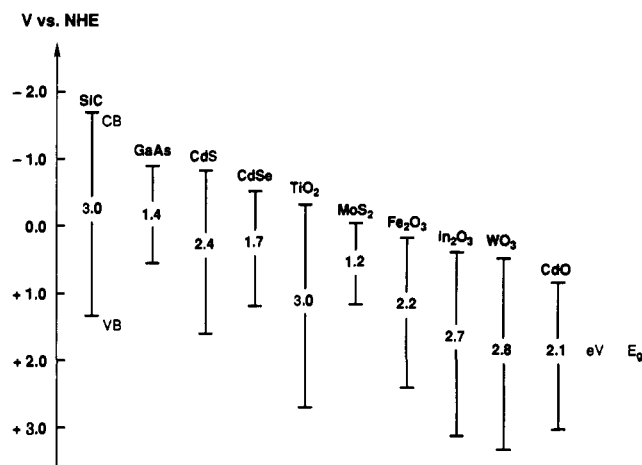
Figure 26. Bandgap energies and conduction and valence band energy levels of various semiconductors at pH 7.

tosensitization, is extensively used in photoelectrochemistry and imaging science. The principle of such a process is illustrated in Figure 25b. In the first case (Figure 25a) excitation of a reactive surface (e.g., semiconductor particle) is followed by its participation in the charge-transfer process with the adsorbed molecules. However in the second case (Figure 25b), the reactive surface acts as a quencher by accepting a charge from the excited molecule adsorbed on its surface. The energies of the conduction and valence bands of the semiconductor and redox potential of the adsorbed molecule control the reaction course of such surface photochemical reactions. The energy levels and bandgap energies of several semiconductors are shown in Figure 26. The photophysical and photochemical properties of submicron size semiconductor particles directly control the selectivity and charge-transfer efficiency of the reactive surface.

A. Properties of Colloidal Semicondcutors

a. Preparation and Characterization of Semiconductor Colloids in Homogeneous and Heterogeneous Media

Most of the semiconductor colloids studied to date are oxides and chalcogenides of various metals.[225-259] Usually the preparation involves precipitation of semiconductor colloid from homogeneous solution by controlled release of anions (or cations) or forced hydrolysis. For example, controlled mixing of a metal ion such as Cd^{2+} with sulfide ions yields small colloidal particles of metal sulfide.[226-232,255-259] Similarly, forced hydrolysis can be employed for the preparation of metal oxides such as TiO_2,[233-237] ZnO,[238-241] WO_3,[242] CdO, and In_2O_3.[243] The size and distribution of the colloidal particles can be controlled by varying the experimental parameters

such as concentration of reactants, reaction temperature, nature of stabilizer, and medium. Other methods of colloidal semiconductor synthesis include phase transformations (e.g., α-Fe_2O_3),[244-247] reaction in the vapor phase (e.g., TiO_2 and Si),[248,249] and dissolution of crystalline powders of layered semiconductors (e.g., MoS_2 and WS_2).[250] A radiolytic method has also been used recently in the preparation of MnO_2,[251] CdS,[252a] and silver halides.[253] The growth of semiconductor particles from molecule to crystal has been probed in these studies by pulse radiolysis. GaAs colloidal particles have been prepared by refluxing a solution of $((CH_3)_3Si)_3As$ and $GaCl_3$ in toluene[254a] and quinoline[254b] at high temperatures (216-237 °C). A new improved procedure to produce quantized GaAs particles has also been reported by Nozik and his co-workers.[254c]

Characterization of the semiconductor particles is usually carried out with absorption and emission spectroscopy,[222-224] TEM,[239,258] NMR,[260] EDS,[2361a] XRD,[261b] and STM[262] techniques. Structural analysis of molecular clusters of encapsulated PbS has been carried out with X-ray absorption spectroscopy.[263]

Efforts have also been made to prepare ultrasmall semiconductor particles in various heterogeneous environments. Microencagement of semiconductor particles in an organized medium controls not only the morphology but also the photocatalytic properties of the semiconductors. These include micelles,[264,265] vesicles,[266,267] bilayer membranes,[269,270] zeolites,[261,271-274] polymer films,[262,275-280] Langmuir-Blodgett films,[281-282] clays,[283,284] and silicate glasses.[285-289] Such preparations provide isolated small semiconductor particles which are stabilized in an organized medium. In most of these studies, CdS has been the popular choice since it can be prepared easily by chemical precipitation and characterized readily by its absorption and emission spectra.

The same method of arrested precipitation can be employed to prepare metal chalcogenides in other organized systems such as clays and zeolites. The methods of preparation of semiconductor clusters in various mimetic membranes have been well documented by Fendler.[31] Phenyl-capped CdSe particles[290] and tailored semiconductor-receptor systems in cyclodextrin[291] have also been prepared. Biosynthesis of CdS quantum clusters in yeasts has also been attempted.[292] The peptide-capped intracellular CdS particles (diameter ~20 Å) are found to be more monodisperse than CdS particles synthesized chemically.

b. Surface Modification of Semiconductor Particles

i. Deposition of Noble Metals. The selectivity and efficiency of a photoelectrochemical reaction can be improved by modifying the surface of the semiconductor
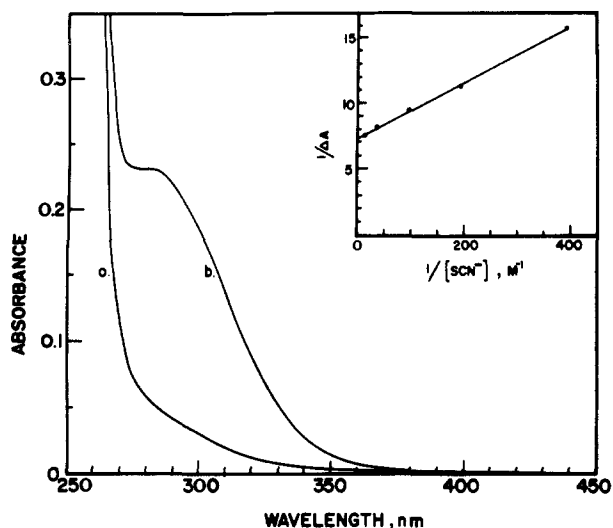
Figure 27. Absorption spectra of (a) 0.005 M SCN⁻ (vs acetonitrile as reference) and 0.005 M SCN⁻ and 28 μM TiO₂ (vs 28 μM TiO₂ in acetonitrile as reference). Insert shows the Benesi-Hildebrand plot for the determination of the apparent association constant for the association between TiO₂ and SCN⁻. Reprinted from ref 60. Copyright 1985 American Chemical Society.

Figure 28. Absorption spectra of ZnO particles in ethanol. Reprinted from ref 241. Copyright 1992 American Chemical Society.

particle with a suitable noble metal. For example, an order of magnitude enhancement in the efficiency of photocatalytic hydrogen production from water has been achieved upon platinization of semiconductor particles. The metal deposit on the semiconductor acts as a sink for the photogenerated electron and catalyzes the production of hydrogen. Platinization can be done by direct photoreduction of $PtCl_6^{2-}$ on the semiconductor particle,[293] stirring the suspensions of semiconductor colloids and platinum colloids together,[294-297] or grinding the two powders (semiconductor and Pt black) in an agate mortar.[298] Other noble metals and metal oxides (e.g., RuO_2) have also been deposited on semiconductor particles to improve the efficiency of the photocatalytic reactions.[299,300]

ii. Complexation with Redox Couples and Sensitizer. Redox species that strongly interact with a semiconductor surface are of great interest in improving the performance of photoelectrochemical activity of the semiconductor system.[301] Such interactions are also useful in controlling the size of the colloidal particle as observed for the colloidal CdS preparation in the presence of various thiols.[252,302-305] The interaction between the semiconductor surface and surface modifier alters their absorption characteristics. These spectral changes include displacement or broadening of the absorption bands, appearance of new charge transfer bands, and changes in the extinction coefficient of absorption. For example, surface complexation of TiO₂ colloid with SCN⁻ results in the appearance of a new absorption band at 285 nm (Figure 27).[60] The apparent association constant as determined by the Benesi–Hildebrand method is 350 M^{-1}. Similarly, complexation of TiO₂ colloids with $Fe(CN)_6^{4-}$,[306a] CdS colloids with ferrocene derivatives,[306b] and CdSe single-crystal surface with 7,7,8,8-tetracyanoquinodimethane[306c] has also been observed.

Semiconductor surface modification which involves attachment of a sensitizer molecule to extend the photoresponse of the large bandgap semiconductor has
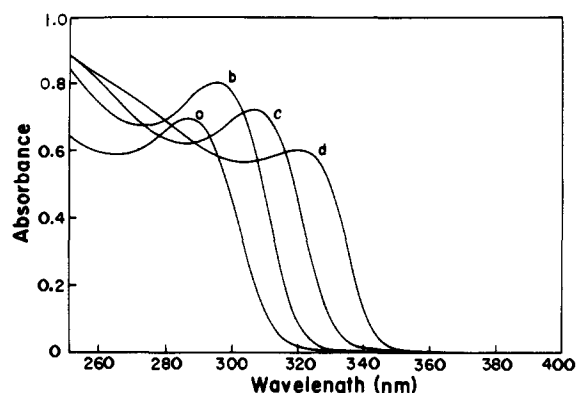
also been studied extensively. TiO₂ colloids have been modified with sensitizers such as squaraines,[55] erythrosin B,[307] eosin Y,[308-309] rose bengal,[310] anthracene-9-carboxylic acid,[56,57] chlorophyllin,[59] and zinc porphyrins.[311] The interaction between the semiconductor surface and the sensitizer can be probed with the electronic absorption and emission spectra of the sensitizer as the energetics of the ground and excited states are altered. For example, the absorption changes observed during the association of a squaraine dye with colloidal TiO₂ involved a red shift in the absorption maxima.[55] These spectral changes are shown in Figure 4. The values of association constants and the spectral changes observed during the surface modification of TiO₂ colloids with various dyes and redox couples are summarized in Table I.

c. Quantum Size Effects

Semiconductor particles which exhibit size-dependent optical and electronic properties are termed quantized particles (or Q particles) or semiconductor clusters. The particles with diameters ≥ 150 Å typically behave as bulk semiconductors. However, similarly prepared crystallites of 15–50-Å diameter which possess some bulk lattice structures differ considerably in electronic properties. These crystallites are molecular clusters in which complete electron delocalization has not yet occurred.

The experimental observation of the transformation from solid-state electronic properties of various semiconductors[312-327] has been the focus of many recent papers. The absorption spectra of ZnO colloids of various particle sizes are compared in Figure 28.[241] The onset of absorption for larger colloids closely matches the absorption edge of bulk ZnO. The absorption edge shifts to blue for smaller size particles as a result of increase in the effective bandgap.

Quantization in these ultrafine particles arises from the confinements of charge carriers in semiconductors with potential wells of small dimensions (less than the DeBroglie wavelength of the electrons and holes). Under these conditions the energy levels available for the electrons and holes in the conduction and valence bands become discrete. Brus,[315,316] Henglein,[319,320] and Friesner[314] and their co-workers[319,320] have modified the above quantum mechanical treatment to explain the various experimental results of wavelength threshold as a function of the diameter of CdS particles. The
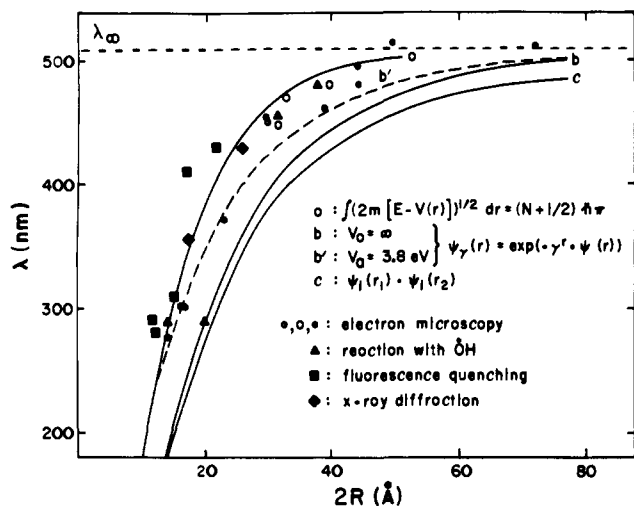
Figure 29. Wavelength $\lambda_{threshold}$ as a function of diameter, $2R$, of CdS particle; λ is the wavelength for macrocrystalline material. Points: experimental data. Curves: calculated fits. Reprinted from ref 320. Copyright 1986 Elsevier Science Publishers, B. V.

Figure 30. (A) Steady-state emission spectra of ZnO colloids in ethanol. The particle size of these colloids were (a) 20, (b) 30, and (c) 40 Å. (B) Time-resolved emission spectra of 1 mM ZnO colloids in ethanol. The spectra were recorded following the 355-nm laser pulse excitation of ZnO colloids at time intervals: (a) 0, (b) 7.6, (c) 26.6, and (d) 266 ns. Reprinted from ref 241. Copyright 1992 American Chemical Society.

comparison of various models and the experimental results are shown in Figure 29. The plot of wavelength of onset of absorption vs the function of particle diameter seems to agree well with the model proposed by Henglein and his co-workers.[319,320] The particle size dependence of other experimental data is also shown.

Quantum confinement can occur in one,[323] two,[328,329] or three dimensions.[330-344] Optical effects due to size quantization in layered-type semiconductors have also been reported.[250,326,345,346] The transition from molecular to crystalline aggregates of AgI and CdS has been probed by pulse radiolysis[252-253] and multichannel spectrophotometry.[347] In addition to its very large effects on optical properties, size quantization also leads to major changes in the effective redox potential of the photogenerated carriers.[325]

d. Emission Characteristics

i. Spectral Characteristics and Yields. Photoluminescence in semiconductors occurs when a photogenerated minority carrier recombines with a previously existing majority carrier. Considerable attention has been given in recent years to the emission of various semiconductor colloids: ZnO,[238-241] ZnS,[231,348] CdS,[305,349-353,355] and CdSe.[289,353] The measurements give valuable information regarding the nature of surface states and the recombination of charge carriers.

The emission spectra of ZnO colloids recorded under steady-state irradiation and laser pulse excitation are shown in Figure 30, parts a and b, respectively. Under steady-state irradiation conditions, these colloids exhibit green emission with a maximum dependent on the particle size. With laser pulse excitation a new band at 380 nm corresponding to the excitonic emission can also be observed. This short-lived excitonic emission is seen only when a high concentration of charge carriers is attained with laser excitations.

Enhancement in the emission yield has been achieved by modifying the colloidal CdS surface with triethylamine and mercaptoethylamine[305] or by activation of the surface with Ag$_2$S or Cd^{2+} ions.[357,358] Similarly, addition of unsaturated hydrocarbons such as 1-C$_4$H$_8$

and C$_2$H$_5$C$\equiv$CH onto the TiO$_2$ catalyst enhanced the luminescence intensity of the semiconductor.[359] Surface defects which promote radiationless recombination of the charge carriers can be blocked upon such modifications.

Charge transfer to an adsorbed substrate usually results in the decrease of the emission yield of the semiconductor colloid. The quenching phenomenon provides an interfacial charge transfer process. It has been shown that viologen compounds or thiazine dyes can efficiently quench the emission of CdS colloids, and by using Poisson statistics, one can determine the number of molecules aggregated in the CdS colloid.[230,265,350,352] However, in the case of ZnO colloid, hole scavengers such as I$^-$ or SCN$^-$ quenched its green emission as they interacted with the surface anionic vacancies.[241]

ii. Emission Lifetimes. The analysis of luminescence decay gives important information regarding kinetic and mechanistic details of charge carrier recombination in colloidal semiconductors. The decay profiles of CdS emission at different wavelengths are shown in Figure 31. A distribution of excited states emitting with different lifetimes and a substantial overlap of emission spectra were noted in these experiments.[353] The shorter-lived states were found to emit at higher energy. Similar wavelength dependence of emission lifetime has been observed for ZnO,[241] ZnS,[318] and CdSe,[289] colloids. The wavelength dependence of the emission lifetime arises from the contribution of the Coulombic

Figure 31. Time dependence and biexponential fits to the luminescence decay of the 22-Å clusters at 10 K, as a function of wavelength. Reprinted from ref 333. Copyright 1986 American Chemical Society.

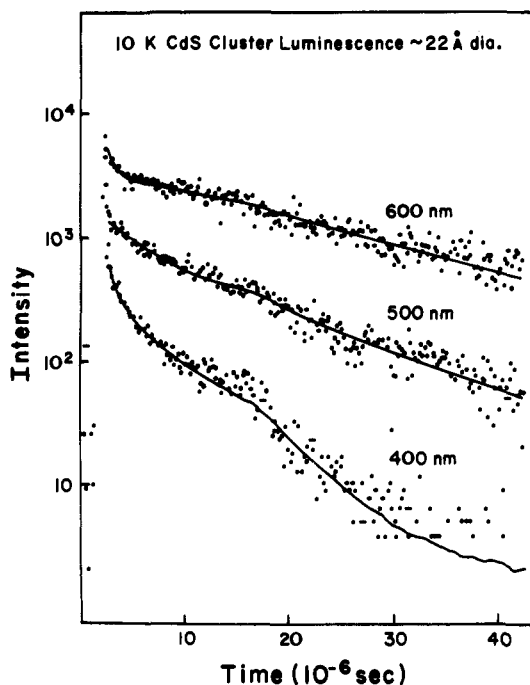energy of interaction of the electron–hole pair to the total energy of the emitted photon[333]

$$h\nu = E_x - (D_+ - D_-) + e^2/\epsilon R \tag{17}$$

where D_+ and D_- are the trap depths for the electron and hole separated by a distance R measured with respect to the lowest delocalized state, E_x. E_x, D_+, and D_- depend upon particle diameter. In a purely radiative tunneling decay, close pairs with a small separating distance, R, emit faster and at higher energy than distant pairs for a fixed particle diameter. The distribution of tunneling distance R was found to be independent of cluster size.

A decrease in the emission lifetime of semiconductor colloids is observed when an electron acceptor[318] or a surface modifier[303] is adsorbed onto the semiconductor surface. The average emission lifetime of CdS colloids in acetonitrile at 640 nm decreased from 156 to 26 ns when the semiconductor surface was modified with the diethyldithiocarbamate anion.[303] A decrease in the emission lifetime observed upon adsorption of Cu^{2+}, I_3^-, and S^{2-} ions on a CdS surface has been explained on the basis of increased surface recombination velocity.[380] On the other hand surface complexation of CdS colloids with mercaptoethylamine leads to the enhancement in the emission lifetimes.[305]

e. Nonlinear Optical Properties

Recently, small semiconductor particles as materials for generating nonlinear optical effects have drawn the attention of many researchers. Commercially available CdS_xSe_{1-x} glasses (with particles of diameter 100–1000 Å) have already been investigated in this context (see, for example, refs 362 and 363). Photoinduced blue shifts in the absorption have also been reported for the colloids of CdS,[230,361,364-372] Cd_3P_2,[373] In_2S_3,[259] PbS,[324] CdSe,[289,374,375] In_2Se_3[258] Se,[376] TiO_2,[236] and ZnO.[377] Such
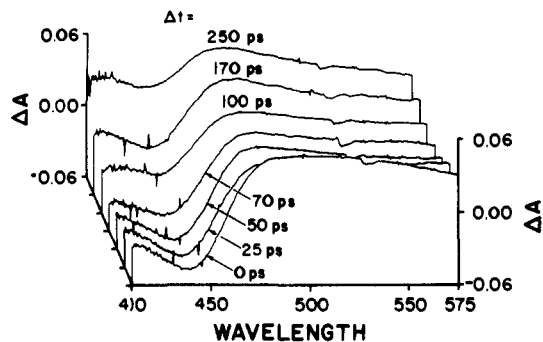

Figure 32. Transient photobleaching of CdS colloids. ΔA vs wavelength recorded at different times following the 355-nm laser pulse excitation (pulse width 18 ps). Reprinted from ref 361. Copyright 1989 American Chemical Society.

photoinduced blue shifts appear as bleaching in the transient absorption spectrum.

Figure 32 shows the change in the absorbance as a function of wavelength at various times following a 355-nm laser pulse excitation of CdS colloids in acetonitrile. The transient absorption spectra exhibit strong bleaching at wavelengths below 500 nm. The bleaching appears within the laser pulse duration of 18 ps and exhibits multiexponential decay with time constants ranging into the nanosecond regime. The origin of this photoinduced blue-shift has been attributed to different mechanisms which included (1) band filling due to excess conduction band electrons or dynamic Burstein-Moss effect,[378-382] (2) a decrease in the oscillator strength of the excitonic transitions due to trapped electrons and holes,[384-366] (3) increase in excitonic energy due to surface-trapped electrons,[369,370] and (4) Coulombic screening by photogenerated free carriers.[380]

f. Trapping of Charge Carriers

Colloidal semiconductor particles contain a high density of defect sites, usually at the semiconductor surface, and the nature of these defect sites depends strongly on the method of chemical synthesis. Upon optical excitation, the free carriers are rapidly trapped at the defect sites and these trapped charge carriers further undergo radiative and radiationless recombination. For example, the lack of direct recombination emission and the observation of strong red emission in CdS colloids show the dominant role of the sulfur vacancies in the trapping of photogenerated charge carriers.

i. Photochemical Changes Associated with Trapping of Electrons. By selectively scavenging the photogenerated holes in a semiconductor colloid, it is possible to monitor the behavior of trapped electrons. EPR studies of photoexcited anatase TiO_2 particles have shown that the photogenerated electrons are trapped at Ti^{4+} sites within the bulk[383] (reactions 18a and b).

$$TiO_2 + h\nu \rightarrow TiO_2 (e_{CB}^- + h_{VB}^+) \tag{18a}$$

$$e_{CB}^- \rightarrow e_t^- \tag{18b}$$
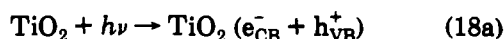
Rothenberger et al.[384] have time-resolved the transient absorption due to trapped electron in colloidal TiO_2 and interpreted their results based on a stochastic kinetic model. As can be seen from Figure 33, the absorption spectrum of the trapped electron appears
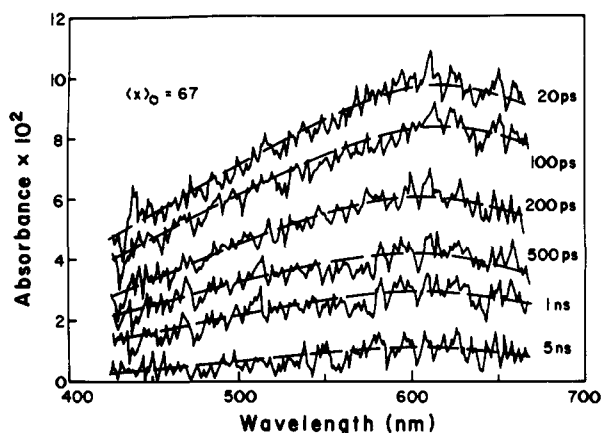
Figure 33. Trapped electrons in TiO_2 colloids. Transient absorption spectra observed at various time intervals after laser pulse excitation of aqueous colloidal TiO_2 (17 g/L, pH 2.7) deaerated with Ar. Average number of electron–hole pairs present initially in one TiO_2 particle is 67. Reprinted from ref 384. Copyright 1985 American Chemical Society.

within the leading edge of the 30-ps laser pulse. The rate constant for the recombination between trapped electrons and holes was determined to be 3.2 (±1.4) × 10^{-11} cm^3 s^{-1}. The effect of hole scavengers in extending the lifetime of the trapped electron in colloidal TiO_2 has also been demonstrated recently.[385] Electron-trapping process has been shown to control the electrochromic and photoelectrochromic properties of WO_3 colloids.[242b]

Similarly, trapped electrons in colloidal metal chalcogenides such as CdS undergo chemical changes by reacting with Cd^{2+} sites. Unfortunately the chemical changes associated with this process cannot be detected from the absorption in the visible region. However, the formation of Cd^0 has been indirectly confirmed in the steady-state photolysis of CdS.[386] Such an accumulation of charges in the minute reaction space of a semiconductor colloid is important in improving the efficiency of interfacial redox reactions.

It is to be noted that high intensity laser pulse excitation of small semiconductor particles can lead to the emission of electrons. This multiphoton process has been studied by monitoring the absorption of hydrated electrons and the holes trapped at the semiconductor surface. Colloidal semiconductors of CdS,[370] Cd_3P_2,[373] and ZnO[377] have been investigated to characterize the chemical effects associated with the photoelectron emission from the semiconductor.

ii. Photochemical Changes Associated with Trapping of Holes. The basic hydroxide groups at the surface of TiO_2 can be considered deep traps for valence band holes. The chemical identity of the trapped hole is considered to be an O^- radical anion at the TiO_2 surface.[234,383] The process of hole trapping in colloidal TiO_2 has been considered to be slower than the trapping of electrons and requires ~250 ns to complete.[384] While the majority of these trapped holes recombine with conduction band and trapped electrons, a small fraction of O^- undergoes dimerization at the surface to form stable titanium peroxide.

The chemical changes associated with trapping of charge carriers in CdS and CdSe have been time-resolved recently.[375,387] The time-resolved transient absorption spectra recorded after 355-nm laser pulse

Figure 34. Formation of S^-_{surf}. Transient absorption spectra recorded at different time intervals following the 355-nm laser pulse ex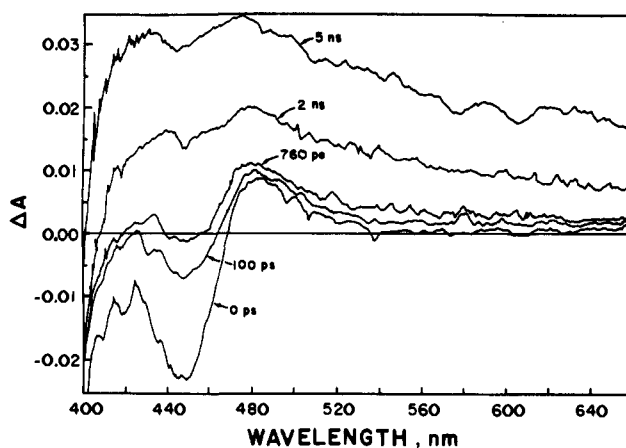citation (pulse width 18 ps) of 0.2 mM colloidal CdS in acetonitrile. Reprinted from ref 387. Copyright 1989 Elsevier Science Publishers, B. V.

excitation of CdS colloids are shown in Figure 34. The observed growth in the absorption at wavelengths greater than 460 nm is attributed to the formation of $S^{•-}$ at the CdS surface (reaction 19), the identity of which had been confirmed earlier by pulse radiolysis measurements.[388] A high quantum yield (ϕ = 0.77) of

$$(CdS)_n + h_t^+ \rightarrow [(CdS)_{n-1}Cd^{2+}S^-_{surf}] \qquad (19)$$
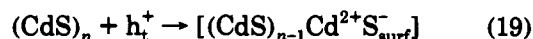
S^-_{surf} formation indicates that a majority of the photogenerated holes are trapped at the CdS surface. The pseudo-first-order kinetic analysis indicates the rate constant for the formation of S^-_{surf} in CdS colloids to be 5 × 10^8 s^{-1} and Se^-_{surf} in CdSe colloids to be 1.1 × 10^8 s^{-1}. The recombination coefficient of electron–hole pairs in CdS particles has been determined to be (9 ± 4) × 10^{-11} cm^3 s^{-1} by Nosaka and Fox.[389] Kumar et al.[390] have also observed annihilation of S^-_{surf} to yield S_2^{2-} (or $S + S^{2-}$).

The doping of semiconductors with transition metal ions such as Fe(III) leads to the drastic retardation of the electron–hole recombination rate.[391] Formation of substitutional Fe(III) on Ti(IV) lattice sites leads to the trapping of valence band holes while the charge-compensating oxygen vacancies scavenge conduction band electrons. As a result, the trapped charge carriers survive for a long period of time.

B. Charge-Transfer Processes In Colloidal Semiconductor Systems

The principle of electron and hole transfer at the photoexcited semiconductor particle has already been described in Figure 25a. Both free and trapped charge carriers participate in these interfacial redox processes. By decreasing the particle size, it is possible to shift the conduction band to more negative potentials and the valence band to more positive potentials as a result of quantization effects. Hence, redox processes that cannot occur in bulk materials can be facilitated in quantized semiconductor particles. Fast kinetic spectroscopy techniques such as laser flash photolysis and pulse radiolysis are found to be useful in elucidating the interfacial charge-transfer dynamics in colloidal semiconductor systems. Other techniques such as
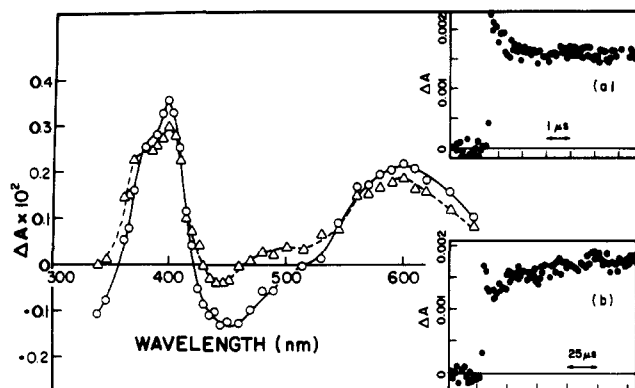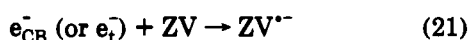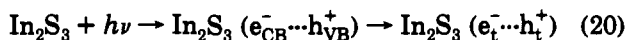
Figure 35. Reduction of zwitterionic viologen in colloidal In$_2$S$_3$ suspension. Time-resolved difference absorption recorded following 355-nm laser pulse excitation of a 0.1 mM colloidal suspension In$_2$S$_3$ containing 4 mM ZV in Ar-saturated 14/86 v/v% water/acetonitrile. The spectra were recorded (O) immediately after and ($\triangle$) at 7 μs after the laser pulse excitation. Absorption–time profiles are shown in the inserts. Reprinted from ref 259. Copyright 1988 American Chemical Society.

microwave absorption,[310,392] transient grating,[393] EPR,[383] diffuse reflectance,[38–41,120–123,394] and resonance Raman spectroscopy[395] have also been employed.

a. Reduction with Photoexcited Semiconductor Particles

i. Mechanistic and Kinetic Aspects of Electron Transfer. Several organic compounds have been extensively used by several researchers to investigate the factors that control electron transfer at the semiconductor colloid. Both picosecond[384,387,396–400] and nanosecond[229,230,234,235,388,401–408] laser flash photolysis have been employed to time resolve the heterogeneous electron-transfer process. For example, the transient absorption spectra in Figure 35 shows the reduction of a zwitterionic viologen, ZV, in a colloidal In$_2$S$_3$ suspension. The transient absorption with maxima around 395 and 600 nm was attributed to the reduced product, ZV$^{•-}$ (reaction 20 and 21). Picosecond laser flash

$$In_2S_3 + h\nu \rightarrow In_2S_3 \, (e^-_{CB}\cdots h^+_{VB}) \rightarrow In_2S_3 \, (e^-_t\cdots h^+_t) \quad (20)$$

$$e^-_{CB} \, (or \, e^-_t) + ZV \rightarrow ZV^{•-} \quad (21)$$

photolysis of the CdS-ZV system has indicated the risetime of ZV$^{•-}$ formation to be less than 20 ps. Therefore, the rate constant for the interfacial electron transfer should be greater than 5×10^{10} s^{-1}. This estimate is in good agreement with the value ($k = 2 \times 10^8$ to 5×10^{10} s^{-1}) proposed by Rosetti and Brus in their picosecond resonance Raman experiments.[395] Such a large value of the rate constant indicates a rapid interfacial electron transfer from the photoexcited CdS to the adsorbed viologen. Strong adsorbate–adsorbent interaction is essential to carry out the reduction process.

A major fraction of ZV$^{•-}$ decays within 500 ps as a result of its reaction with trapped holes (or S$^-_{surf}$). A fraction of ZV$^{•-}$ survives as it diffuses away from the surface (see inserts in Figure 35). Negatively charged Nafion, which is used to stabilize the colloids, drives ZV$^{•-}$ away from the particle surface by electrostatic
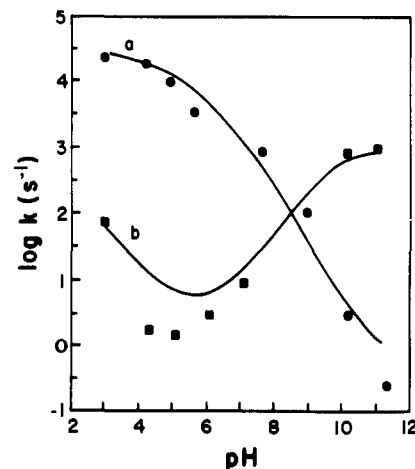

Figure 36. Calculated rate constants (solid line) based on the electrophoretic data are compared with the experimental results for the electron transfer between iron(III) oxide colloids and (a) ZV$^-$ ($\bullet$) and (b) MV$^+$ ($\blacksquare$). Reprinted from ref 247. Copyright 1988 American Chemical Society.

repulsion. The role of ionic charge of the polymeric stabilizer in influencing the rate of heterogeneous electron transfer has been studied recently.[407,408] The influence of electrostatic interaction on the stabilization of viologen radical in negatively charged SiO$_2$[138,410] and TiO$_2$-coated SiO$_2$[410] colloidal systems and in micellar systems[411] has also been discussed. The dimerization of MV$^{•+}$ has been noted in some experiments.[397,400] The desirable experimental conditions for efficient reduction on a semiconductor particle have been discussed by Gerischer.[412] A large increase in reduction efficiency can be achieved by locally contacting the particles with suitable metals, due to the formation of an accumulation layer at this contact. The reduction process is quite efficient when the acceptor molecule is adsorbed on the semiconductor particle. In a few cases dynamic electron transfer has also been reported (e.g., reduction of tetranitromethane[402] and methyl viologen[229,413] in aqueous TiO$_2$ solvents).

Albery et al.[414] have proposed a general model which considered a Gaussian distribution of the logarithm of the rate constant about some mean and the width of distribution as an additional parameter. In the case of colloidal semiconductors, the dispersion in the kinetic transients is caused by the dispersion in the radii. A good agreement for the radial dispersion between the value found from dynamic light scattering and the value found from kinetic analysis has been demonstrated for colloidal semiconductor systems.

However, Darwent and his co-workers[406] and Meisel and his co-workers[247] have shown that the potential distribution around colloidal oxides coupled with the charge of the reducing species could significantly affect the rate of electron transfer to and from the colloid. Figure 36 shows good agreement between the calculated rate constants based on electrophoretic data and the experimentally obtained rate constant for the electron transfer between ZV$^{•-}$ (or MV$^{•+}$) and iron(III) oxide colloids at various pH. The manipulation of the surface potential by control of pH and ionic strength can improve the efficiency of charge transfer process. The discrete range of particle sizes in a colloidal semiconductor system leads to a multiexponential kinetic
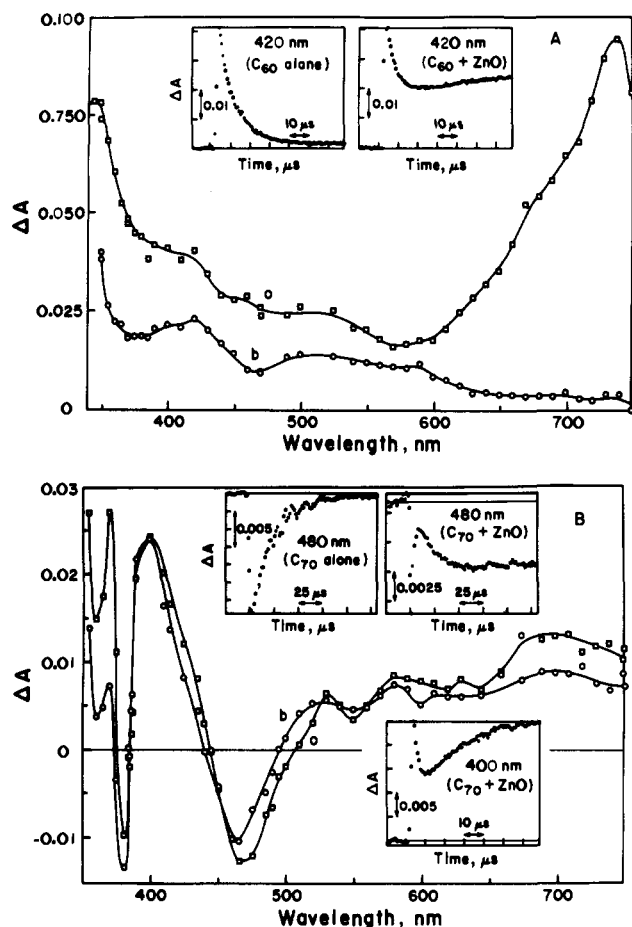
Figure 37. Time-resolved difference absorption spectra recorded following 308-nm laser pulse excitation of a 5 mM ZnO colloidal suspension containing (A) C_{60} and (B) C_{70} in 50/50 (v/v %) benzene–ethanol. The concentration of fullerene was kept around 30 μM. The spectra were recorded at (a; $\square$) 1 μs and (b, O) 65 μs after the laser pulse excitation. Examples of absorption–time profiles at different monitoring wavelengths (see inserts) show the formation of fullerene anion only in the presence of ZnO. Reprinted from ref 403. Copyright 1991 American Chemical Society.

behavior for the heterogeneous electron transfer since k_{et} is dependent on the particle size.

ii. Quantum Efficiency of Reduction. Laser flash photolysis techniques have also been used to probe the reduction of organic dyes such as thiazine, oxazine, phenazine, squaraine, and methyl orange in various colloidal semiconductors: TiO_2,[12-16,403,404,415-417,420] CdS,[230,415,418] In_2S_3,[259] and In_2Se_3.[419] Bandgap excitation of the semiconductor leads to one-electron reduction of the dye to yield semireduced dye, which then disproportionates to yield a two-electron reduction product (leuco dye). Multielectron transfer on a single semiconductor particle is not so commonly observed. Recently, one-electron reduction of fullerenes (C_{60} and C_{70}) has also been carried out in colloidal ZnO suspension.[403] Figure 37 shows the absorption spectra of triplet excited states (short-time spectra) and radical anions (long-time spectra) of C_{60} and C_{70} after 355-nm laser pulse excitation of a ZnO colloidal suspension containing the respective fullerene. The anion is formed as a result of direct reduction of fullerene at the excited ZnO surface. The triplet excited states of fullerenes were observed as a result of simultaneous excitation of fullerenes along with ZnO colloids. The values of

Table III. Photocatalytic Reduction in Colloidal Semiconductor Systems

semi-conductor	substrate	E° (A/A$^-$) (V vs NHE)	K_a	ϕ	ref
TiO_2	methyl viologen	−0.44		1.0	229
				0.35	402
	phenosafranin	0.25	2.1	0.05	415
	thionine	0.064	29.0	0.10	58
	methylene blue	0.01	7.2	0.06	404
	oxazine 725	−0.02	5.2	0.05	404
	nile blue A	−0.10	14.3	0.03	404
	tetranitromethane			0.17	402
WO_3	oxazine 725	−0.02		0.5	242b
CdS	methyl viologen	−0.44		0.6	229
	phenosafranin	0.25		0.02	415
	methylene blue	0.01	0.7	0.08	230
	oxazine 725	−0.02	1.5	0.05	230
	nile blue A	−0.10	3.0	0.04	230
CdSe	zwitterionic viologen	−0.44	4.3	0.1	374
In_2S_3	zwitterionic viologen	−0.44	30.0	0.07	419
	oxazine 725	−0.02	1.5	0.04	419
	nile blue A	−0.10	2.7	0.02	419
In_2Se_3	zwitterionic viologen	−0.44		0.01	419
CdS/TiO_2	methyl viologen	0.44		0.95	437

$$ZnO(e) + C_{60} \text{ (or } C_{70}) \rightarrow ZnO + C_{60}{}^- \text{ (or } C_{70}{}^-) \quad (22)$$
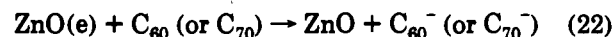
quantum yield of reduction and equilibrium constant (K_a) for the association between the semiconductor and the electron acceptors for various colloidal semiconductor systems are summarized in Table III. The quantum yield of reduction is dependent both on K_a and on the energetics of the semiconductor conduction band and the redox couple. The difference between the semiconductor conduction band and the reduction potential of the redox couple ($\Delta E = E_{CB} - E^\circ_{D/D^-}$) acts as a driving force for the heterogeneous electron transfer at the semiconductor colloid.

Electron transfer reactions of semiconductor colloids have also been investigated in other media such as micellar solutions, vesicles, BLMs, polymer films and zeolites. There have been several studies which address the topic of generating H_2 from water by utilizing a relay compound such as methyl viologen. This topic, by itself, has become another major aspect of semiconductor-assisted photocatalysis, the details of which can be found in earlier review articles.[12,31,217,219]

b. Oxidation with Photoexcited Semiconductor Particles

Photogenerated holes can be utilized to oxidize substrates at the semiconductor surface. The holes trapped at the TiO_2 surface can survive for a duration of microseconds to milliseconds[234,384] and can react with OH$^-$ to generate OH$^\bullet$ radicals in aqueous medium. These OH$^\bullet$ radicals can also participate in the oxidation process. One of the initial studies of the oxidative process involves laser flash photolysis of the colloidal TiO_2/thiocyanate system.[229] The oxidation product $(SCN)_2{}^{\bullet-}$ was characterized from its absorbance at 480 nm. The formation of $(SCN)_2{}^{\bullet-}$ was completed within

$$h_{VB}^+ \text{ (or } h_t^+) + SCN^- \rightarrow SCN^\bullet \xrightarrow{(SCN^-)} (SCN)_2{}^{\bullet-} \quad (23)$$
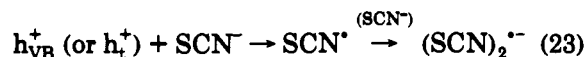
the laser pulse duration as a result of the association

Table IV. Photocatalytic Oxidation in Colloidal Semiconductor Systems

semi-conductor	sub-strate	$E°(X_2^{--}/2X^-)$ (V vs NHE)	K_a $(10^4 M^{-1})$	ϕ	ref(s)
TiO$_2$	SCN$^-$	1.3	350	0.04	60
	I$^-$	1.0		0.8	421
	Br$^-$	1.7		0.16	422
	Cl$^-$	2.3		0.08	421
CdS	Et$_2$NCS$_2^-$	0.05	1900, 170	0.28	303,387
In$_2$S$_3$	I$^-$	1.0		0.15	259, 419
In$_2$Se$_3$	I$^-$	1.0		0.03	419
ZnO	SCN$^-$	1.3		0.035	241b
ZnO/ZnS	SCN$^-$	1.3		0.09	241b
ZnO/ZnSe	SCN$^-$	1.3		0.32	241a

of SCN$^-$ with TiO$_2$.[305] Scavenging of holes by SCN$^-$ had a marked effect on the reduction of tetranitromethane[402] and oxazine dyes[305] in the TiO$_2$ colloidal system. Simultaneous capture of holes and electrons at the TiO$_2$ surface with suitable scavengers enhanced the efficiency of interfacial charge transfer by a factor of 2.

Similarly, oxidation of halide ions was investigated in various colloidal semiconductor suspensions by laser flash photolysis.[230,259,402,421] The quantum yields of various oxidation processes are summarized in Table IV. The energetics of the semiconductor valence band and the oxidation potential of the redox couple influence the photocatalytic oxidation.[402,421] For example, the enhancement in the efficiency of halide oxidation at TiO$_2$ follows the sequence Cl$^-$ < Br$^-$ < I$^-$, correlating with the decrease in the oxidation potential. By decreasing the pH it is possible to shift the valence band of TiO$_2$ to more positive potentials, and thus to enhance the quantum efficiency of halide oxidation.

The oxidation of diethyldithiocarbamate anion (NCEt$_2$S$_2^-$) in colloidal CdS suspension has been investigated[303,375,387] to resolve the kinetic components of reactions of valence band and trapped holes (reactions 24 and 25).

$$h_{VB}^+ + Et_2NCS_2^- \rightarrow Et_2NCS_2^• \qquad (24)$$

$$h_t^+ + Et_2NCS_2^- \rightarrow Et_2NCS_2^• \qquad (25)$$

The formation of Et$_2$NCS$_2^•$ following the laser pulse excitation of CdS colloids can be monitored from its absorption band at 600 nm (Figure 38). The rate constants for these two processes, reactions 24 and 25, are estimated to be >5 × 10^{10} s^{-1} and ~10^{10} s^{-1}, respectively. Only a small fraction (~15%) of NCEt$_2$S$_2^•$ decayed during the time period of 1 ns, probably by reacting with trapped electrons, and the rest undergoes dimerization as it diffuses away from the CdS surface (k = 4.6 × 10^9 M^{-1} s^{-1}).[303]

The oxidation of several other organic compounds such as 2-propanol,[404,422] cystein,[423] and methyl orange[417] has also been investigated. The oxidation of N$_3^-$ to N$_3^•$ radical in CdS and ZnO suspension has been investigated by the ESR spin-trapping technique using phenyl-tert-butylnitrone (PBN) as a spin trap.[424] Draper and Fox[394] have employed diffuse reflectance laser flash photolysis to elucidate the mechanism of oxidation of several inorganic and organic compounds in TiO$_2$ particulate systems.

Charge-transfer processes of various colloidal semiconductors with radiolytically generated reducing spe-
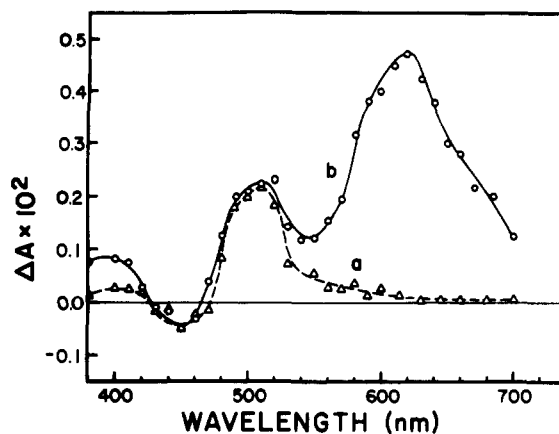

Figure 38. Formation of Et$_2$NCS$_2$ in colloidal CdS suspension. Transient absorption spectra recorded immediately after the 355-nm laser pulse excitation of 0.2 mM colloidal CdS in acetonitrile containing (a) no Et$_2$NCS$_2^-$ and (b) 2.5 mM Et$_2$NCS$_2^-$. Reprinted from ref 303. Copyright 1989 American Chemical Society.

cies such as hydrated electrons, COO$^{•-}$, (CH$_3$)$_2$CO$^•$H, or oxidizing species such as OH$^•$, (SCN)$_2^{•-}$, I$_2^{•-}$, Br$_2^{•-}$, or Cl$_2^{•-}$ radicals have been investigated by various researchers.[247,261,325,386,388,425-435] These studies are useful in understanding the behavior of trapped charge carriers and the optical and chemical effects caused as a result of charge trapping.

c. Photocorrosion of Semiconductor Surfaces

Trapped charge carriers, if not quickly scavenged with a suitable redox couple, can induce irreversible chemical changes at the semiconductor surface. Characterization of photochemical events that lead to the corrosion of the semiconductor is important for improving the photostability of the colloidal semiconductor system. Photocorrosion processes in the metal sulfides and selenides have been investigated by several research groups.[228,258,399,430,432-435]

Photolysis and pulse radiolysis experiments have been carried out to demonstrate the dependence of semiconductor corrosion on the size of the colloid.[325,341,354,433] Enhanced photoredox chemistry of quantized particles has a pronounced effect on the photocorrosion process. Because of the increase in the effective bandgap, the band edges of the quantized semiconductor particle attain new positions relative to the cathodic and anodic corrosion potentials. Cathodic and anodic corrosion processes in extremely small particles are energetically favored when the conduction band moves above the cathodic corrosion potential and the valence band below the anodic corrosion potential, respectively.

d. Coupled Semiconductors

An interesting approach for achieving a better charge separation in semiconductor particulate systems involves coupling of two semiconductor colloids with different energy levels. For example, in a colloidal CdS/TiO$_2$ system a photogenerated electron can be injected from CdS into a TiO$_2$ particle while the holes remain in the CdS particle (Figure 39). The difference in the energy levels of the two semiconductor systems plays an important role in achieving such a charge separation. The feasibility of sensitizing the large bandgap semi-
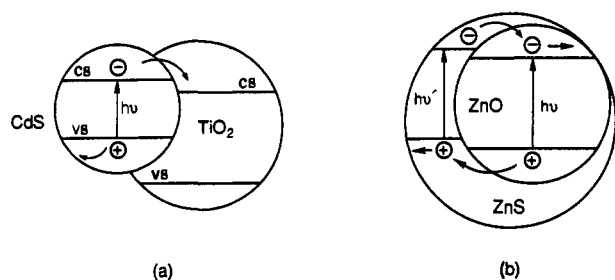
Figure 39. Schematic diagram representing the interaction between two semiconductor colloids: (a) CdS/TiO$_2$ and (b) ZnO/CdSe coupled semiconductor systems. Reprinted from ref 241. Copyright 1992 American Chemical Society.
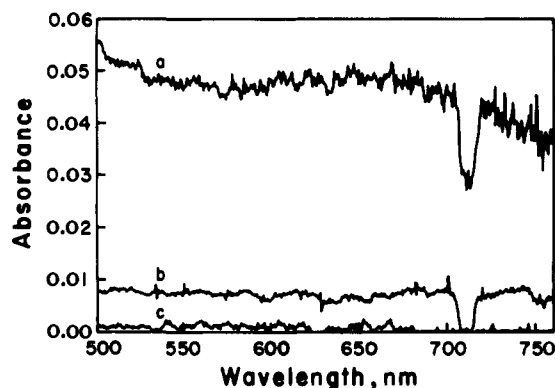

Figure 40. Transient absorption spectra recorded immediately after the 355-nm laser pulse (pulse width 18 ps) excitation of colloidal suspension containing (a) CdS (0.75 mM)/TiO$_2$ (1.5 mM), (b) CdS alone (0.75 mM), and (c) TiO$_2$ alone (1.5 mM). Reprinted from ref 440. Copyright 1990 American Chemical Society.

conductor ZnO with a deposit of CdS film has been demonstrated by Gerischer and Lübke.[436]

These coupled semiconductor systems have been referred to as "sandwich structures" in the past.[437,438] Enhanced yields of H$_2$ from the reduction of H$_2$S has been observed in the CdS particulate system upon addition of TiO$_2$ powder.[439] Recently, charge-transfer processes in several mixed colloidal semiconductor systems, CdS/TiO$_2$,[385,437,440,441] CdS/ZnO,[437,442] CdS/AgI,[440] Cd$_3$P$_2$/TiO$_2$ and Cd$_3$P$_2$/ZnO,[438] ZnO/ZnS,[443] ZnO/ZnSe,[241] and AgI/Ag$_2$S[444] have been reported.

The charge injection process in a coupled semiconductor system has been further demonstrated by carrying out methyl viologen reduction at the TiO$_2$ semiconductor particle, but with excitation of CdS semiconductor in the CdS/TiO$_2$ system.[437] The efficient quenching of CdS emission and high quantum yield for reduction of MV^{2+} in the presence of colloidal TiO$_2$ indicates an efficient charge injection process with a quantum efficiency of 100%. The electron injection into ZnO has been found to be less efficient and occurs only in the case of Q-CdS particles. Similarly, enhanced efficiency of SCN$^-$ oxidation has been observed in ZnO/ZnSe and ZnO/ZnS coupled semiconductor systems (Table IV).

The primary photochemical events associated with charge separation in the CdS/TiO$_2$ system can be probed with transient absorption measurements.[440] The transient absorption spectra recorded immediately after the laser pulse excitation of CdS in a CdS/TiO$_2$ system are shown in Figure 40. The broad absorption in the region of 500–760 nm is similar to the one shown in

Figure 33 and corresponds to the charge trapped at the Ti^{4+} site of TiO$_2$ colloid. This transient formation is completed within the laser pulse duration of 18 ps. This suggests that the rate constant for the charge injection process is $>5 \times 10^{10}$ s^{-1}.

The improved charge separation in coupled semiconductor also enhances the process of hole trapping and this process can be followed by monitoring the absorbance of S$^-_{surf}$. As a result of improved hole trapping efficiency an increase in the photoanodic corrosion has been observed in aerated suspensions of the CdS/TiO$_2$ system.[432] However, by using a suitable redox couple it is possible to suppress the photoanodic corrosion and carry out a useful oxidation process. The photocatalytic applications of coupled semiconductor systems have yet to be explored. But it is evident that the rectification properties of these coupled semiconductor systems are attractive enough to lead us to explore their feasibility in designing molecular devices and integrated chemical systems for solar energy conversion. The use of coupled particles in improving the performance of semiconductor electrodes has been demonstrated recently.[441,442]

e. Phototransformations of Organic Compounds

Early contributions in the area of organic phototransformations came from Bard and his co-workers.[445–449] Photocatalytic processes such as the photo-Kolbe reaction and amino acid synthesis have been performed with platinized TiO$_2$ under bandgap excitation. Heterogeneous photocatalysis has also been employed in the polymerization of methyl methacrylate and 1-vinylpyrene.[449–454] DeMayo and his co-workers[455–457] have reported CdS powder mediated cis–trans isomerization of several derivatives of styrene. The conversion of cis to trans isomer proceeds via the olefin radical cation intermediate which is formed at the photoexcited CdS surface. The role of various semiconductors in initiating and controlling organic reactivity has been explored by several research workers. Such transformations on photoexcited semiconductor surfaces include oxidation of olefins, arenes, alkanes, amines and alcohols, alcohols, cycloadditions and retrocycloadditions, and geometric isomerizations. Various developments in this area have been reviewed recently by Fox.[21–24,458,459]

f. Photocatalytic Degradation of Chemical Contaminants

Semiconductor particulate systems can provide a cheap and convenient way of treating several undesirable chemicals. The principle of such a treatment lies in initiating an oxidation or reduction process at the semiconductor surface. Addition of other reactants can drive the secondary chemical reactions to yield a desirable product.

For example, H$_2$S, which is a byproduct in the coal and petroleum industry, can be oxidized to S at the CdS semiconductor surface.[460] A quantum yield of ~50% has been reported for the reaction between sulfide anions and photogenerated valence band holes in CdS suspensions. The oxidation of S^{2-} and HS$^-$ in colloidal In$_2$S$_3$ suspension has been demonstrated by laser flash photolysis.[259] Loading of CdS particles with RuO$_2$ enhances the efficiency of H$_2$S cleavage.[460–464]
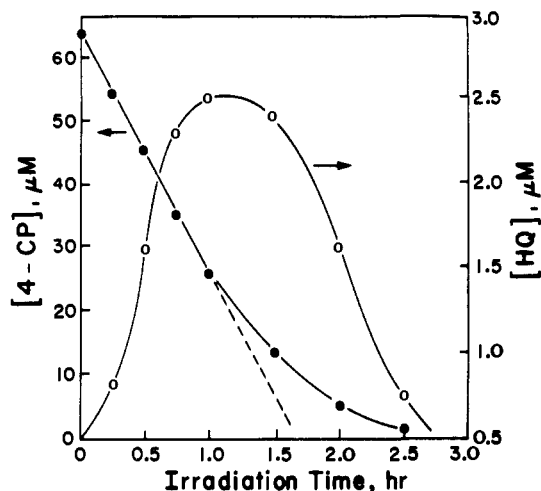
Figure 41. Degradation of 4-CP (●) and the formation and degradation of HQ (O) as a function of irradiation time. Initial [4-CP] = 63 μM. Other conditions are as follows: initial pH, 5.85; flow rate, 250 mL min^{-1}; temperature, 30 $\pm$ 2 °C. Reprinted from ref 478b. Copyright 1989 American Chemical Society.

Addition of sulfite also facilitates the H_2S cleavage process by removing S from this surface to generate a desirable product, thiosulfate.[461-463] In a similar way,

$$S + SO_3{}^{2-} \rightarrow S_2O_3{}^{2-} \qquad (26)$$
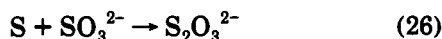
the photocatalytic transformation of CN^- to SCN^- has been carried out in Rh-loaded CdS particulate systems.[465]

Photoassisted catalytic degradation of organic materials such as hydrocarbons,[466] haloaromatics,[467-471] phenols,[472] halogenated biphenyls,[473] chlorinated organics,[474] surfactants,[475] and diethylnitrophenyl phosphate[476] in TiO_2 suspensions has been carried out. For example, complete mineralization of chlorophenols into CO_2 and HCl can be achieved upon bandgap excitation of the semiconductor with sunlight for a few hours. The photodegradation of chlorophenols has been the topic of many recent investigations. Figure 41 illustrates one such example of photodegradation of 4-chlorophenol in a TiO_2 suspension. The above cited references are only a few representative examples. For further details, readers are advised to refer to recent reviews in this area.[27-29,477]

While many studies have addressed the kinetic details of photocatalytic processes,[466,477,478] efforts are still being made to establish the reaction mechanism controlling the mineralization of chlorophenol and other aromatics. Most of the mechanistic studies suggest the hydroxyl free radical (formed as a result of hole scavenging by OH^- at the TiO_2 surface) as the primary charge-transfer intermediate (see for example ref 478) and consider the essential role of oxygen[479] to be electron scavenging. Some recent studies have questioned this approach.[480-482] For example, Draper and Fox[394b] failed to detect any of the expected intermediate OH adducts of the aromatics on the TiO_2 surface. A recent FTIR study (Figure 42) shows direct evidence for the formation of hydroquinone during the UV photolysis of dry TiO_2 powder on which 4-chlorophenol was chemisorbed. Further studies in this area are essential to establish
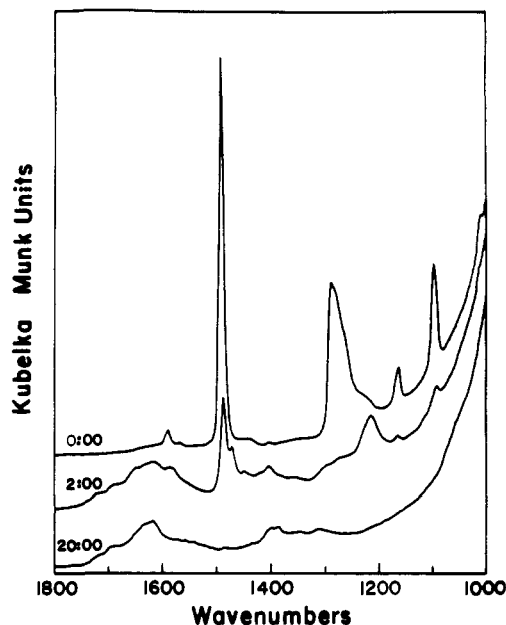
Figure 42. Diffuse reflectance FTIR spectra recorded during the photodegradation of 4-chlorophenol adsorbed on TiO_2. The samples were analyzed following the UV irradiation for (a) 0, (b) 2, and (c) 20 h. Spectrum a corresponds to the chemisorbed chlorophenol, spectrum b corresponds to the reaction intermediates (e.g., hydroquinone), and spectrum c shows the disappearance of organic molecules bound to the TiO_2 surface. Reprinted from ref 482. Copyright 1992 Elsevier Science Publishers, B. V.
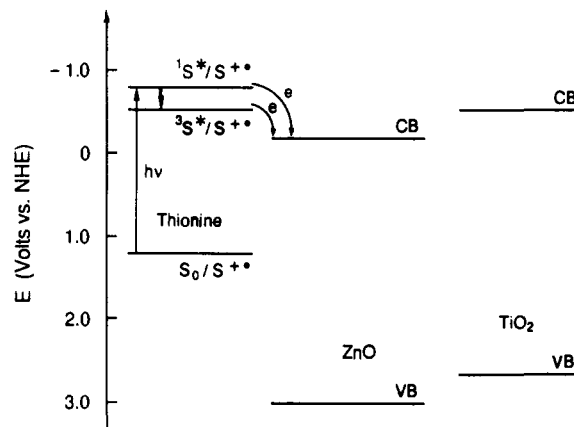
Figure 43. Schematic diagram illustrating participation of singlet and triplet excited states of a sensitizer (thionine) in injecting electrons into the conduction band of a large bandgap semiconductor (TiO_2 and ZnO). Reprinted from ref 498. Copyright 1992 American Chemical Society.

a unified mechanism for the TiO_2-assisted degradation of organic compounds.

V. Reactive Surface as a Quencher

As indicated in Figure 25b, the semiconductor support materials are capable of interacting with the excited state of the adsorbed molecules (sensitizers). This process, which is referred to as photosensitization, is associated with the process of charge injection from the excited state into the conduction band of the semiconductor.[483-487] The energy-level diagram which describes the participation of singlet and triplet excited states in the charge injection process is illustrated in Figure 43. Spectroscopic techniques such as emission,[57,59,307,308,496] nanosecond[308,311] and picosecond[55,488-490]
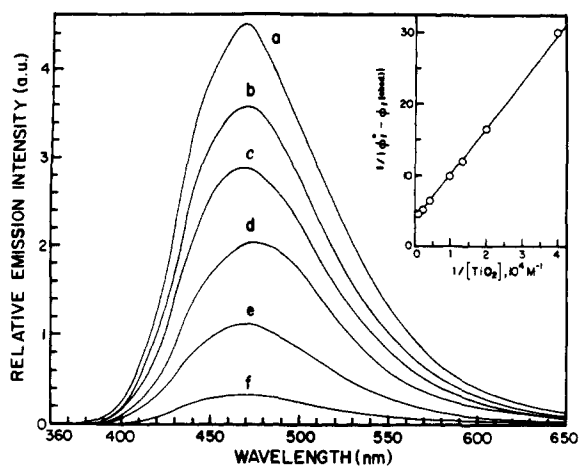
Figure 44. Fluorescence emission spectra of 20 mM anthracene-9-carboxylic acid in acetonitrile at various concentrations of TiO_2: (a) 0, (b) 0.05, (c) 0.1, (d) 0.25, (e) 0.5, and (f) 1 mM. The excitation wavelength was at 355 nm, and the spectra were corrected for the photomultiplier response. Insert shows the dependence of $1/(\Phi°_f - \Phi_f(obsd))$ on the reciprocal concentration of TiO_2 (see eq 28 for details). Reprinted from ref 57. Copyright 1989 American Chemical Society.

laser flash photolysis, diffuse reflectance laser flash photolysis,[38-41] microwave absorption,[310,491] and internal reflection flash photolysis[492] have been employed to investigate the interaction between an excited sensitizer and the reactive semiconductor surface. The mechanistic and kinetic information gathered from these studies will be discussed.

Dyes such as erythrosin B,[307] eosin,[308,309] rose bengal,[39,310] rhodamine B,[43,493-495] cresyl violet,[496] thionine,[497,498] chlorophyllin,[59] anthracene-9-carboxylate,[57,490] porphyrins,[311,499] phthalocyanines,[500] carbocyanines,[501,502] $Ru(bpy)_3^{2+}$ and its analogues,[466,503-507] and phenylfluorone,[508] which have high extinction coefficients in the visible, are often employed to extend the photoresponse of the semiconductor in the photoelectrochemical systems. One of the important criteria for achieving efficient excited-state quenching is to adsorb these dyes on the semiconductor surface with an electrostatic, hydrophobic, or chemical interaction. The interaction between the sensitizer and the semiconductor surface can be probed with the electronic absorption and emission spectra of the sensitizer as the energetics of its ground and excited states are altered. One such example has been demonstrated in the case of the squaraine dye/TiO_2 system (Figure 4).

A. Excited-State Quenching by the Semiconductor Colloids

The quenching of singlet excited sensitizer by a colloidal semiconductor such as TiO_2 is probed by measuring the emission yield and emission lifetime measurements. For example, the quenching of the excited singlet of anthracene-9-carboxylic acid by colloidal TiO_2 is shown in Figure 44. As indicated by these and other studies,[55,307,308,310,311] the quenching mechanism involves electron injection from the excited singlet of the sensitizer into the conduction band of the semiconductor. However, in the case of the eosin/TiO_2 system, it has been shown that self-quenching can also contribute to the decrease in the emission yield at high dye coverages.[308]
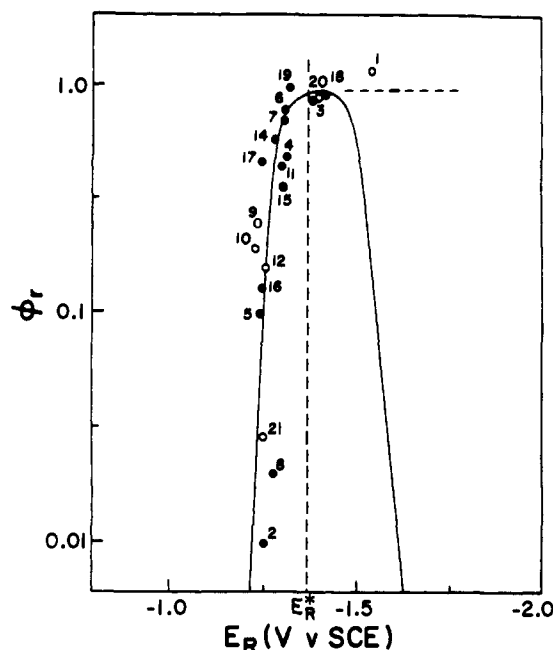

Figure 45. Dependence of Φ_{et} on the electrochemical reduction potential of the sensitizing dye. The solid curve is derived from Marcus theory (see ref 509 for experimental details). Reprinted from ref 57. Copyright 1989 American Chemical Society.

The quenching data have been treated by considering an equilibrium between the associated and unassociated dye with an apparent association constant K_{app}.[57,59] The observed fluorescence quantum yield, $\phi_f(obsd)$, of the sensitizer in colloidal TiO_2 can then be related to the fluorescence yields of unadsorbed ($\phi°_f$) and adsorbed (ϕ'_f) sensitizer molecules by

$$\phi_f(obsd) = (1 - \alpha)\ \phi°_f + \alpha\phi'_f \qquad (27)$$

where α is the degree of association between the semiconductor and sensitizer. At relatively high semiconductor colloid (e.g., TiO_2) concentrations, α can be equated to $(K_{app}[TiO_2])/(1 - K_{app}[TiO_2])$ and eq 27 can be simplified to

$$\frac{1}{\phi° - \phi_f(obsd)} = \frac{1}{\phi°_f - \phi'_f} + \frac{1}{K_{app}(\phi°_f - \phi'_f)[TiO_2]} \qquad (28)$$

The validity of this treatment has been demonstrated in TiO_2/chlorophyllin[59] and TiO_2/9AC[312] systems where the plot of $1/(\phi° - \phi_f(obsd))$ vs $1/[TiO_2]$ was shown to be linear (see for example insert in Figure 44). This method enables one to determine the association constant and the quantum yield of the sensitizer in the adsorbed state. The net quenching efficiency expressed as $(\phi°_f - \phi'_f)/\phi°_f$ was in the range of 70 to ~100% for several different systems and was dependent on the energy difference between the semiconductor conduction band and the oxidation potential of the excited sensitizer.

Tani and his co-workers have observed that the quantum efficiency (ϕ_{et}) of photoinduced electron transfer from sensitizing dyes (cyanine dyes) to silver bromide microcrystals is dependent on the sensitizer reduction potential.[509] The dependence of ϕ_{et} on the reduction potential of the dye (Figure 45) has been explained on the basis of Marcus theory with a small
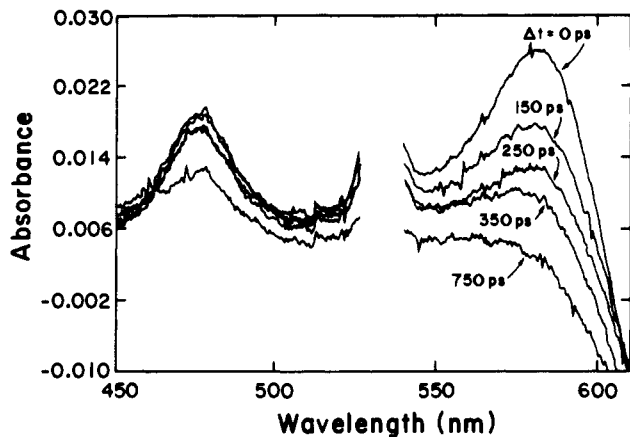
Figure 46. Production of dye cation radical in TiO_2/Sq system. Time-resolved transient absorption spectra recorded after 532-nm laser pulse excitation of SQ in 50/50 (v/v%) dichloromethane–acetonitrile containing 2.5 mM colloidal TiO_2. The absorption maxima at 475 and 580 nm correspond to the unadsorbed $^1Sq^*$ and Sq^+ respectively. Reprinted from ref 55. Copyright 1991 Elsevier Science Publishers, B. V.

rearrangement energy (0.05 eV) and without the inverted region. Spitler[510] has employed a quantitative photoconductive model to explain the data of Tani et al.[509] The model predicts an energetic threshold for spectral sensitization, correlating to a high speed of spectral sensitization of a dye with a highly negative electrochemical reduction potential.

B. Transient Absorbance Studies

a. Quenching of Singlet Excited State

The identification of the electron transfer product in a charge injection process (eq 29) was first attempted by Moser and Grätzel,[308] where S represents the

$$TiO_2 + {}^1S^* \xrightarrow{k_{et}} TiO_2(e) + S^{\cdot+} \qquad (29)$$
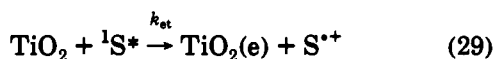
sensitizer molecule. Recently, picosecond laser flash photolysis of squaraine dye (Sq) in colloidal TiO_2 suspensions has been carried out to investigate the ultrafast photochemical events associated with the charge injection process. The absorption peak of the transient at 580 nm obtained upon 532-nm laser excitation of the dye (Figure 46) confirms the formation of squaraine cation radical. The mechanism of cation radical formation in the colloidal TiO_2/eosin system has also been established by time-resolved resonance Raman spectroscopy.[309] The net charge-transfer efficiency in the case of the eosin/TiO_2 system is $\sim 38\%$.[308] However, much smaller ($<1\%$) efficiencies have been observed when 9AC[57] or chlorophyllin[59] is chosen as a sensitizer.

b. Quenching of Triplet Excited State

In most of the examples discussed above, only the singlet excited state of the sensitizer is able to participate in the charge injection process. The yield and lifetime of the triplet excited state are relatively unaffected in the presence of TiO_2. In some cases, the poor reactivity of the triplet excited state has been attributed to the lack of a driving force for the triplet sensitizer (e.g. $\Delta E \approx 0.1$ V for the 9AC/TiO_2 system)
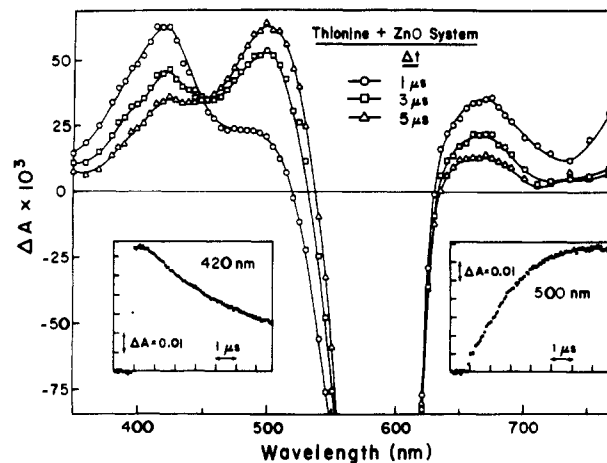
Figure 47. Quenching of triplet excited state thionine on ZnO surface. Time-resolved transient absorption spectra recorded following the 532-nm excitation of 25 μM thionine and 7 mM ZnO colloids in ethanol. Inserts show the decay of $^3TH^{+*}$ at 420 nm and the formation of TH^{2+} at 500 nm, respectively. Reprinted from ref 498. Copyright 1992 American Chemical Society.

a. With Interaction/ Adsorption   **b. With no direct Interaction**
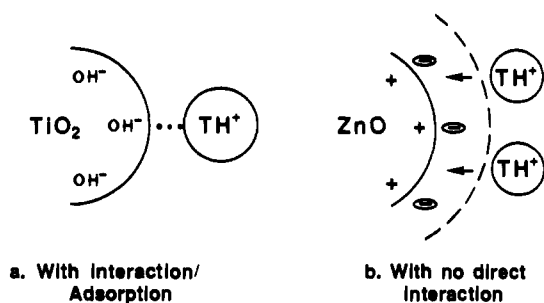
Figure 48. Possible modes of interaction between sensitizer and the semiconductor colloid. (a) Static quenching of the sensitizer can occur when its interaction with the semiconductor surface is strong. (b) Dynamic quenching can occur when there is no direct interaction between the semiconductor and the sensitizer. Reprinted from ref 498. Copyright 1992 American Chemical Society.

to inject an electron into the conduction band of the semiconductor.

However, recently charge injection via triplet excited state has been observed in the eosin (EO)/TiO_2[492] and thionine (TH^+)/ZnO[498] systems. The transient absorption spectra recorded in Figure 47 indicate the formation of dye cation radical (absorption maximum at 500 nm) as the triplet excited state (absorption maximum at 420 nm) is quenched by ZnO. The

$$^3TH^{+*} + ZnO \rightarrow TH^{\cdot 2+} + ZnO(e) \qquad (30)$$
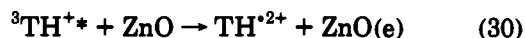
maximum quantum efficiency for the net charge transfer is 10%. Surprisingly, no such electron-transfer quenching can be observed for the singlet excited state. The difference in reactivity of the two excited states in different colloidal semiconductor systems has been summarized on the basis of interaction between the sensitizer and the semiconductor (Figure 48). In the first category, the sensitizer is strongly bound to the semiconductor (e.g. thionine/TiO_2[497] or Sq/TiO_2[55]) and the charge injection process proceeds via the singlet excited state. In the second category, when there is no direct interaction between the sensitizer and the semiconductor (e.g., thionine/ZnO system[498]), one can
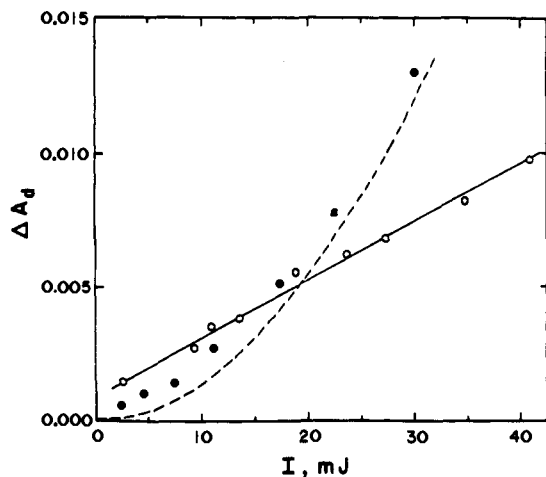
Figure 49. Dependence of the relative yield of RB⁺ (as measured from ΔA_d at 400 nm) on the laser pulse intensity: (O) rose bengal adsorbed on TiO_2 (0.4 mg/g of TiO_2) and (●) rose bengal adsorbed on alumina (0.4 mg/g of Al_2O_3). The dashed curve represents the dependence of yield of RB⁺ on the square of excitation intensity. Reprinted from ref 39. Copyright 1989 American Chemical Society.

expect the triplet excited state to participate in a diffusion-controlled charge injection process.

The charge injection process on a semiconductor surface (reaction 29) as well as the photoionization of adsorbed molecules on a nonreactive surface (reaction 12) yields the same reaction product (i.e., cation radical of the adsorbate). But it should be noted that the former (charge injection) process is monophotonic while the latter (photoionization) is biphotonic. The dependence of the rose bengal cation radical yield on the laser intensity (Figure 49) are distinctly different for TiO_2 and Al_2O_3 samples. This example shows how the reactive and nonreactive surfaces can control the photochemical behavior of the adsorbed molecules.[39] Similar influence of support material has also been observed in the degradation of 2,3-diphenylisobenzofuran on alumina and TiO_2.[41]

C. Kinetics of Charge-Transfer Processes

a. Forward Electron Transfer

The sensitizer molecules adsorbed on the TiO_2 surface have a significantly shorter fluorescence lifetime than in the homogeneous solution and this decrease in lifetime can be correlated with the charge injection process. If we assume that the observed decrease in the fluorescence lifetime is entirely due to the electron injection process (reaction 29) and that the other radiative and nonradiative decay processes of the sensitizer associated with TiO_2 colloid occur at the same rate as in neat solvent, we can correlate the observed lifetime by the expression

$$1/\tau_{ads} = 1/\tau + k_{et} \tag{31}$$

where τ and τ_{ads} are the lifetimes of the sensitizer in a neat solvent and adsorbed on TiO_2 surface, respectively, and k_{et} is the specific rate constant of the charge injection process. For example, fluorescence lifetimes of 400 and 150 ps are observed for chlorophyllin in the unadsorbed and adsorbed state.[59] The value of k_{et} obtained from eq 31 then corresponds to 4.2×10^9 s⁻¹. This high value of the rate constant for the heteroge-
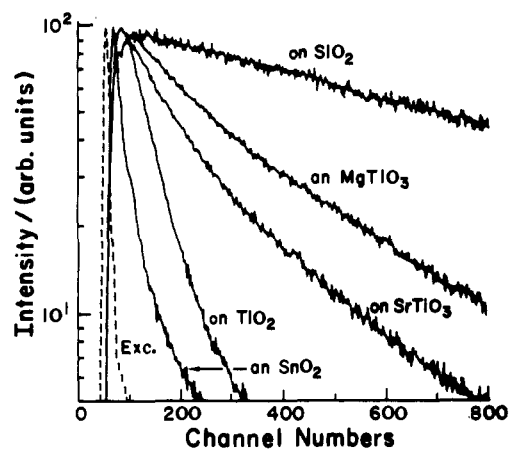
Figure 50. Fluorescence decays of Rh B adsorbed on metal oxide powders in vacuo (4.88 ps/channel). The excitation pulse (dotted line) shape is also shown. Reprinted from ref 495. Copyright 1988 Elsevier Science Publishers, B. V.

neous electron transfer is very similar to that determined for the eosin/TiO_2 system using picosecond laser flash photolysis.[489] In these studies the rate of EO⁺ formation (k_{obs}) is related to k_{et} by the expression

$$k_{et} = k_{obsd}\phi(EO^{•+}) \tag{32}$$

The rate constant for charge injection from excited eosin into the conduction band of TiO_2 colloid has been determined to be 2×10^9 s⁻¹.

A recent picosecond laser flash photolysis study[490] has indicated prompt appearance of sensitizer cation radical, 9AC⁺ (abs max 720 nm) following 355-nm laser pulse excitation (pulse duration ~ 18 ps). The rate constant for the charge injection process is estimated as $\geq 5 \times 10^{10}$ s⁻¹. Such a rate constant indicates a strong exchange coupling between the excited singlet state of the sensitizer and the d-band states of the TiO_2 conduction band.[219]

The fluorescence decay of rhodamine B (Rh B) adsorbed on various oxide semiconductor powders has been measured in vacuo to establish the dependence of electron transfer rates on the type of semiconductor substrate.[495] The fluorescence decay curve of Rh B on various substrates are compared in Figure 50. The electron-transfer rates increase from 5.6×10^8 s⁻¹ to 2×10^{10} s⁻¹ as the energy difference of the singlet excited state oxidation potential $(E^0_{D^*/D^+})$ and the conduction band of the semiconductor (E_c) increases from 0.03 eV (for ZnO) to 1.56 eV (for WO_3).

According to the model proposed by Gerischer[511,512] and Spitler[513] the probability of an electron transfer (j_c) from conduction band with an energy level E_c is proportional to an exponential factor described by the expression

$$j_c \propto \exp\left(-\frac{(E_c - E^o_{D^*/D^+})^2}{4L^*kT}\right) \tag{33}$$

where L* represents the reorganization energy in the excited state and is in the range of 0.5–1.5 eV. The energy difference $(E_c - E^o_{D^*/D^+})$ acts as a driving force for the charge injection process and governs the efficiency of sensitization. The pH dependence of the sensitization efficiency has also been explained on the basis of similar thermodynamic considerations.[492]
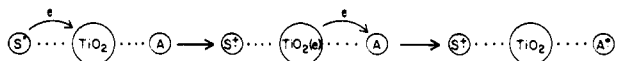
Figure 51. Charge separation in a sensitizer–semiconductor–acceptor system. The semiconductor colloid acts as a mediator in promoting the sensitizing reduction of the acceptor molecule. Reprinted from ref 57. Copyright 1989 American Chemical Society.

b. Back Electron Transfer

The time-resolved absorption spectra recorded in Figure 46 also indicate the decay of $Sq^{\bullet+}$ in the subnanosecond time domain ($k \approx 10^{10}$ s^{-1}) as a result of its reaction with the injected charge (reaction 34).

$$Sq^{\bullet+} + TiO_2(e) \rightarrow Sq + TiO_2 \qquad (34)$$
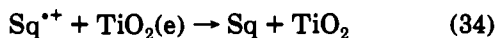
Less than 10% of Sq survived this back-reaction by diffusing away from the TiO_2 surface. In the case of the eosin/TiO_2 system, a biphasic decay has been observed for the radical, $EO^{\bullet}$. The initial fast component of this decay is attributed to the recombination of $EO^{\bullet}$ with the injected charge. The rate constant for this process is determined to be 2×10^5 s^{-1} which is 10^4 times slower than that for the electron injection process. The fraction of $EO^{\bullet}$ ($\sim 50\%$) that has survived the back electron transfer desorbs from the TiO_2 surface and undergoes bulk recombination. Similarly, a much slower back electron transfer ($k = (1-5) \times 10^5$ s^{-1}) has been observed for sensitizers such as porphyrins,[311] $Ru(bpy)_3{}^{2+}$ and its analogues,[486] and $Fe(CN)_6{}^{4-}$.[306]

In the case of the thionine/ZnO system, the back electron transfer, which is dependent on the ZnO concentration, varies from 1.77×10^4 to 5.72×10^4 s^{-1}. This lower value of the rate constant is attributed to the weak interaction between the sensitizer and the semiconductor colloid.

This shows that suppression of the back electron transfer process is an important aspect of achieving an efficient charge separation. There are two different approaches for improving the efficiency of charge separation: (1) depositing a noble metal on the semiconductor surface, such that it acts as a trap for the injected electrons and (2) employing a sacrificial electron donor which rapidly regenerates the sensitizer at the semiconductor surface. These aspects need to be addressed further before one can consider sensitizer/semiconductor systems for the design of photoactive molecular assemblies.

D. Utilization of Charge Injected into the Semiconductor

As mentioned earlier, the application of a photosensitization process involves the utilization of the charge injected into the semiconductor. This aspect has conveniently been studied in photoelectrochemical cells by driving away the injected charge via an external circuit (see for example refs 311, 486, 503, 505, and 514). By monitoring the sensitized photocurrent under controlled experimental conditions, one can elucidate the mechanistic details of photosensitization in such systems.

It is of interest to see how the charge injected into the semiconductor particle can be utilized to reduce another substrate. One can also compare this approach of charge separation (Figure 51) in the colloidal
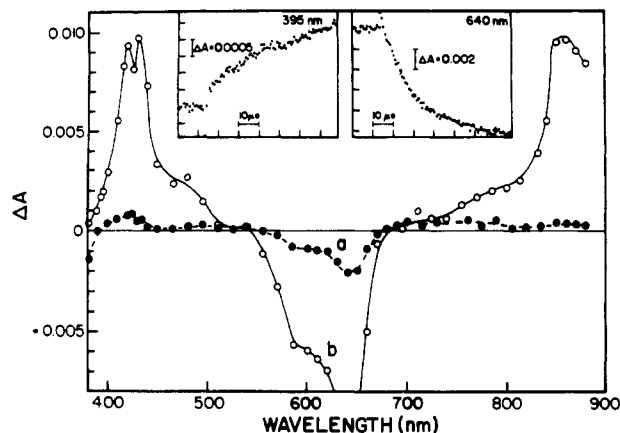

Figure 52. Sensitized reduction of Ox725. Transient absorption spectra recorded upon 355-nm laser pulse excitation of 20 μM 9AC and 5 mM Ox725: (a, ●) in acetonitrile and (b, O) in acetonitrile containing 2 mM TiO_2. The spectra were recorded 110 μs after the laser pulse excitation. Inserts show the formation of Ox^- (395 nm) and depletion of Ox725 (640 nm) in TiO_2 suspensions. Reprinted from ref 57. Copyright 1989 American Chemical Society.

semiconductor system ($S^{\bullet+}$–SC–$A^{\bullet-}$), to the concept of achieving charge separation in a carotenoid–porphyrin–quinone triad ($C^{\bullet+}$–P–$Q^{\bullet-}$).[515] The feasibility of the scheme presented in Figure 51 has recently been demonstrated[57] in the photosensitized reduction of N,N,N',N'-tetraethyloxonine perchlorate (Ox^+) in the colloidal TiO_2 system (reaction 35). Figure 52 shows

$$TiO_2(e) + Ox^+ \rightarrow TiO_2 + Ox^{\bullet} \qquad (35)$$

the transient absorption spectra recorded following the excitation of 9AC and Ox 725 in the absence and presence of TiO_2 colloids. The formation of $Ox^{\bullet}$ on the TiO_2 surface (abs max 420 nm) as characterized in laser flash photolysis experiments, is completed in ~ 100 μs. No such reduction was seen when the sensitizer was excluded. The dependence of reduction yield on the TiO_2 concentration has highlighted the role of the semiconductor and the sensitizer in promoting the electron transfer in the microheterogeneous system. A maximum quantum efficiency of 1.5% has been achieved for the sensitized reduction of Ox^+ in these experiments.

By using a similar principle, visible-light-induced photooxidation of iodide in a dye-sensitized TiO_2 colloid system has been carried out.[516] The dye sensitization of semiconductor particles has also been extended to other redox processes. A bifunctional redox catalyst composed of Pt and RuO_2 codeposited on the colloidal TiO_2 semiconductor has been sensitized with $Ru(bpy)_3{}^{2+}$ for the purpose of water cleavage.[220,517,518] The electron which is injected from the sensitizer into the semiconductor migrates to the Pt deposit where H_2 evolution occurs. The oxidized form of the sensitizer ($Ru(bpy)_3{}^{3+}$) generates oxygen from water. This aspect has also been demonstrated in electrochemical experiments by sensitizing a SnO_2 electrode.[519] Various other inorganic and organic sensitizers have also been used to produce H_2 from water in TiO_2 and Pt/TiO_2 particulate systems.[520] A maximum quantum efficiency of 0.1 has been reported for H_2 production with $Ru(bpy)_3{}^{2+}$ as sensitizer in these studies. Visible-light photolysis of hydrogen iodide using sensitized layered semiconductor

particles has also been reported.[521] Efforts are also being made to employ naturally occurring humic substances as sensitizers to carry out the reduction of dyes and other organic compounds with visible light.[522]

VI. Concluding Remarks

This review has sought to highlight the photophysical and photochemical processes of molecules adsorbed on reactive and nonreactive surfaces, the reactivity being controlled by the surface morphology and the intrinsic properties of the support material. Site-specific interactions, pore-size effects, electrostatic effects, surface mobility of the adsorbed molecules, and redox properties are some of the parameters that influence the mechanism and kinetics of photochemical processes on solid surfaces. Surface photochemistry has already grown out of its infancy and now emerges as a major field in photochemical research. The recent development of ultrafine semiconductor particles with many interesting photocatalytic properties has added a new dimension to the challenges of the future. The ability of such semiconductor microelectrodes to carry out redox processes with greater efficiency and selectivity than in homogeneous solutions has made them potential candidates for the conversion and storage of solar energy, and in the mineralization of chemical pollutants. The challenge for the next decade lies not only in developing new experimental and theoretical approaches to better understand the mechanistic and kinetic details of the surface photochemical processes, but also in designing novel microheterogeneous assemblies which promote an efficient photoinduced charge separation and mimic the natural photosynthetic system.

References

(1) Adamson, A. W. *Physical Chemistry of Surfaces*; Wiley: New York, 1982.
(2) Thomas J. K. *Chemistry of Excitation at Interfaces*; ACS Monograph 191; American Chemical Society: Washington, DC, 1983.
(3) Fox, M. A., Ed. *Organic Transformations in Nonhomogeneous Media*; ACS Symposium Series 278; American Chemical Society; Washington, DC, 1985.
(4) Kalyanasundaram, K. *Photochemistry in Microheterogeneous Systems*; Academic Press: New York, 1987.
(5) Anpo, M.; Matsuura, T. *Photochemistry on Solid Surfaces*; Elsevier: New York, 1989.
(6) (a) De Mayo, P. *Pure Appl. Chem.* **1982**, *54*, 163. (b) Turro, N. J. *Pure Appl. Chem.* **1986**, *58*, 1219.
(7) (a) Ramamurthy, V. *Tetrahedron* **1986**, *42*, 5753. (b) Ramamurthy, V. *Adv. Photochem.* **1992**, in press. (c) Ramamurthy, V. *Photochemistry in Organized and Constrained Media*; VCH: New York, 1991.
(8) Oelkrug, D.; Flemming, W.; Füllerman, R.; Günter, R.; Honnen, W.; Krabichler, G.; Schäfer S.; Uhl, S. *Pure Appl. Chem.* **1986**, *58*, 1207.
(9) Thomas, J. K. *J. Phys. Chem.* **1987**, *91*, 267.
(10) (a) Anpo, M.; Nishiguchi, H. *Res. Chem. Intermed.* **1990**, *13*, 73. (b) Anpo, M. *Res. Chem. Intermed.* **1989**, *11*, 67.
(11) Gafney, H. D. *Coord. Chem. Rev.* **1990**, *104*, 113.
(12) Bard, A. J. *J. Phys. Chem.* **1982**, *86*, 172.
(13) Bockris, J. O'M.; Uosaki, K. *Adv. Chem. Ser.* **1977**, *163*, 33.

(14) Gerischer, H. In *Photochemical Conversions*; Braun, A. M., Ed.; Presses Polytechnique Romandes: Lousanne, Switzerland, 1983; p 211.
(15) Memming, R. *Top. Curr. Chem.* **1988**, *143*, 79.
(16) Burevich, Yu. Ya; Pleskov, Yu. V. *Russ. Chem. Rev.* **1983**, *52*, 318.
(17) Heller, A. *Science* **1984**, *233*, 1141.
(18) Nozik, A. J. *Ann. Rev. Phys. Chem.* **1978**, *29*, 189.
(19) Wrighton, M. S. *Pure Appl. Chem.* **1985**, *57*, 57.
(20) Rajeshwar, K.; Singh, P.; Dubow, J. *Electrochim. Acta* **1978**, *23*, 1117.
(21) Fox, M. A. *Acc. Chem. Res.* **1983**, *16*, 314.
(22) Fox, M. A. In *Topics in Organic Electrochemistry*; Fry, A. J., Britton, W. E., Eds.; Plenum Press: New York, 1986, p 77.
(23) Fox, M. A. *Top. Curr. Chem.* **1987**, *142* (Electrochemistry I), 71.
(24) Fox, M. A., Channon, M., Eds. *Photoinduced Electron Transfer*; Elsevier: Amsterdam, 1988; Part D-6.
(25) Fox, M. A. *Res. Chem. Intermed.* **1991**, *15*, 153.
(26) Grätzel, M. A., Ed. *Energy Resources Through Photochemistry and Catalysis*; Academic Press: New York, 1983.
(27) Childs, L.; Ollis, D. F. *J. Catal.* **1980**, *66*, 383.
(28) Ollis, D. F.; Pelizzetti, E.; Serpone, N. *Environ. Sci. Technol.* **1991**, *25*, 1523.
(29) Serpone, N.; Pelizzetti, E. *Photocatalysis. Fundamentals and Applications*; Wiley Interscience: New York, 1989.
(30) Anpo, N.; Kubokawa, Y. *Rev. Chem. Intermed.* **1987**, *8*, 105.
(31) Fendler, J. H. *Chem. Rev.* **1987**, *87*, 877.
(32) Fendler, J. H. *J. Phys. Chem.* **1985**, *89*, 2730.
(33) Norris, J. R., Jr., Meisel, D., Eds. *Photochemical Energy Conversion*; Elsevier: New York, 1989; p 297.
(34) Borgarello, E.; Serpone, N.; Grätzel, M.; Pelizzetti, E. *Int. J. Hydrogen Energy* **1985**, *10*, 737.
(35) Kamat, P. V. In *Kinetics and Catalysis in Microheterogeneous Systems*; Grätzel, M., Kalyanasundaram, K., Ed.; Marcel Dekker, Inc.: New York, 1991, pp 375–436.
(36) (a) White, J. M. *J. Vac. Sci. Technol.* **1992**, *B10*, 191. (b) Heilweil, E. J.; Casassa, M. P.; Cavanagh, R. R.; Stephenson, J. C. *Annu. Rev. Phys. Chem.* **1989**, *40*, 143.
(37) Rempfer, K.; Uhl, S.; Oelkrug, D. *J. Mol. Struct.* **1964**, *114*, 225.
(38) Kamat, P. V.; Gopidas, K. R.; Weir D. *Chem. Phys. Lett.* **1988**, *149*, 491.
(39) Gopidas, K. R.; Kamat, P. V. *J. Phys. Chem.* **1989**, *93*, 6428.
(40) Gopidas, K. R.; Kamat, P. V.; George, M. V. *Mol. Cryst. Liq. Cryst.* **1990**, *183*, 403.
(41) Vinodgopal, K.; Kamat, P. V. *J. Phys. Chem.* **1992**, *96*, 5054.
(42) Fujii, T.; Shimiju, E.; Suzuki, S. *J. Chem. Soc., Faraday Trans. 1* **1988**, *84*, 4387.
(43) Vyshkvarko, A. A.; Kiselev, V. F.; Pashenko, V. Z.; Plotnikov, G. S. *J. Lumin.* **1991**, *47*, 327.
(44) Furlong, D. N.; Sasse, W. H. F. *Colloids Surfaces* **1983**, *7*, 29.
(45) Ford, W. E.; Kamat, P. V. *J. Phys. Chem.* **1989**, *93*, 6423.
(46) Queitevis, E. L.; Horng, M.-L.; Chen, S.-Y. *Proc. Am. Inst. Phys. Conf.* **1988**, *172*, 697.
(47) Queitevis, E. L.; Horng, M.-L.; Chen, S.-Y. *J. Phys. Chem.* **1988**, *92*, 256.
(48) Kamat, P. V. *J. Electroanal. Chem.* **1984**, *163*, 389.
(49) Avnir, D.; Grauer, Z.; Yariv, S.; Huppert, D.; Rojanski, D. *Nouv. J. Chimie* **1986**, *10*, 153.
(50) Ghosh, P. K.; Bard, A. J. *J. Phys. Chem.* **1984**, *88*, 5519.
(51) Kennelly, T.; Gafney, H. D.; Braun, M. *J. Am. Chem. Soc.* **1985**, *107*, 4431.
(52) Shi, W.; Wolfgang, S.; Strekas, T. C.; Gafney, H. D. *J. Phys. Chem.* **1988**, *92*, 2329.
(53) Fan, J.; Shi, W.; Tysoe, T. C.; Strekas, T. C.; Gafney, H. D. *J. Phys. Chem.* **1989**, *93*, 373.
(54) Avnir, D.; Levy, D.; Reisfeld, R. *J. Phys. Chem.* **1984**, *88*, 5956.
(55) Kamat, P. V. ; Das, S.; Thomas, K. G.; George, M. V. *Chem. Phys. Lett.* **1991**, *178*, 75.
(56) Kamat, P. V.; Ford, W. E. *Chem. Phys. Lett.* **1987**, *135*, 421.
(57) Kamat, P. V. *J. Phys. Chem.* **1989**, *93*, 859.
(58) Kamat, P. V. *J. Photochem.* **1985**, *28*, 513.
(59) Kamat, P. V.; Chauvet, J.-P.; Fessenden, R. W. *J. Phys. Chem.* **1986**, *90*, 1389.
(60) Kamat, P. V. *Langmuir* **1985**, *1*, 608.
(61) Kamat, P. V.; Ford, W. E. *J. Phys. Chem.* **1992**, *55*, 159.
(62) Hiemenz, P. C., *Principles of Colloid and Surface Chemistry*; Marcel Dekker: New York, 1986.
(63) (a) Tunesi, S.; Anderson, M. *J. Phys. Chem.* **1991**, *95*, 3399. (b) Cunningham, J.; Al-Sayyed, G. *J. Chem. Soc., Faraday Trans.* **1990**, *86*, 3935.
(64) Benesi, H. A.; Hildebrand, J. H. *J. Am. Chem. Soc.* **1949**, *71*, 2703.
(65) Schmehl, R. H.; Whitten, D. G. *J. Am. Chem. Soc.* **1980**, *102*, 1938.
(66) Takagi, K.; Aoshima, K.; Sawaki, Y.; Iwamura, H. *J. Chem. Soc., Perkin Trans. 2* **1986**, 1771.
(67) Kamat, P. V.; Ford, W. E. *J. Phys. Chem.* **1989**, *93*, 1405.
(68) De Boer, J. H. *Z. Phys. Chem., Abt. B* **1931**, *14*, 163.
(69) Weis, L. D.; Evans, T. R.; Leermakers, P. A. *J. Am. Chem. Soc.* **1968**, *90*, 6109.
(70) Nicholls, C. H.; Leermakers, P. A. *Adv. Photochem.* **1971**, *8*, 315.
(71) Piciulo, P. L.; Sutherland, J. W. *J. Am. Chem. Soc.* **1979**, *101*, 3123.

(72) Bauer, R. K.; Borenstein, R.; De Mayo, P.; Okada, K.; Rafalska, M.; Ware, W. R.; Wu, K. C. J. Am. Chem. Soc. 1982, 104, 4635.
(73) Bauer, R. K.; De Mayo, P.; Ware, W. R.; Wu, K. C. J. Phys. Chem. 1982, 86, 3781.
(74) Bauer, R. K.; De Mayo, P.; Okada, K.; Ware, W. R.; Wu, K. C. J. Phys. Chem. 1983, 87, 460.
(75) Bauer, R. K.; De Mayo, P.; Natarajan, L. V.; Ware, W. R. Can. J. Chem. 1984, 62, 1279.
(76) De Mayo, P.; Natarajan, L. V.; Ware, W. R. J. Phys. Chem. 1985, 89, 3526.
(77) De Mayo, P.; Natarajan, L. V.; Ware, W. R. Chem. Phys. Lett. 1984, 107, 187.
(78) Avnir, D.; Busse, R.; Ottolenghi, M.; Weller, E.; Zachariasse, K. A. J. Phys. Chem. 1985, 89, 3521.
(79) Fujii, T.; Shimizu, E. Chem. Phys. Lett. 1987, 137, 448.
(80) (a) Fujii, T.; Shimizu, E.; Suzuki, S. J. Chem. Soc., Faraday Trans. 1, 1988, 84, 4387. (b) Suzuki, S.; Fujii, T. Stud. Surf. Sci. Catal. 1989, 47, 79.
(81) Hara K.; De Mayo, P.; Ware, W. R.; Weedon, A. V.; Wong, G. S. K.; Wu, K. C. Chem. Phys. Lett. 1980, 69, 105.
(82) (a) Lochmueller, C. H.; Colben, A. S.; Hunnicutt, M. L.; Harris, J. M. J. Am. Chem. Soc. 1984, 106, 4077. (b) Lochmueller, C. H.; Wenzel, T. J. J. Phys. Chem. 1990, 94, 4230.
(83) Francis, C.; Lin, J.; Singer, L. A. Chem. Phys. Lett. 1983, 94, 162.
(84) Ståhlberg, J.; Almgren, M.; Alsins. J. Anal. Chem. 1988, 60, 2487.
(85) Wellner, E.; Rojanski, D.; Ottolenghi, M.; Huppert, D.; Avnir, D. J. Am. Chem. Soc. 1987, 109, 575.
(86) Zachariasse, K. A. Stud. Surf. Sci. Catal. 1989, 47, 48.
(87) Slama-Schwok, A.; Ottolenghi, M.; Avnir, D. Nature 1992, 355, 240.
(88) Yankovich, V. N.; Osipov, V. V.; Eremenko, A. M.; Chuiko, A. A. Teor. Eksp. Khim. 1987, 23, 121.
(89) Oelkrug, D.; Radjaipour, M.; Erbse, H. Z. Phys. Chem., N.F. 1974, 88, 23.
(90) Oelkrug, D.; Radjaipour, M. Z. Phys. Chem. 1980, 123, 163.
(91) Beck, G.; Thomas, J. K. Chem. Phys. Lett. 1985, 94, 553.
(92) Pankasem, S.; Thomas, J. K. J. Phys. Chem. 1991, 95, 7385.
(93) Hara, K.; Ware, W. R. J.Chem. Phys. 1980, 51, 61.
(94) Suib, S. L.; Kostapapas, A. J. Am. Chem. Soc. 1984, 106, 7705.
(95) Baretz, B. H.; Turro, N. J. J. Photochem. 1984, 24, 201.
(96) (a) Nakamura, T.; Thomas, J. K. J. Phys. Chem. 1986, 90, 641. (b) Nakamura, T.; Thomas, J. K. Langmuir 1985, 1, 568.
(97) (a) Delaguardia, R. A.; Thomas, J. K. J. Phys. Chem. 1984, 88, 964. (b) Delaguardia, R. A.; Thomas, J. K. J. Phys. Chem. 1983, 87, 3550.
(98) Viaene, K.; Caigui, J.; Schoonheydt, R. A.; DeSchryver, F. C. Langmuir 1987, 3, 107-111.
(99) Kalyanasundaram, K.; Thomas, J. K. J. Phys. Chem. 1977, 99, 2039.
(100) Ishida, H.; Takahashi, H.; Tsubomura, H. Bull. Chem. Soc. Jpn. 1970, 43, 3130.
(101) Ishida, H.; Takahashi, H.; Tsubomura, H. J. Am. Chem. Soc. 1970, 92, 275.
(102) Ishida, H.; Tsubomura, H. J. Photochem. 1973, 2, 285.
(103) Bogar, R. G.; Thomas, J. C.; Callis, J. B. Anal. Chem. 1985, 89, 3521.
(104) James, D. R.; Liu, Y.-S.; De Mayo, P.; Ware, W. R. Chem. Phys. Lett. 1985, 120, 460.
(105) Cehelnik, E. D.; Cundall, R. B.; Lockwood, J. R.; Palmer, T. F. Chem. Phys. Lett. 1974, 27, 568.
(106) Levy, A.; Avnir, D.; Ottolenghi, M. Chem. Phys. Lett. 1985, 121, 233.
(107) Lin, C. T.; Hsu, W. L.; Yang, C. L.; El-Sayed, M. A. J. Phys. Chem. 1987, 91, 4556.
(108) Lin, C. T.; Hsu, W. L. J. Phys. Chem. 1988, 92, 1889.
(109) Honnen, W.; Krabichler, G.; Uhl, S.; Oelkrug, D. J. Phys. Chem. 1983, 87, 4872.
(110) Uhl, S.; Oelkrug, D. J. Mol. Struct. 1988, 175, 117.
(111) Oelkrug, D.; Uhl, S.; Weller, F.; Willsher, C. J. J. Phys. Chem. 1989, 93, 4551.
(112) Suzuki, S.; Fujii, T. In ref 5; p 79.
(113) (a) Kemnitz, K.; Murao, T.; Yamazaki, I.; Nakashima, N.; Yoshihara, K. Chem. Phys. Lett. 1983, 101, 337. (b) Kemnitz, K.; Tamai, N.; Yamazaki, I.; Nakashima, N.; Yoshihara, K. J. Phys. Chem. 1987, 91, 1423.
(114) (a) Ernst, L. Appl. Surface Sci. 1981, 7, 196. (b) Ernst, L. Surface Sci. 1982, 116, 351. (c) Ernst, L. Ber. Bunsen-ges. Phys. Chem. 1983, 87, 63.
(115) Huston, A. L.; Reimann, C. T. Chem. Phys. 1991, 149, 401.
(116) Schulman, E. M.; Walling, C. J. Phys. Chem. 1973, 77, 902.
(117) Oelkrug, D.; Plauschinat, M.; Kessler, R. W. J. Lumin. 1979, 18/19, 434.
(118) Dalterio, R. A.; Hurtubise Anal. Chem. 1982, 54, 224.
(119) (a) Anpo, M.; Tanakashi, I.; Kubokawa, Y. J. Phys. Chem. 1980, 84, 3440. (b) Anpo, M.; Tanakashi, I.; Kubokawa, Y. J. Chem. Soc., Faraday Trans. 1 1982, 78, 2121. (c) Anpo, M.; Suzuki, T.; Kubokawa, Y.; Tanaka, F.; Yamashita, S. J. Phys. Chem. 1984, 88, 5778.
(120) Kessler, R. W.; Wilkinson, F. J. Chem. Soc., Faraday Trans. 1 1981, 77, 309.

(121) Wilkinson, F. J. Chem. Soc., Faraday Trans. 2 1986, 82, 2073.
(122) Oelkrug, D.; Krabichler, G.; Honnen, W.; Wilkinson, F.; Willsher, C. J. J. Phys. Chem. 1988, 92, 3589.
(123) Wilkinson, F.; Willsher, C. J. Chem. Phys. Lett. 1984, 104, 272.
(124) Turro, N. J.; Zimmt, M. B.; Gould, I. R. J. Am. Chem. Soc. 1985, 107, 5826.
(125) Kazanis, S.; Azarani, A.; Johnston, L. J. J. Phys. Chem. 1991, 95, 4430.
(126) Drake, J. M.; Levitz, P.; Turro, N. J.; Nitsche, S.; Cassidy, K. F. J. Phys. Chem. 1988, 92, 4680.
(127) Wilkinson, F.; Willsher C. J.; Leicester, P. A.; Barr, J. R. M.; Smith, M. J. C. J. Chem. Soc., Chem. Commun. 1986, 1216.
(128) Oelkrug, D.; Reich, S.; Wilkinson, F.; Leicester, A. J. Phys. Chem. 1991, 95, 269.
(129) Piciulo, P. L.; Sutherland, J. W. J. Am. Chem. Soc. 1979, 101, 3123.
(130) Gevaert, M.; Kamat, P. V. Chem. Phys. Lett., submitted for publication.
(131) Gevaert, M.; Kamat, P. V. J. Chem. Soc., Chem. Commun., in press.
(132) Casal, H. L.; Scaiano, J. C. Can J. Chem. 1984, 62, 628.
(133) Casal, H. L.; Scaiano, J. C. Can J. Chem. 1985, 63, 1308.
(134) Schoonheydt, R. A.; Cenens, J.; De Schrijver, F. C. J. Chem. Soc., Chem. Commun. 1986, 82, 281.
(135) Basu, A.; Gafney H. D.; Perettie, D. J.; Clark, J. B. J. Phys. Chem. 1983, 87, 4532.
(136) Wolfgang, S.; Gafney H. D. J. Phys. Chem. 1983, 87, 4532.
(137) Shi, W.; Wolfgang, S.; Strekas, T. C.; Gafney H. D. J. Phys. Chem. 1985, 89, 974.
(138) Willner, J.; Yang, J.; Loane, C.; Otvos, J. W.; Calvin, M. J. Phys. Chem. 1981, 85, 3277.
(139) Wheeler, J.; Thomas, J. K. J. Phys. Chem. 1982, 86, 4540.
(140) Krueger, J. S.; Mallouk, T. E. In Kinetics and Catalysis in Microheterogeneous Systems; Grätzel, M., Kalyanasundaram, K., Ed.; Surfactant Science Series; Marcel Dekker, Inc.: New York, 1991; Vol. 18, 461.
(141) (a) Krenske, D.; Abdo, S.; Van Damme, H.; Cruz, M.; Fripiat, J. J. J. Phys. Chem. 1980, 84, 2447. (b) Nijs, H.; Cruz, M.; Fripiat, J. J.; Van Damme, H. J. Chem. Soc., Chem. Commun. 1981, 1026. (c) Abdo, S.; Canesson, P.; Cruz, M.; Van Damme, H.; Fripiat, J. J.; Cruz, M. J. Phys. Chem. 1981, 85, 797. (d) Nijs, H.; Fripiat, J. J.; Van Damme, H. Nouv. J. Chem. 1982, 6, 551. (e) Nijs, H.; Fripiat, J. J.; Van Damme, H. J. Phys. Chem. 1983, 87, 1279. (f) Nijs, H.; Fripiat, J. J.; Van Damme, H. J. Phys. Chem. 1983, 87, 1279.
(142) Turro, N. J.; Kumar, C. V.; Grauer, Z.; Barton, J. K. Langmuir 1987, 3, 1056.
(143) Kamat, P. V.; Ford, W. E. Photochem. Photobiol. 1992, 55, 159.
(144) Schoonheydt, R. A.; De Pauw, P.; Dominique, V.; DeSchryver, F. C. J. Phys. Chem. 1984, 88, 5113.
(145) (a) Quale, W. H.; Lunsford, J. H. Inorg. Chem. 1982, 21, 97. (b) DeWilde, W.; Peeters, G.; Lunsford, J. H. J. Phys. Chem. 1980, 84, 2306.
(146) Incavo, J. A.; Datta, P. K. J. Phys. Chem. 1990, 94, 3075.
(147) Turbeville, W.; Robins, D. S.; Dutta, P. K. J. Phys. Chem. 1992, 96, 5024.
(148) Yamagishi, A.; Soma, M. J. Am. Chem. Soc. 1981, 103, 4640.
(149) Yamagishi, A. J. Am. Chem. Soc. 1985, 107, 732.
(150) Joshi, V.; Kotkar, D.; Ghosh, P. K. J. Am. Chem. Soc. 1986, 108, 4650.
(151) (a) Joshi, V.; Kotkar, D.; Ghosh, P. K. J. Chem. Soc., Chem. Commun. 1987, 789. (b) Joshi, V.; Kotkar, D.; Ghosh, P. K. J. Am. Chem. Soc. 1989, 111, 5604.
(152) Kamat, P. V.; Gopidas, K. R.; Mukherjee, T.; Joshi, V.; Kotkar, D.; Pathak, V. S.; Ghosh, P. K. J. Phys. Chem. 1991, 95, 10009.
(153) Cao, G.; Garcia, M. E.; Alcala, M.; Burgess, L. F.; Mallouk, T. E. J. Am. Chem. Soc. 1992, 114, 7574.
(154) Wendlandt W. W.; Hecht, H. G. Reflectance Spectroscopy; Interscience: New York, 1966.
(155) Hecht, H. G. J. Res., Natl. Bur. Stand.—A. Phys. Chem. 1976, 567.
(156) Kubelka, P.; Munk, F. Z. Tech. Phys. 1931, 12, 593.
(157) Kessler, R. W.; Krabichler, G.; Uhl, S.; Oelkrug, D.; Hagan, W. P.; Hyslop, J.; Wilkinson, F. Opt. Acta 1983, 30, 1099.
(158) Wilkinson, F. J.; Willsher, C. Tetrahedron 1987, 43, 1197.
(159) Stone, F. S. In Surface Properties and Catalysis by Non-Metals; Bonnelle, Ed.; D. Reidel Publishing Co.: Dordrecht, the Netherlands, 1983, p 237.
(160) Sancier, K. M.; Morrison, S. R. Surf. Sci. 1979, 83, 29.
(161) Volodin, A. M.; Cherkashin, A. E. Kinet. Catal. 1981, 22, 598.
(162) Tavadyan, L. A. Kinet. Catal. 1983, 24, 332.
(163) Turro, N. J.; Waterman, K. C.; Welsh, K. M.; Paczkowski, M. A.; Zimmt, M. B.; Cheng, C.-C.; Mahler, W. Langmuir 1988, 4, 677.
(164) Wu, Y.; Piekara-Sady, L.; Kispert, L. D. Chem. Phys. Lett. 1991, 180, 569.
(165) Dozier, W. D.; Drake, J. M.; Klafter, J. Phys. Rev. Lett. 1986, 56, 197.
(166) Bryukhanov, V. V.; Ketsle, G. A.; Regir, K. F.; Runov, V. K.; Smagulov, Zh. K. Opt. Spectrosc. (USSR), 1989, 66, 546.
(167) Klafter, J.; Blueman, A. Chem. Phys. Lett. 1988, 148, 557.
(168) Levitz, P.; Drake, J. M.; Klafter, J. Chem. Phys. Lett. 1988, 148, 557.
(169) Pines-Rojanski, D.; Huppert, D.; Avnir, D. Chem. Phys. Lett. 1987, 139, 109.

(170) Even, U.; Rademann, K.; Jortner, J. *Phys. Rev. Lett.* **1984**, *52*, 2164.
(171) Levitz, P.; Drake, J. M. *Phys. Rev. Lett.* **1987**, *58*, 686.
(172) Kopelman, R.; Parus, S.; Prasad, J. *Phys. Rev. Lett.* **1986**, *56*, 1742.
(173) Avnir, D. *J. Am. Chem. Soc.* **1987**, *109*, 2931.
(174) Che, M.; Tench, A. J. *Adv. Catal.* **1983**, *32*, 1.
(175) Midden, W. R.; Wang, S. Y. *J. Am. Chem. Soc.* **1983**, *105*, 4129.
(176) Turro N. J.; Gould, I. R.; Zimmt, M. B.; Cheng, C.-C. *Chem. Phys. Lett.* **1985**, *119*, 484.
(177) Freeman, D. L.; Doll, J. D. *J. Chem. Phys.* **1983**, *78*, 6002.
(178) Cukier, R. I. *J.Chem. Phys.* **1983**, *79*, 2430.
(179) Blueman, A.; Zumophen, G.; Klafter, J. J. *Phys. Rev. B* **1984**, *30*, 5379.
(180) Vinodgopal, K.; Kamat, P. V. *J. Photochem. Photobiol. A: Chem.* **1992**, *63*, 119.
(181) Pettit, T. L.; Fox, M. A. *J. Phys. Chem.* **1986**, *90*, 1353.
(182) Khulbe, K. C.; Mann, R. S.; Sarkar, M. S. *React. Kinet. Catal. Lett.* **1977**, *7*, 35.
(183) Hecht, H. G.; Jensen, J. L. *J. Photochem.* **1978**, *9*, 33.
(184) Ramamurthy, V.; Casper, J. V.; Corbin, D. R. *Tetrahedron Lett.* **1990**, *31*, 1097
(185) Ramamurthy, V.; Casper, J. V.; Corbin, D. R.; Eaton, D. F.; Kauffman, J. S.; Dybiwski, C. *J. Photochem. Photobiol. A: Chem.* **1990**, *51*, 259.
(186) Breuer, H. D.; Jacob, H. *Chem. Phys. Lett.* **1980**, *73*, 172.
(187) Fukunishi, K.; Tatsuma, M.; Rahman, S. M. F. U.; Kuwabara, M.; Yamanaka, H.; Nomura, M. *Bull. Chem. Soc. Jpn.* **1990**, *63*, 3701.
(188) Kerzhner, B. K.; Kofanov, V. I.; Vrubel', T. L. *J. Gen. Chem. USSR* **1983**, *52*, 2076.
(189) Kerzhner, B. K.; Vrubel', T. L.; Kofanov, V. I. *J. Gen. Chem. USSR* **1987**, *57*, 1049
(190) Rau, H.; *Ber. Bunsen-ges. Phys. Chem.* **1971**, *75*, 1347.
(191) Rau, H.; Luddeke, E. *J. Am. Chem. Soc.* **1982**, *104*, 1616.
(192) Moesta, H. *Disc. Faraday Soc.* **1974**, *58*, 244.
(193) Grutsch, P. A.; Kutal, C. *J. Chem. Soc., Chem. Commun.* **1982**, 894.
(194) Gessner, F.; Olea, A.; Lobaugh, J. H.; Johnston, L. J.; Scaiano, J. C. *J. Org. Chem.* **1989**, *54*, 259.
(195) Faulkner, L. R.; Suib, S. L.; Renschler, C. L.; Green, J. M.; Bross, P. R. In *Chemistry in Energy Production*; Wymer, R. G., Keller, O. L., Eds.; John Wiley and Sons: New York, 1982, pp 99–114.
(196) Dutta, P. K.; Incavo, J. A. *J. Phys. Chem.* **1987**, *91*, 4443.
(197) Persaud, L.; Bard, A. J.; Campion, A.; Fox, M. A.; Mallouk, T. E.; Webber, S. E.; White, J. M. *J. Am. Chem. Soc.* **1987**, *109*, 7309.
(198) Kreuger, J. S.; Mayer, J. E.; Mallouk, T. E. *J. Am. Chem. Soc.* **1988**, *110*, 8232.
(199) Rong, D.; Hong, H.-G.; Kim, Y. I.; Krueger, J. S.; Mayer, J. E.; Mallouk, T. E. *Coord. Chem. Rev.* **1990**, *97*, 237.
(200) Kim, Y. I.; Mallouk, T. E. *J. Phys. Chem.* **1992**, *96*, 2879.
(201) Colón, J. L.; Yang, C.-Y.; Clearfield, A.; Martin, C. R. *J. Phys. Chem.* **1988**, *92*, 5777.
(202) Colón, J. L.; Yang, C.-Y.; Clearfield, A.; Martin, C. R. *J. Phys. Chem.* **1990**, *94*, 874.
(203) Liu, X.; Liu, K.-K.; Thomas, J. K. *J. Phys. Chem.* **1989**, *93*, 4120.
(204) DellaGuardia, R. A.; Thomas, J. K. *J. Phys. Chem.* **1983**, *87*, 990.
(205) Turro, N. J. *Tetrahedron* **1987**, 1589.
(206) Kazanis, S.; Azarani, A.; Johnston, L. J. *J. Phys. Chem.* **1991**, *95*, 4430.
(207) Wilkinson, F.; Willsher, C. J.; Casal, H. L.; Johnston, L. J.; Scaiano, J. C. *Can. J. Chem.* **1986**, *64*, 539.
(208) Kelly, G.; Willsher, C. J.; Wilkinson, F.; Netto-Ferreira, J. C.; Olea, A.; Weir, D.; Johnston, L. J.; Scaiano, J. C. *Can. J. Chem.* **1989**, 812.
(209) Avnir, D.; De Mayo, P.; Ono, I. *J. Chem. Soc., Chem. Commun.* **1978**, 1109.
(210) Leffler, J. E.; Zapanicic. *J. Am. Chem. Soc.* **1980**, *102*, 259.
(211) Leffler, J. E.; Barbas, J. T. *J. Am Chem. Soc.* **1981**, *103*, 7768.
(212) Abdel-Malik, M. M.; De Mayo, P. *Can. J. Chem.* **1984**, *62*, 1275.
(213) Johnston, L. J.; De Mayo, P.; Wong, S.K *J. Chem. Soc., Chem. Commun.* **1982**, 1106.
(214) Johnston, L. J.; De Mayo, P.; Wong, S.K. *J. Org. Chem.* **1984**, *49*, 20.
(215) Berger, R. M.; Weir, D. *Chem. Phys. Lett.* **1990**, *169*, 213.
(216) Lewis, N. *Annu. Rev. Phys. Chem.* **1991**, *42*, 543.
(217) Willner, I.; Willner, B. S. *Int. J. Hydrogen Energy* **1988**, *13*, 593.
(218) Grätzel, M. *Acc. Chem. Res.* **1981**, *41*, 376.
(219) Grätzel, M. *Heterogeneous Photochemical Electron Transfer*; CRC Press, Inc.: Boca Raton, FL, 1989, Chapter 3.
(220) Kalyanasundaram, K.; Grätzel, M.; Pelizzetti, E. *Coord. Chem. Rev.* **1986**, *69*, 57.
(221) (a) Henglein, A. *Top. Curr. Chem.* **1988**, *143*, 113. (b) Henglein, A. *Chem. Rev.* **1989**, *89*, 1861.
(222) *Quantum Size Particles*; Kamat, P. V., Meisel, D., Guest Ed. *Israel J. Chemistry* 1992.
(223) Kamat, P. V.; Dimitrijević, N. M. *Solar Energy* **1990**, *44*, 83.
(224) Brus, L. E. *J. Phys. Chem.* **1986**, *90*, 2555.
(225) Matijević, E. *Langmuir* **1986**, *2*, 12.
(226) Kuczynski, J.; Thomas, J. K. *Chem. Phys. Lett.* **1982**, *88*, 445.
(227) Kalyanasundaram, K.; Borgarello, E.; Duonghong, D.; Grätzel, M. *Angew. Chem.* **1981**, *93*, 1012.
(228) Henglein, A. *Ber. Bunsen-ges Phys. Chem.* **1982**, *86*, 301.

(229) Duonghong, D.; Ramsden, J.; Grätzel, M. *J. Am. Chem. Soc.* **1982**, *104*, 2977.
(230) Kamat, P. V.; Dimitrijević, N. M.; Fessenden, R. W. *J. Phys. Chem.* **1987**, *91*, 396.
(231) Becker, W. G.; Bard, A. J. *J. Phys. Chem.* **1983**, *87*, 4888.
(232) Wilhemy, D. M.; Matijević, E. *J. Chem. Soc., Faraday Trans. 1* **1984**, *80*, 563.
(233) Kiwi, J.; Borgarello, E.; Duonghong, D.; Grätzel, M. In *Preparation of Catalysts III*; Poncelet, G., Grange, P., Jacobs, P. A., Eds.; Elsevier Science: Amsterdam, 1983, p 135.
(234) Bahnemann, D.; Henglein, A.; Lilie, J.; Spanhel, L. *J. Phys. Chem.* **1984**, *88*, 709.
(235) Fox, M. A.; Chen, C. C.; Lindig, B. *J. Am. Chem. Soc.* **1982**, *104*, 5828.
(236) Kormann, C.; Bahnemann, D. W.; Hoffmann, M. R. *J. Phys. Chem.* **1988**, *92*, 5196.
(237) Nishimoto, S.; Ohtani, B.; Kajiwara, H.; Kagiya, T. *J. Chem. Soc., Faraday Trans. 1* **1985**, *81*, 61.
(238) Rabani, J.; Behar, D. *J. Phys. Chem.* **1989**, *93*, 2559.
(239) Bahnemann, D. W.; Kormann, C.; Hoffmann, M. R. *J. Phys. Chem.* **1987**, *91*, 3789.
(240) Spanhel, L.; Anderson, M. A. *J. Am. Chem. Soc.* **1991**, *113*, 2826.
(241) (a) Kamat, P. V.; Patrick, B. *J. Phys. Chem.* **1992**, *96*, 6829. (b) Kamat, P. V.; Patrick, B. In *Proceedings of the 44th Annual Meeting, Society for Imaging Science and Technology*, 1991; p 293.
(242) (a) Nenadović, M. T.; Rajh, T.; Micić, O. I.; Nozik, A. J. *J. Phys. Chem.* **1984**, *88*, 5827. (b) Hotchandani, S.; Bedja, I.; Kamat, P. V. *J. Phys. Chem.*, submitted for publication.
(243) Fojtik, A.; Henglein, A.; Katsikas, L.; Weller, H. *Chem. Phys. Lett.* **1987**, *138*, 535.
(244) (a) Sorum, C. H. *J. Am. Chem. Soc.* **1928**, *50*, 1263. (b) Matijevic, E. *Annu. Rev. Mater. Sci.* **1985**, *15*, 483.
(245) Stramel, R. D.; Thomas, J. K. *J. Colloid. Interface Sci.* **1986**, *110*, 121.
(246) Kiwi, J.; Grätzel, M. *J. Chem. Soc., Faraday Trans. 1* **1987**, *83*, 1101.
(247) Mulvaney, P.; Swayambunathan, V.; Grieser, F.; Meisel, D. *J. Phys. Chem.* **1988**, *92*, 6732.
(248) Visca, M.; Matijević, E. *J. Colloid Interface Sci.* **1979**, *68*, 308.
(249) Fojtik, A.; Weller, H.; Fiechler, S.; Henglein, A. *Chem. Phys. Lett.* **1987**, *134*, 477.
(250) Peterson, M. W.; Nenadović, M. T.; Rajh, T.; Herak, R.; Micić, O. I.; Goral, J. P.; Nozik, A. J. *J. Phys. Chem.* **1988**, *92*, 1400.
(251) Baral, S.; Lume-Pereira, C.; Janata, E.; Henglein, A. *J. Phys. Chem.* **1986**, *90*, 6025.
(252) (a) Hayes, D.; Micić, O. I.; Nenadović, M. T.; Swayanbunathan, V.; Meisel, D. *J. Phys. Chem.* **1989**, *93*, 4603. (b) Hayes, D.; Meisel, D.; Micić, O. I. *Colloids Surf.* **1991**, *55*, 121. (c) Silvester, E. J.; Grieser, F.; Sexton, B. A.; Healy, T. W. *Langmuir* **1991**, *7*, 2917.
(253) (a) Schmidt, K. M.; Patel, R.; Meisel, D. *J. Am. Chem. Soc.* **1988**, *110*, 4882. (b) Hayes, D.; Schmidt, K. H.; Meisel, D. *J. Phys. Chem.* **1989**, *93*, 6100. (c) Johansson, K. P.; McLendon, G.; Marchetti, A. P. *Chem. Phys. Lett.* **1991**, *171*, 321. (d) Micić, O. I.; Meglic, M.; Lawless, D.; Sharma, D. K.; Serpone, N. *Langmuir* **1990**, *6*, 487.
(254) (a) Wells, R. L.; Pitt, C. G.; McOhail, A. T.; Purdy, A. P.; Shafieezad, S.; Hallock, R. B. *Chem. Mater.* **1989**, *1*, 4. (b) Olshavsky, M. A.; Goldstein, A. N.; Alivisatos, A. P. *J. Am. Chem. Soc.* **1990**, *112*, 9438. (c) Uchida, H.; Curtis, C. J.; Kamat, P. V.; Jones, K. M.; Nozik, A. J. *J. Phys. Chem.* **1992**, *96*, 3.
(255) Fischer, Ch.-H.; Weller, H.; Fojtik, A.; Lume-Periera, C.; Janata, E.; Henglein, A. *Ber. Bunsen-ges. Phys. Chem.* **1986**, *90*, 46.
(256) Fischer, Ch.-H.; Lillie, J.; Weller, H.; Katsikas, L.; Henglein, A. *Ber. Bunsen-ges Phys. Chem.* **1989**, *93*, 61.
(257) Rajh, T.; Peterson, M. W.; Turner, J. A.; Nozik, A. J. *J. Electroanal. Chem.* **1987**, *228*, 55.
(258) Dimitrijević, N. M.; Kamat, P. V. *Langmuir* **1987**, *3*, 1004.
(259) Kamat, P. V.; Dimitrijević, N. M.; Fessenden, R. W. *J. Phys. Chem.* **1988**, *92*, 2324.
(260) Mac Dougall, J. E.; Eckert, H.; Stucky, G. D.; Herron, N.; Wang, Y.; Moller, K.; Bein, T; Cox, D. *J. Am. Chem. Soc.* **1989**, *111*, 8006.
(261) (a) Gills, L.; Zongguan; Meisel, D. *J. Phys. Chem.* **1988**, *92*, 822. (b) Ookubo, A.; Kanezaki, E.; Ooi, K. *Langmuir* **1990**, *6*, 206.
(262) Zen, J.-M.; Fan, R.-R. F.; Chen, G.; Bard, A. J. *Langmuir* **1989**, *5*, 1355.
(263) Moller, K.; Bein, T.; Herron, N.; Mahler, W.; Wang, Y. *Inorg. Chem.* **1989**, *28*, 2914.
(264) Meyer, M.; Wallberg, C.; Kurihara, K.; Fendler, J. H. *J. Chem. Soc., Chem. Commun.* **1984**, 90.
(265) (a) Lianos, P.; Thomas, J. K. *Chem. Phys. Lett.* **1986**, *125*, 299. (b) Pileni, M. P.; Lisiecki, I.; Motte, L.; Petit, C. *Res. Chem. Intermed.* **1992**, *17*, 101.
(266) (a) Tricot, Y. M.; Fendler, J. H. *J. Am. Chem. Soc.* **1984**, *106*, 7359. (b) Tricot, Y. M.; Emerson, A.; Fendler, H. J. *J. Phys. Chem.* **1985**, *89*, 4721.
(267) Tricot, Y. M.; Manassen, J. *J. Phys. Chem.* **1988**, *92*, 5239.
(268) Zhao, X. K.; Baral, S.; Rolandi, R.; Fendler, J. H. *J. Am. Chem. Soc.* **1988**, *110*, 1012.
(269) Baral, S.; Fendler, J. H. In *Photoinduced Electron Transfer*; Fox, M. A., Chanon, M., Eds.; Elsevier: 1988, Part B, 541.

(270) Baral, S.; Fendler, J. H. *J. Am. Chem. Soc.* 1989, *111*, 1604.
(271) Wang, Y.; Herron, N. *J. Phys. Chem.* 1987, *91*, 257.
(272) Herron, N.; Wang, Y.; Eddy, M. M.; Stucky, G. D.; Cox, D. E.; Moller, K.; Bein, T. *J. Am. Chem. Soc.* 1989, *111*, 530.
(273) Liu, X.; Thomas, J. K. *Langmuir* 1989, *5*, 58.
(274) Mallouk, T. E. *Proceedings of the Thirteenth DOE Solar Photochemistry Conference*; Argonne National Laboratory: Argonne, IL, 1988, p 37.
(275) Meissner, D.; Memming, R.; Kastening, *Chem. Phys. Lett.* 1983, *96*, 34.
(276) (a) Krishnan, M.; White, J. R.; Fox, M. A.; Bard, A. J. *J. Am. Chem. Soc.* 1983, *105*, 7002. (b) Finlayson, M. F.; Park, K. H.; Kakuta, N.; Bard, A. J.; Campion, A.; Fox, M. A.; Webber, S. E.; White, J. M. *J. Lumin.* 1988, *39*, 205.
(277) (a) Wang, Y.; Mahler, W. *Opt. Commun.* 1987, *61*, 233. (b) Mahler, W. *Inorg. Chem.* 1988, *27*, 436.
(278) Honda, K.; Kuwana, A.; Chiba, K.; Iskikawa, A.; Miyama, H. *Chem. Lett.* 1988, 195.
(279) Dalas, E.; Sakkopoulos, S.; Kallitsis, J.; Vitoratos, E.; Koutsoukos, P. G. *Langmuir* 1990, *6*, 1356.
(280) Gopidas, K. R.; Kamat, P. V. *Mater. Lett.* 1990, *9*, 372.
(281) Smotkin, E. S.; Lee, C.; Bard, A. J.; Campion, A.; Fox, M. A.; Mallouk, T. E.; Webber, S. E.; White, J. M. *Chem. Phys. Lett.* 1988, *152*, 265.
(282) Bohorquez, M.; Kamat, P. V.; Patterson, L. K. *Chem. Phys. Lett.*, submitted for publication.
(283) Stramel, R. D.; Nakamura, T.; Thomas, J. K. *Chem. Phys. Lett.* 1986, *130*, 423.
(284) Yoneyama, H.; Haga, S.; Yamanaka, S. *J. Phys. Chem.* 1989, *93*, 4833.
(285) Ekomov, A. J.; Onushchenko, A. *JETP Lett.* 1984, *40*, 1136.
(286) (a) Rajh, T.; Vucemilovic, M. I.; Dimitrijević, N. M.; Micić, O. I.; Nozik, A. J. *Chem. Phys. Lett.* 1988, *143*, 305. (b) Rajh, T.; Micić, O. I.; Lawless, D.; Serpone, N. *J. Phys. Chem.* 1992, *96*, 4633.
(287) Kuczynski, J.; Thomas, J. K. *J. Phys. Chem.* 1985, *89*, 2720.
(288) Modes, S.; Lianos, P. *Chem. Phys. Lett.* 1988, *153*, 351.
(289) Slama-Schwok, A.; Avnir, D.; Ottolenghi, M. *J. Phys. Chem.* 1989, *93*, 7544.
(290) Steigerwald, M. L.; Alivisatos, A. P.; Gibson, J. M.; Harris, T. D.; Kortan, R.; Muller, A. J.; Thayer, A. M.; Duncan, T. M.; Douglass, D. C.; Brus, L. E. *J. Am. Chem. Soc.* 1988, *110*, 3046.
(291) Wilner, I.; Eichen, Y. *J. Am. Chem. Soc.* 1987, *109*, 6862.
(292) Dameron, C. T.; Reese, R. N.; Mehra, R. K.; Kortan, A. R.; Carroll, P. J.; Steigerwald, M. L.; Brus, L. E.; Winge, D. R. *Nature* 1989, *338*, 596.
(293) Krautler, B.; Bard, A. J. *J. Am. Chem. Soc.* 1978, *100*, 4317.
(294) Mills, A.; Porter, G. *J. Chem. Soc., Faraday Trans. 1* 1982, *78*, 3659.
(295) Sakata, T.; Kawai, T.; Hashimoto, K. *Chem. Phys. Lett.* 1982, *88*, 50.
(296) (a) Baba, R.; Nakabayashi, S.; Fuhishima, A.; Honda, K. *J. Phys. Chem.* 1985, *89*, 1902. (b) Prahov, L. T.; Disdier, J.; Herrman, J.-M.; Pichat, P. *Int. J. Hydrogen Energy* 1984, *9*, 397.
(297) Duonghong, D.; Borgarello, E.; Grätzel, M. *J. Am. Chem. Soc.* 1981, *103*, 4685.
(298) Anpo, M.; Chiba, K.; Tomonari, M.; Coluccia, S.; Che, M.; Fox, M. A. *Bull. Chem. Soc. Jpn.* 1991, *64*, 543.
(299) Harriman, A.; Porter, G.; Walters, P. *J. Chem. Soc. Faraday Trans. 1* 1981, *77*, 2373.
(300) Mills, A. *J. Chem. Soc., Dalton Trans.* 1982, 1213.
(301) Thackeray, J. W.; Natan, M. J.; Ng, P.; Wrighton, M. S. *J. Am. Chem. Soc.* 1986, *108*, 3570.
(302) Nosaka, Y.; Yamaguchi, K.; Miyama, H.; Hayashi, H. *Chem. Lett.* 1988, 605.
(303) Kamat, P. V.; Dimitrijević, N. M. *J. Phys. Chem.* 1989, *93*, 4259.
(304) Fischer, C.-H.; Henglein, A. *J. Phys. Chem.* 1989, *93*, 5578.
(305) Kamat, P. V.; De Lind, M.; Hotchandani, S. *Israel J. Chem.* 1992, in press.
(306) (a) Brachnou, E.; Vlachopoulos, N.; Grätzel, M. *J. Chem. Soc., Chem. Commun.* 1987, 868. (b) Chandler, R. R.; Coffer, J. L.; Atherton, S. J.; Snowden, P. T. *J. Phys. Chem.* 1992, *96*, 2713. (c) Zhang, J. Z.; Ellis, A. B. *J. Phys. Chem.* 1992, *96*, 2700.
(307) Kamat, P. V.; Fox, M. A. *Chem. Phys. Lett.* 1983, *102*, 379.
(308) Moser, J.; Grätzel, M. *J. Am. Chem. Soc.* 1984, *106*, 6557.
(309) (a) Rossetti, R.; Brus, L. E. *J. Am. Chem. Soc.* 1984, *106*, 4336. (b) Umapathy, S.; Cartner, A. M.; Parker, A. W.; Hester, R. J. *Phys. Chem.* 1990, *94*, 8880.
(310) Fessenden, R. W.; Kamat, P. V. *Chem. Phys. Lett.* 1984, *123*, 233.
(311) Kalyanasundaram, K.; Vlachopoulos, N.; Krishnan, V.; Monnier, A.; Grätzel, M. *J. Phys. Chem.* 1987, *91*, 2342.
(312) (a) Steigerwald, M. L.; Brus, L. E. *Acc. Chem. Res.* 1990, *23*, 183. (b) Bawendi, M. G.; Steigerwald, M. L.; Brus, L. E. *Ann. Rev. Phys. Chem.* 1990, *41*, 477.
(313) Wang, Y.; Herron, N. *J. Phys. Chem.* 1991, *95*, 525.
(314) Rama Krishna, M. V.; Friesner, R. A. *J. Chem. Phys.* 1991, *95*, 8309.
(315) Brus, L. E. *J. Phys. Chem.* 1983, *79*, 5566.
(316) Brus, L. E. *J. Chem. Phys.* 1984, *80*, 4403.
(317) Rossetti, R.; Ellison, J. L.; Gibson, J. M.; Brus, L. E. *J. Phys. Chem.* 1984, *80*, 4464.
(318) Weller, H.; Koch, U.; Gutierrez, M.; Henglein, A. *Ber. Bunsen-ges. Phys. Chem.* 1984, *88*, 649.
(319) Fojtik, A.; Weller, H.; Koch, U.; Henglein, A. *Ber. Bunsen-ges. Phys. Chem.* 1984, *88*, 969.
(320) Weller, H.; Schmidt, M. H.; Koch, U.; Fojtik, A.; Baral, S.; Henglein, A., Kunath, W.; Weiss, K.; Dieman, E. *Chem. Phys. Lett.* 1986, *124*, 557.
(321) Sandroff, C. J.; Hwang, D. M.; Chung, W. M. *J. Phys. Chem.* 1986, *90*, 5337.
(322) Shinada, S.; Sugano, S. *J. Phys. Soc. Jpn.* 1966, *21*, 1936.
(323) Ploog, K.; Döhler, G. H. *Adv. Phys.* 1983, *32*, 285.
(324) Wang, Y.; Suna, A.; Mahler, W.; Kasowski, R. *J. Chem. Phys.* 1987, *87*, 7315.
(325) Nedeljkovic, J. M.; Nenadovic, M. T.; Micić, O. I.; Nozik, A. J. *J. Phys. Chem.* 1986, *90*, 12.
(326) Nozik, A. J.; Williams, F.; Nenadovic, M. T.; Rajh, T.; Micić, O. I. *J. Phys. Chem.* 1985, *89*, 397.
(327) Mohan, V.; Anderson, J. B. *Chem. Phys. Lett.* 1989, *156*, 520.
(328) Petroff, P. M.; Gössard, A. C.; Logan, R. A.; Wiegmann, W. *Appl. Phys. Lett.* 1982, *41*, 633.
(329) Laviron, M.; Aversuch, P.; Godfrin, H.; Rapp, R. E. *J. Phys. (Paris)* 1985, *44*, L-1021.
(330) Henglein, A.; Fojtik, A.; Weller, H. *Ber. Bunsen-ges Phys. Chem.* 1987, *91*, 441.
(331) Rossetti, R.; Hull, R.; Gibson, J. M.; Brus, L. E. *J. Chem. Phys.* 1985, *82*, 552.
(332) Rossetti, R.; Hull, R.; Gibson, J. M.; Brus, L. E. *J. Chem. Phys.* 1985, *83*, 1406.
(333) Chestnoy, N.; Harris, T. D.; Brus, L. E. *J. Phys. Chem.* 1986, *90*, 3393.
(334) Fojtik, A.; Weller, H.; Henglein, A. *Chem. Phys. Lett.* 1985, *120*, 552.
(335) Chestnoy, N.; Hull, R.; Brus, L. E. *J. Chem. Phys.* 1986, *85*, 2237.
(336) Sandroff, C. J.; Hwang, D. M.; Chung, W. M. *Phys. Rev. B* 1986, *33*, 5953.
(337) Sandroff, C. J.; Farrow, L. A. *Chem. Phys. Lett.* 1986, *130*, 458.
(338) Warnock, J.; Anwshalom, D. D. *Phys. Rev. B* 1986, *32*, 5529.
(339) Warnock, J.; Anwshalom, D. D. *Appl. Phys. Lett.* 1986, *48*, 425.
(340) Fojtik, A.; Jirkovsky, J. *Chem. Phys. Lett.* 1987, *137*, 226.
(341) Nenadovic, M. T.; Nedeljkovic, J. M.; Micić, O. I. *J. Chem. Soc., Faraday Trans. 1* 1987, *83*, 1127.
(342) (a) Ekimov, A. I.; Onuschenko, A. A. *JETP Lett.* 1981, *34*, 345. (b) Ekimov, A. I.; Efros, A. L.; Onuschenko, A. A. *Solid State Commun.* 1985, *56*, 921.
(343) O'Neil, M.; McLendon, G. *Chem. Phys. Lett.* 1988, *147*, 565.
(344) Nosaka, Y.; Tamaguchi, K.; Miyama, H.; Hayashi, H. *Chem. Phys. Lett.* 1988, 605.
(345) Micić, O. I.; Zongguan, L. I.; Mills, G.; Sullivan, J. C.; Meisel, D. *J. Phys. Chem.* 1987, *91*, 6221.
(346) Peterson, M. W.; Micić, O. I.; Nozik, A. J. *J. Phys. Chem.* 1988, *92*, 4160.
(347) (a) Tanaka, T.; Iwasaki, M. *J. Photogr. Sci.* 1983, *31*, 13. (b) Tanaka, T.; Iwasaki, M. *J. Imaging Sci.* 1985, *29*, 86.
(348) Henglein, A.; Gutiérrez, M. *Ber. Bunsen-ges Phys. Chem.* 1983, *87*, 852.
(349) Rossetti, R.; Brus, L. *J. Phys. Chem.* 1982, *86*, 4470.
(350) Ramsden, J. J.; Grätzel, M. *J. Chem. Soc., Faraday Trans. 1* 1984, *80*, 919.
(351) Uchihara, T.; Matsumura, M.; Yamamoto, A.; Tsubomura, H. *J. Phys. Chem.* 1989, *93*, 5870.
(352) Ramsden, J. J.; Webber, S. E.; Grätzel, M. *J. Phys. Chem.* 1985, *89*, 2740.
(353) Ferrer, I. J.; Salvador, P. *Chem. Phys. Lett.* 1987, *142*, 399.
(354) Dimitrijević, N. M. *J. Chem. Soc. Faraday Trans. 1* 1987, *83*, 1193.
(355) Dannhauser, T.; O'Neil, M.; Johansson, K.; Whitten, D.; McLendon, G. *J. Phys. Chem.* 1986, *90*, 6074.
(356) Lambe, J. J.; Klick, C. C.; Dexter, D. L. *Phys. Rev.* 1956, *103*, 1715.
(357) Spanhel, L.; Weller, H.; Fojtik, A.; Henglein, A. *Ber. Bunsen-ges Phys. Chem.* 1987, *91*, 88.
(358) Spanhel, L.; Weller, H.; Henglein, A. *J. Am. Chem. Soc.* 1987, *109*, 5649.
(359) Anpo, M.; Tomonari, M.; Fox, M. A. *J. Phys. Chem.* 1989, *93*, 7300.
(360) Benjamin, D.; Huppert, D. *J. Phys. Chem.* 1988, *92*, 4676.
(361) Kamat, P. V.; Dimitrijević, N. M.; Nozik, A. J. *J. Phys. Chem.* 1989, *93*, 2873.
(362) Chemela, D. S.; Miller, D. A. M. *J. Opt. Soc. Am.* 1985, *B2*, 1155.
(363) (a) Jain, R. K.; Lind, R. C. *J. Opt. Soc. Am.* 1983, *73*, 647. (b) Borrelli, N. F.; Hall, D. W.; Holland, H. J.; Smith, D. W. *J. Appl. Phys.* 1987, *61*, 5339.
(364) Hilenski, E. F.; Lucas, P. A.; Wang, Y. *J. Phys. Chem.* 1988, *89*, 3435.
(365) Wang, Y.; Herron, N.; Mahler, W.; Suma, A. *J. Opt. Soc. Am.* 1989, *B6*, 808.
(366) Cheng, L.-T.; Herron, N.; Wang, Y. *J. Appl. Phys.* 1989, *66*, 3417.
(367) Kuczynski, J. P.; Milosavljevic, B. H.; Thomas, J. K. *J. Phys. Chem.* 1984, *88*, 980.
(368) Albery, W. J.; Brown, G. T.; Darwent, J. R.; Saievar-Iranizad, E. *J. Chem. Soc., Faraday Trans, 1* 1985, *81*, 1999.
(369) Henglein, A.; Kumar, A.; Janata, E.; Weller, H. *Chem. Phys. Lett.* 1986, *132*, 133.

(370) Haase, M.; Weller, H.; Henglein, A. *J. Phys. Chem.* **1988**, *92*, 4706.

(371) Liu, C.; Bard, A. J. *J. Phys. Chem.* **1989**, *93*, 3232.

(372) Liu, C.; Bard, A. J. *J. Phys. Chem.* **1989**, *93*, 7749.

(373) Haase, M.; Weller, H.; Henglein, A. *Ber. Bunsen-ges Phys. Chem.* **1988**, *92*, 1103.

(374) Dimitrijević, N. M.; Kamat, P. V. *J. Phys. Chem.* **1987**, *91*, 2096.

(375) Kamat, P. V.; Gopidas, K. R.; Dimitrijević, N. M. *Mol. Cryst. Liq. Cryst.* **1990**, *183*, 439.

(376) Dimitrijević, N. M.; Kamat, P. V. *Langmuir* **1988**, *4*, 782.

(377) Haase, M.; Weller, H.; Henglein, A. *J. Phys. Chem.* **1988**, *92*, 482.

(378) Burstein, B. E. *Phys. Rev.* **1954**, *93*, 632.

(379) Moss, T. S. *Proc. Phys. Soc. (London) B* **1954**, *76*, 775.

(380) Banyai, L.; Koch, S. W. *Phys. Rev. Lett.* **1986**, *57*, 2722.

(381) Moss, T. *Phys. Status Solidi* **1980**, *101*, 555.

(382) Dapkus, P. D.; Holonyak, N.; Burnham, R. D.; Keune, D. L. *Appl. Phys. Lett.* **1980**, *16*, 93.

(383) Howe, R. F.; Grätzel, M. *J. Phys. Chem.* **1987**, *91*, 3906.

(384) Rothenberger, G.; Moser, J.; Grätzel, M.; Serpone, N.; Sharma, D. K. *J. Am. Chem. Soc.* **1985**, *107*, 8054.

(385) Kamat, P. V.; Gopidas, K. R. In Picosecond and Femtosecond Spectroscopy from Laboratory to Real World. *Proceedings of the SPIE's Technical Symposium on Laser Spectroscopy*, 1990; pp 115–122.

(386) Gutiérrez, M.; Henglein, A. *Ber. Bunsen-ges Phys. Chem.* **1978**, *87*, 474.

(387) Kamat, P. V.; Ebbesen, T. W.; Dimitrijević, N. M.; Nozik, A. J. *Chem. Phys. Lett.* **1989**, *157*, 384.

(388) Baral, S.; Fojtik, A.; Weller, H.; Henglein, A. *J. Am. Chem. Soc.* **1986**, *108*, 375.

(389) Nosaka, Y.; Fox, M. A. *J. Phys. Chem.* **1986**, *90*, 6521.

(390) Kumar, A.; Janata, E.; Henglein, A. *J. Phys. Chem.* **1988**, *92*, 2587.

(391) Moser, J.; Gallay, R.; Grätzel, M. *Helv. Chim. Acta* **1987**, *70*, 1596.

(392) Warman, J. M.; deHaas, M. P.; van Hövell tgot Westerflier, S. W. F. M.; Binsma, J. J. M.; Kolar, Z. I. *J. Phys. Chem.* **1989**, *93*, 5895.

(393) Morgan, J. R.; Natarajan, L. V. *J. Phys. Chem.* **1989**, *93*, 5.

(394) (a) Draper, R. B.; Fox, M. A. *J. Phys. Chem.* **1990**, *94*, 4628. (b) Draper, R. B.; Fox, M. A. *Langmuir* **1990**, *6*, 1396.

(395) (a) Rossetti, R.; Beck, S. M.; Brus, L. E. *J. Am. Chem. Soc.* **1984**, *106*, 980. (b) Rossetti, R.; Brus, L. E. *J. Phys. Chem.* **1986**, *90*, 558.

(396) Watanabe, T.; Honda, K. *J. Phys. Chem.* **1982**, *86*, 2617.

(397) Serpone, N.; Sharma, D. K.; Jamieson, M. A.; Grätzel, M.; Ramsden, J. J. *Chem. Phys. Lett.* **1985**, *115*, 473.

(398) Arbour, C.; Sharma, D. K.; Langford, C. H. *J. Chem. Soc., Chem. Commun.* **1987**, 917.

(399) Serpone, N.; Sharma, D. K.; Moser, J.; Grätzel, M. *Chem. Phys. Lett.* **1987**, *136*, 47.

(400) Nosaka, Y.; Miyama, H.; Terauchi, M.; Kobayashi, T. *J. Phys. Chem.* **1988**, *92*, 255.

(401) Henglein, A. *Pure Appl. Chem.* **1984**, *56*, 1215.

(402) Bahnemann, D.; Henglein, A.; Spanhel, L. *Faraday Discuss. Chem. Soc.* **1984**, *78*, 151.

(403) Kamat, P. V. *J. Am. Chem. Soc.* **1991**, *113*, 9705.

(404) Kamat, P. V. *J. Chem. Soc., Faraday Trans. 1* **1985**, 509.

(405) Ramsden, J. J. *Proc. R. Soc. London A* **1987**, *410*, 89.

(406) (a) Brown, G. R.; Darwent, J. R. *J. Chem. Soc., Chem. Commun.* **1985**, 98. (b) Brown, G. T.; Darwent, J. R.; Fletcher, P. D. I. *J. Am. Chem. Soc.* **1985**, *107*, 6446.

(407) (a) Nosaka, Y.; Fox, M. A. *Langmuir* **1987**, *3*, 1147. (b) Nosaka, Y.; Yamaguchi, K.; Kuwabara, A.; Miyama, H.; Baba, R.; Fujishima, A. *J. Photochem. Photobiol. A: Chem.* **1992**, *64*, 375.

(408) Rajh, T.; Rabani, J. *Langmuir* **1991**, *7*, 2054.

(409) Frank, A. J.; Willner, I.; Zafrir, G.; Degani, Y. *J. Am. Chem. Soc.* **1987**, *109*, 3568.

(410) Laane, C.; Willner, I.; Otvos, J. W.; Calvin, M. *Proc. Natl. Acad. Sci. U.S.A.* **1981**, *78*, 5928.

(411) Kuczynski, J.; Thomas, J. K. *Langmuir* **1985**, *1*, 158.

(412) Gerischer, H. *J. Phys. Chem.* **1984**, *88*, 6096.

(413) Grätzel, M.; Frank, A. J. *J. Phys. Chem.* **1982**, *86*, 2964.

(414) Albery, W. J.; Bartlet, P. N.; Wilde, C. P.; Darwent, J. R. *J. Am. Chem. Soc.* **1985**, *107*, 1854.

(415) Gopidas, K. R.; Kamat, P. V. *Langmuir* **1989**, *5*, 22.

(416) Patrick, B.; George, M. V.; Kamat, P. V.; Das, S.; Thomas, K. G. *J. Chem. Soc., Faraday Trans. 1* **1992**, *88*, 671.

(417) (a) Brown, G. T.; Darwent, J. R. *J. Chem. Soc. Faraday Trans.* **1984**, *80*, 1631. (b) Brown, G. T.; Darwent, J. R. *J. Phys. Chem.* **1984**, *88*, 4955.

(418) Mills, A.; Williams, G. *J. Chem. Soc., Faraday Trans. 1* **1987**, *83*, 2647.

(419) Kamat, P. V.; Dimitrijević, N. M. *Proceedings of the Symposium on Photoelectrochemistry and Electrosynthesis of Semiconductor Materials*; The Electrochemical Society: Pennington, NJ, 1988; Vol. 88-14, 90.

(420) Moser, J.; Grätzel, M. *J. Am. Chem. Soc.* **1983**, *105*, 6547.

(421) Moser, J.; Grätzel, M. *Helv. Chim. Acta* **1982**, *65*, 142.

(422) Henglein, A. *Ber. Bunsen-ges Phys. Chem.* **1982**, *86*, 241.

(423) Darwent, J. R. *J. Chem. Soc., Faraday Trans. 1* **1984**, *80*, 193.

(424) Amadelli, R.; Maldotti, A.; Bartocci, C.; Carassiti, V. *J. Phys. Chem.* **1989**, *93*, 6448.

(425) Lawless, D.; Serpone, N.; Meisel, D. *J. Phys. Chem.* **1991**, *95*, 5166.

(426) Mulvaney, P.; Cooper, R.; Grieser, F.; Meisel, D. *Langmuir* **1988**, *4*, 1206.

(427) Dimitrijević, N. M.; Kamat, P. V. *Radiat. Phys. Chem.* **1988**, *32*, 53.

(428) Resch, U.; Weller, H.; Henglein, A. *Langmuir* **1989**, *5*, 1015.

(429) Micić, O. I.; Nenadović, M. T.; Rajh, T.; Dimitrijević, N. M.; Nozik, A. J. In *Homogeneous and Heterogeneous Photocatalysis*; Pelizzetti, E., Serpone, N., Eds.; D. Reidel Publishing Co.: Dordrecht, the Netherlands, 1986, p 213.

(430) Vucemilović, M. I.; Micić, O. I. *Radiat. Phys. Chem.* **1988**, *32*, 79.

(431) Henglein, A.; Lilie, J. *J. Am. Chem. Soc.* **1981**, *103*, 1059.

(432) Henglein, A. *J. Phys. Chem.* **1982**, *86*, 2291.

(433) Vucemilovic, M. I.; Vukelić; Rajh, T. *J. Photochem. Photobiol. A: Chemistry* **1988**, *42*, 157.

(434) Hayes, R.; Freeman, P. A.; Mulvaney, P.; Grieser, F.; Healy, T. W.; Furlong, D. N. *Ber. Bunsen-ges Phys. Chem.* **1987**, *91*, 231.

(435) Mills, G.; Zongguan, L.; Meisel, D. *J. Phys. Chem.* **1988**, *92*, 822.

(436) Gerischer, H.; Lübke, M. *J. Electroanal. Chem.* **1986**, *204*, 225.

(437) Spanhel, L.; Weller, H.; Henglein, A. *J. Am. Chem. Soc.* **1987**, *109*, 6632.

(438) Spanhel, L.; Henglein, A.; Weller, H. *Ber. Bunsen-ges Phys. Chem.* **1987**, *91*, 1359.

(439) Serpone, N.; Borgarello, E.; Grätzel, M. *J. Chem. Soc., Chem. Commun.* **1983**, 142.

(440) Gopidas, K. R.; Bohorquez, M.; Kamat, P. V. *J. Phys. Chem.* **1990**, *94*, 6436.

(441) Vogel, R.; Pohl, K.; Weller, H. *Chem. Phys. Lett.* **1990**, *174*, 241.

(442) (a) Hotchandani, S.; Kamat, P. V. *J. Phys. Chem.* **1992**, *96*, 6834. (b) Hotchandani, S.; Kamat, P. V. *Chem. Phys. Lett.* **1992**, *191*, 320.

(443) Rabani, J. *J. Phys. Chem.* **1989**, *93*, 7707.

(444) Henglein, A.; Gutiérrez, M.; Weller, H.; Fojtik, A.; Jirkovvsky, J. *Ber. Bunsen-ges Phys. Chem.* **1989**, *93*, 593.

(445) Kraeutler, B.; Bard, A. J. *J. Am. Chem. Soc.* **1978**, *100*, 2239.

(446) Kraeutler, B.; Bard, A. J. *J. Am. Chem. Soc.* **1978**, *100*, 5985.

(447) Izumi, I.; Fan, F. R. F.; Bard, A. J. *J. Phys. Chem.* **1979**, *101*, 3127.

(448) Reiche, H.; Bard, A. J. *J. Am. Chem. Soc.* **1979**, *101*, 3127.

(449) Kraeutter, B.; Reiche, H.; Bard, A. J.; Hocker, R. B. *J. Polym. Sci. Polym. Lett. Ed.* **1979**, *17*, 535.

(450) Funt, B. L.; Tan, S. R. *J. Polym. Sci. Polym. Chem. Ed.* **1984**, *22*, 605.

(451) Kamat, P. V.; Basheer, R. A.; Fox, M. A. *Macromolecules* **1985**, *18*, 1366.

(452) Kamat, P. V.; Todesco, R. V. *J. Polym. Sci., Polym. Chem. Ed.* **1987**, *25*, 1035.

(453) Hoffman, A. J.; Yee, H.; Mills, G.; Hoffmann, M. R. *J. Phys. Chem.* **1992**, *96*, 5540.

(454) Hoffman, A. J.; Mills, G.; Yee, H.; Hoffmann, M. R. *J. Phys. Chem.* **1992**, *96*, 5546.

(455) Al-Ekabi, H.; DeMayo, P. *J. Chem. Soc., Chem. Commun.* **1984**, 1231.

(456) Al-Ekabi, H.; DeMayo, P. *J. Phys. Chem.* **1985**, *89*, 5815.

(457) Hasegawa, T.; DeMayo, P. *Langmuir* **1986**, *2*, 362.

(458) Fox, M. A. In *Topics in Organic Electrochemistry*; Fry, A. J., Britton, W. E., Eds.; Plenum Press: New York, 1986.

(459) Fox, M. A. *Top. Curr. Chem.* **1987**, *142* (Electrochemistry I), 71.

(460) Borgarello, E.; Kalyanasundaram, K.; Grätzel, M.; Pelizzetti, E. *Helv. Chim. Acta* **1982**, *65*, 243.

(461) Bühler, N.; Meier, K.; Reber, J. F. *J. Phys. Chem.* **1984**, *88*, 3261.

(462) Thewissen, D. H. H. W.; Timmer, K.; Eenhorst-Reinten, M.; Tinnemans, A. H. A.; Mackor, A. *Nouv. J. Chim.* **1983**, *7*, 191.

(463) Borgarello, E.; Erbs, W.; Grätzel, M.; Pellizzetti, E. *Nouv. J. Chim.* **1983**, *7*, 195.

(464) Borgarello, E.; Serpone, N.; Grätzel, M. *Int. J. Hydrogen Energy* **1985**, *10*, 737.

(465) Borgarello, E.; Terzian, R.; Serpone, N.; Pelizzetti, E.; Barbeni, M. *Inorg. Chem.* **1986**, *25*, 2135.

(466) Izumi, I.; Dunn, W. W.; Wilbourn, K. O.; Fan, F. F.; Bard, A. J. *J. Phys. Chem.* **1980**, *84*, 3207.

(467) Barbeni, M.; Pramaura, E.; Pelizzetti, E.; Borgarello, E.; Grätzel, M.; Serpone, N. *Nouv. J. Chim.* **1985**, *9*, 67.

(468) Al-Ekabi, H.; Serpone, N. *J. Phys. Chem.* **1988**, *92*, 5726.

(469) Matthews, R. W. *J. Chem. Soc., Faraday Trans. 1* **1984**, *80*, 457.

(470) (a) Matthews, R. W. *J. Catal.* **1988**, *111*, 264. (b) Pelizzetti, E.; Carlin, V.; Minero, C.; Grätzel, M. *New J. Chem.* **1991**, *15*, 351. (c) Al-Sayyed, G.; D'Oliveira, J.-C.; Pichat, P. *J. Photochem. Photobiol. A: Chem.* **1991**, *58*, 99.

(471) D'Oliveira, J.-C.; Al-Sayyed, G.; Pichat, P. *Environ. Sci. Technol.* **1990**, *24*, 990.

(472) (a) Okamoto, K.; Yamamoto, Y.; Tanaka, H.; Tanaka, M. *Bull. Chem. Soc. Jpn.* **1985**, *58*, 2015. (b) Sclafani, A.; Palmisano, L.; Davi, E. *New J. Chem.* **1990**, *14*, 265. (c) Grabner, G.; Li, G.; Quint, R. M.; Quint, R.; Getoff, N. *J. Chem. Soc. Faraday Trans.* **1991**, *87*, 1097. (d) Wei, T.-Y.; Wan, C.-C. *Ind. Eng. Chem. Res.* **1991**, *30*, 1293.

(473) (a) Ménassa, P. E.; Mak, M. K. S.; Langford, C. H. *Environ. Tech. Lett.* **1988**, *9*, 825. (b) Minero, C.; Catozzo, F.; Pelizzetti, E. *Langmuir* **1992**, *8*, 481.

(474) (a) Hisanaga, T.; Harada, K.; Tanaka, K. *J. Photochem. Photobiol. A: Chem.* **1990,** *54,* 113. (b) Mao, Y.; Schöneich, C.; Asmus, K.-D. *J. Phys. Chem.* **1991,** *95,* 10080. (c) Kondo, M. M.; Jardim, W. F. *Water Res.* **1991,** *25,* 823. (d) Kormann, C.; Bahnemann, D. W.; Hoffmann, M. R. *Environ. Sci. Technol.* **1991,** *25,* 494. (e) Dibble, L. A.; Raupp, G. B. *Catal. Lett.* **1990,** *4,* 345. (f) Dibble, L. A.; Raupp, G. B. *Environ. Sci. Technol.* **1992,** *26,* 492.

(475) Hidaka, H.; Zhao, J.; Pelizzetti, E.; Serpone, N. *J. Phys. Chem.* **1992,** *96,* 2226.

(476) Grätzel, C. K.; Joursek, M.; Grätzel, M. *J. Mol. Catal.* **1987,** *39,* 347.

(477) (a)Turchi, C. S.; Ollis, D. F. *J. Catal.* **1989,** *112,* 483. (b) Turchi, C. S.; Ollis, D. F. *J. Catal.* **1990,** *113,* 178.

(478) (a) Augugliaro, P.; Palmisano, L.; Sclafani, A.; Minero, C.; Pelizzetti, E. *Toxicol. Environ. Chem.* **1988,** *16,* 89. (b) Al-Ekabi, H.; Serpone, N.; Pelizzetti, E.; Minero, C.; Fox, M. A.; Draper, R. B. *Langmuir* **1989,** *5,* 250.

(479) (a) Gerischer, H.; Heller, A. *J. Phys. Chem.* **1991,** *95,* 5261. (b) Gerischer, H.; Heller, A. *J. Electrochem. Soc.* **1992,** *139,* 113. (c) Wang, C.-M.; Heller, A.; Gerischer, H. *J. Am. Chem. Soc.* **1992,** *114,* 5230.

(480) Lawless, D.; Serpone, N.; Meisel, D. *J. Phys. Chem.* **1991,** *95,* 5166.

(481) Boonstra, A. H.; Mustsaers, C. A. H. A. *J. Phys. Chem.* **1975,** *79,* 1940.

(482) Stafford, U.; Gray, K. A.; Kamat, P. V.; Varma, A. *Chem. Phys. Lett.* **1992,** in press.

(483) Gerischer, H.; Willig, F. *Top. Curr. Chem.* **1976,** *61,* 31.

(484) Meir, H. *Photochem. Photobiol.* **1972,** *16,* 219.

(485) Vlachopoulos, N.; Liska, P.; Augustynski, J.; Grätzel, M. *J. Am. Chem. Soc.* **1988,** *110,* 1216.

(486) De Silvestro, J.; Grätzel, M.; Kevan, L.; Moser, J. *J. Am. Chem. Soc.* **1985,** *107,* 2988.

(487) Spitler, M.; Parkinson, B. A. *Langmuir* **1986,** *2,* 549.

(488) (a) Kirk, A. D.; Langford, C. H.; Joly, C. S.; Lesagi, R.; Sharma, D. K. *J. Chem. Soc., Chem. Commun.* **1984,** 961. (b)Arbour, C.; Sharma, D. K.; Langford, C. H. *J. Phys. Chem.* **1990,** *94,* 331.

(489) Moser, J.; Grätzel, M.; Sharma, D. K.; Serpone, N. *Helv. Chim. Acta* **1985,** *68,* 1686.

(490) Kamat, P. V. *Langmuir* **1990,** *6,* 512.

(491) Levy, B. In *Photochemical Conversion and Storage of Solar Energy*; Pelizzetti, E., Schiravello, M., Eds.; Kluwer Academic Publishers: Boston, 1991, p 337.

(492) Ryan, M. A.; Fitzgerald, E. C.; Spitler, M. T. *J. Phys. Chem.* **1989,** *93,* 6150.

(493) Liang, Y.; Ponte Goncalves, A. M.; Negus, D. K. *J. Phys. Chem.* **1983,** *87,* 1.

(494) Hashimoto, K.; Hiramoto, M.; Sakata, T. *J. Phys. Chem.* **1988,** *92,* 4272.

(495) Hashimoto, K.; Hiramoto, M.; Sakata, T. *Chem. Phys. Lett.* **1988,** *148,* 215.

(496) (a) Crackel, R. L.; Struve, W. S. *Chem. Phys. Lett.* **1985,** *120,* 473. (b) Eichberger, R.; Willig, F. *Chem. Phys.* **1990,** *141,* 159. (c) Willig, F.; Eichberger, R.; Sundaresan, N. S.; Parkinson, B. A. *J. Am. Chem. Soc.* **1990,** *112,* 2702.

(497) Kamat, P. V.; Patrick, B. In *Electrochemistry in Colloids and Dispersions*; Mackay, R. A., Texter, J., Eds.; VCH Publishers, Inc.: New York, 1992, p 447.

(498) Patrick, B.; Kamat, P. V. *J. Phys. Chem.* **1992,** *96,* 1423.

(499) Suto, S.; Yashima, M.; Uchida, W.; Goto, T. *J. Lumin.* **1987,** *38,* 308.

(500) Fan, F. R. F.; Bard, A. J. *J. Am. Chem. Soc.* **1979,** *101,* 6139.

(501) Kemnitz, K.; Yoshihara, K.; Tani, T. *J. Phys. Chem.* **1990,** *94,* 3099.

(502) Sviridov, D. V.; Kulak, A. I.; Shapiro, B. I. *High Energy Chem.* **1990,** *24,* 126.

(503) Gosh, P. K.; Spiro, T. G. *J. Am. Chem. Soc.* **1980,** *102,* 5543.

(504) Borgarello, E.; Kiwi, J.; Pelizzetti, E.; Grätzel, M. *J. Am. Chem. Soc.* **1981,** *103,* 6324.

(505) O'Regan, B.; Grätzel, M. *Nature* **1991,** *353,* 737.

(506) Hashimoto, T.; Kawai, T.; Sakata, T. *Nouv. J. Chim.* **1983,** *7,* 249.

(507) (a) Kajiwara, T.; Hasimoto, K.; Kawai, T.; Sakata, T. *J. Phys. Chem.* **1982,** *86,* 4516. (b) Hashiomoto, K.; Hiramoto, M.; Kawai, T.; Sakata, T. *J. Phys. Chem.* **1988,** *92,* 4636.

(508) Frei, H.; Fitzmaurice, D. J.; Grätzel, M. *Langmuir* **1990,** *6,* 198.

(509) Tani, T.; Suzumoto, T.; Ohzeki, K. *J. Phys. Chem.* **1990,** *94,* 1298.

(510) Ryan, M. A.; Spitler, M. T. *J. Imaging Sci.* **1991,** *35,* 351.

(511) Gerischer, H. *Adv. Electrochem. Eng.* **1961,** *1,* 139.

(512) Gerischer, H. *Photochem. Photobiol.* **1972,** *16,* 243.

(513) Sonntag, L. P.; Spitler, M. J. *J. Phys. Chem.* **1985,** *89,* 1453.

(514) Kamat, P. V.; Fox, M. A.; Fatiadi, A. J. *J. Am. Chem. Soc.* **1984,** *106,* 1191.

(515) Gust, D.; Moore, T. A. *Science* **1989,** *244,* 35.

(516) Fitzmaurice, D. J.; Frei, H. *Langmuir* **1991,** *7,* 1129.

(517) Borgarello, E.; Kiwi, J.; Pelizzetti, E.; Visca, M.; Grätzel, M. *J. Am. Chem. Soc.* **1981,** *103,* 6324.

(518) Borgarello, E.; Kiwi, J.; Pelizzetti, E.; Visca, M.; Grätzel, M. *Nature* **1981,** *289,* 158.

(519) Memming, R.; Schröppel, F.; Bringmann, U. *J. Electroanal. Chem.* **1979,** *100,* 37.

(520) Hashimoto, K.; Kawai, T.; Sakata, T. *Nouv. J. Chim.* **1983,** *7,* 249.

(521) Kim, Y. I.; Salim, S.; Hug, M. J.; Mallouk, T. E. *J. Am. Chem. Soc.* **1991,** *113,* 9561.

(522) Vinodgopal, K.; Kamat, P. V. *Environ. Sci. Tech.* **1992,** *26,* 1963.